(5)

IMPROVEMENTS IN THE POTASSIUM-ARGON DATING METHOD AND THEIR APPLICATION TO STUDIES OF THE HONOLULU VOLCANIC SERIES

A DISSERTATION SUBMITTED TO THE GRADUATE DIVISION OF THE UNIVERSITY OF HAWAII IN PARTIAL FULFILLMENT OF THE REQUIREMENTS FOR THE DEGREE OF DOCTOR OF PHILOSOPHY IN CHEMISTRY DECEMBER 1970

by

John Wilbur Gramlich

Dissertation Committee:

John J. Naughton, Chairman
Gordon A. Macdonald
Richard G. Inskeep
John W. Gilje
Robert W. Buddemeier

We certify that we have read this dissertation and that in our opinion it is satisfactory in scope and quality as a dissertation for the degree of Doctor of Philosophy in Chemistry.

DISSERTATION COMMITTEE

John J. Vaughan
Chairman

Gordon A. Macdonald

Robert W. Buddemeier

Richard G. Inskeep

John M. Gelb

ACKNOWLEDGMENTS

Grateful acknowledgment is made to the following persons for their assistance in this research:

Virginia Lewis for developing the techniques required to obtain accurate potassium analyses, and for obtaining the potassium analyses reported in this paper.

Dr. I. Lynus Barnes and the staff of the Analytical Mass Spectrometry Section, Analytical Chemistry Division, National Bureau of Standards, for the expanded scale recorder and several suggestions for instrumental improvements.

Clarence Williams for performing minor miracles with pyrex and quartz.

Bill Barnes for replacing transistors and diodes as fast as the author could burn them out.

Ted Jordan for assistance with several machine shop problems.

Dr. Kost A. Pankiwskyj for supplying the sample of Salt Lake lava, and assistance with several geological and petrographic problems.

Dr. Harold T. Stearns for his aid in locating samples, and for his interest in this research.

Glen Bauer of the Honolulu Board of Water Supply for the sample of Punchbowl lava.

Ken Kum for many painstaking hours of mineral separations.

Dale Hammond and Clarles Fein for their assistance in obtaining last minute numbers.

Sister Mary Roger Brennan for a shoulder to cry on in times of crisis.

TABLE OF CONTENTS

LIST OF TABLES

LIST OF FIGURES

I. INTRODUCTION

A. The Potassium-Argon Method

Several million years ago, the serenity of the blue Pacific was suddenly shattered by the roar of a hydro-magmatic explosion, as hot lava came in contact with sea water: Pele, the Hawaiian volcano goddess had come to life. For millions of years she poured lava onto the ocean floor, gradually building up mountains which eventually broke above the ocean's surface. As the waves wore away at the fresh lava, Pele poured more lava onto the surface, in a struggle for survival. Gradually, small marine organisms built up protective reefs to hold back the threatening surf. This island-building process continued in a south-easterly direction for approximately 1600 miles and the results comprise the islands, reefs, and shoals known as the Hawaiian Archipelago.

Near the end of the last ice age, small bands of relatively primitive people migrated into the Pacific, possibly from the southwest (1). They slowly continued their migration to the northeast until they finally reached the Hawaiian Islands, perhaps less than a thousand years ago. As the first man set foot on the gray basaltic rock of the Hawaiian Islands, he must have asked himself "how

long have these islands been here"; man, with his nearly infinite curiosity, has been asking this question ever since.

1. Historical

One of the techniques which can help answer the question of geological age is the potassium-argon method of geochronology. In 1905, J. J. Thompson, using a gold leaf electrometer, showed that an alloy of sodium and potassium emitted negative particles (2). The following year, Campbell and Wood (3) showed that this radiation came from potassium. They used fractional crystallization to separate pure potassium salts, and were able to show that the amount of radiation was always proportional to the amount of potassium present, and was independent of the chemical state of the element. In 1921, Aston (4), using mass spectrographic analysis, showed that potassium contained at least two isotopes with masses of 39 and 41. However, neither of these isotopes were capable of emitting beta particles. To account for the radiation emitted by potassium, Newman and Walke (5), and Klemperer (6) proposed the existence of an isotope of mass 40. They hypothesized that ^{40}K would decay by beta emission to ^{40}Ca. Later the same year, A. O. Nier (7), using a mass spectrometer with greater resolving power than was available to Aston, discovered the isotope ^{40}K, and found its abundance to be 1.19×10^{-4} of the

total amount of potassium. This work was almost immediately confirmed by Brewer (8). Two years later, Smythe and Hemmendinger (9) found that all of the beta activity of potassium was due to the newly discovered isotope ^{40}K.

In 1937, C. F. Von Weizsacker (10) proposed that ^{40}Ar was a product of radioactive decay of ^{40}K. It was known at the time that an excess of ^{40}Ar existed in the earth's atmosphere. All other chemically analogous elements show a steady decline in terrestrial abundance with increasing atomic weight. The rare gases in the atmosphere also follow this trend, with the exception of helium, which has an abnormally low concentration due to escape from the outer atmosphere, and ^{40}Ar, which is abnormally high. From the ^{40}Ar abundance evidence, Von Weizsacker concluded that the total activity of potassium was due to potassium-40, and that the entire excess of ^{40}Ar in the atmosphere was due to the decay of ^{40}K. He proposed the existence of the process of electron capture by the nucleus to explain the formation of ^{40}Ar. Von Weizsacker was also the first to suggest that the measurement of the ^{40}K and ^{40}Ar content of minerals might be used as a method of geochronological dating. The first to find an excess of ^{40}Ar in geologic materials were Aldrich and Nier (11), who, in 1948, using mass spectrometric techniques, found an excess of ^{40}Ar in old samples of orthoclase, microcline, sylvite, and langbeinite.

The first reliable age to be measured by the potassium-argon method was obtained by Wolfgang Gentner and his co-workers at the University of Freiburg. They measured the potassium and argon-40 content of a sylvite from the salt mine at Buggingen, Baden, Germany, and obtained an age of 20 million years (12,13). Later they corrected this age for argon losses from diffusion, and reported an age of 25 million years (14,15). Thus, by the middle of the 1950's, the potassium-argon method was well on the way to becoming a useful geochronological tool.

2. Mode of Decay and Mathematical Relationships

In addition to decay by electron capture to ^{40}Ar, potassium-40 also decays to ^{40}Ca by beta emissions: the complete decay scheme is shown in Figure 1. As a result of this decay process, the relative abundance of ^{40}K is continuously decreasing, while that of ^{40}Ca and ^{40}Ar is continuously increasing with time. However, it is only necessary to know the present relative abundance of ^{40}K to use the potassium-argon method. The most generally accepted values for the natural abundances of potassium and argon isotopes are those obtained by Nier (16), and are listed in Table 1. More recent determinations of the abundance of ^{40}K give a value of 0.0118 atom percent (17,18,19), but the older value continues to be the most widely accepted. However, according to Damon (20), Professor Nier now accepts the more recent value.

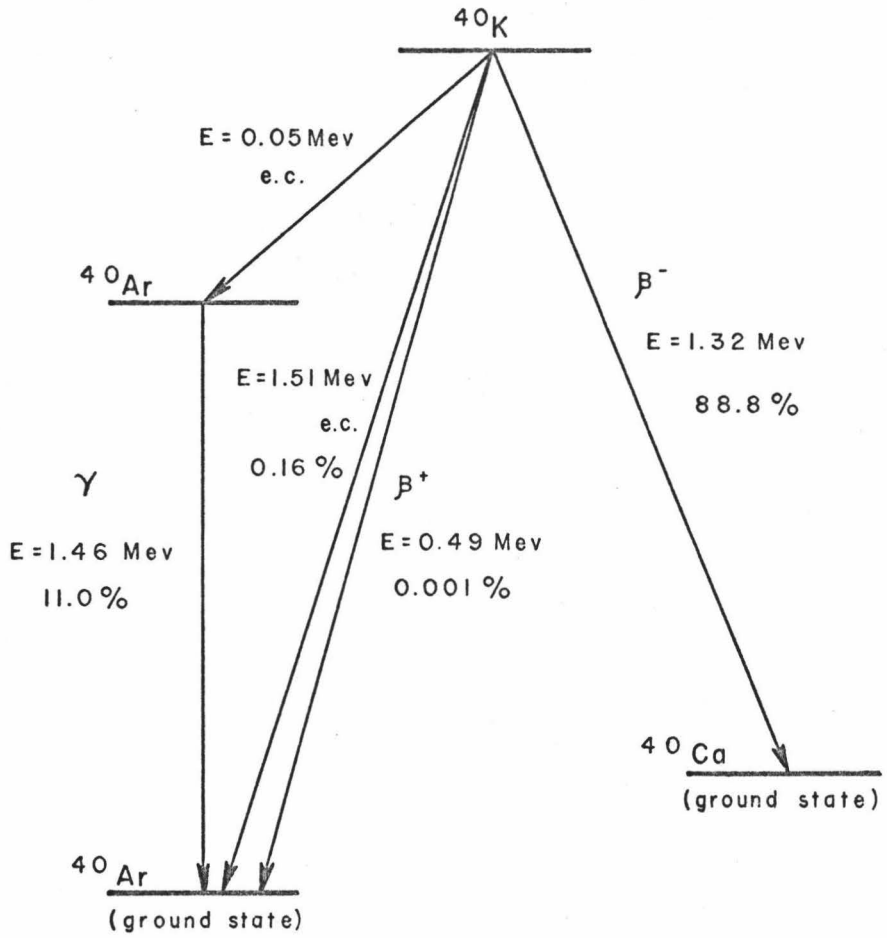

$^{40}K/K = 0.000119$

$T_{1/2} = 1.31 \times 10^{9}$ yr.

$\lambda_e = 0.585 \times 10^{-10}$ yr.$^{-1}$

$\lambda_\beta = 4.72 \times 10^{-10}$ yr.$^{-1}$

Figure 1: Decay Scheme of Potassium-40

Table 1

Isotopic Abundances of Potassium and Atmospheric Argon

Isotope	Relative Atomic Abundance
^{41}K	6.91 ± 0.04 %
^{40}K	0.0119 ± 0.0001 %
^{39}K	93.08 ± 0.04 %
^{40}Ar	99.600 %
^{38}Ar	0.063 %
^{36}Ar	0.337 %

The decay constants for beta emission and electron capture, λ_β and λ_e, are required to determine the decay of ^{40}K. The values most frequently used in potassium-argon age determinations are $\lambda_\beta = 4.72 \times 10^{-10}$ year^{-1} reported by Endt and Kluyver (21), and $\lambda_e = 0.584 \times 10^{-10}$ year^{-1}, an average of the values determined by Wetherill (22) and McNair et al. (23). Both of these values assume a ^{40}K abundance of 0.0119 percent. Higher constants, such as those reported by Folinsbee (24), where $\lambda_\beta = 4.65 \times 10^{-10}$ year^{-1}, and $\lambda_e = 0.589 \times 10^{-10}$ year^{-1}, are derived from a ^{40}K abundance of 0.0118 percent. Some American workers (20) recommend using the values $\lambda_\beta = 4.78 \times 10^{-10}$ year^{-1} and $\lambda_e = 0.588 \times 10^{-10}$ year^{-1}, while some Russian laboratories are now using the constants $\lambda_\beta = 4.68 \times 10^{-10}$ year^{-1} and $\lambda_e = 0.585 \times 10^{-10}$ year^{-1}, based on Firsov's review of experimental data (25). Probably some of the new values for the isotopic abundance of ^{40}K, and the decay constants are more accurate than the older, more commonly used values, but as Smith (26) points out, until new values are internationally agreed upon, only confusion will result from the use of yet another set of decay constants.

The equation for calculating geologic ages from potassium-argon data is:

$$t = \frac{1}{\lambda_\beta + \lambda_e} \ln \left[\frac{^{40}Ar^*}{^{40}K} \frac{\lambda_e + \lambda_\beta}{\lambda_\beta} + 1 \right]$$

where $^{40}Ar^*$ is the radiogenic argon produced from the decay of ^{40}K in the material being dated. The derivation of this equation from the basic laws of radioactive decay is given in Appendix A. Substituting the most frequently used values for the decay constants, the age equation becomes:

$$t = 1.885 \ln (9.068 \ ^{40}Ar^*/^{40}K + 1) \times 10^9$$

where t is the age in millions of years. For geologically young materials, this equation can be simplified to:

$$t = 1.709 \ ^{40}Ar^*/^{40}K \times 10^{10}$$

For late Tertiary and Pleistocene rocks, the error resulting from the use of this equation is negligible and only reaches 1 percent at about 35 million years.

3. Basic Assumptions

Several basic assumptions must be made when the above equations are used to calculate ages by the potassium-argon method. They are as follows:

1. The rate of decay of ^{40}K is constant regardless of its chemical or physical state.
2. The decay constants for ^{40}K are accurately known.
3. At the time of formation, there was no radiogenic argon trapped in the sample.
4. The sample has been a closed system since the time of formation; that is, there has been no loss or gain of ^{40}K or ^{40}Ar, except as a result of radioactive decay of ^{40}K.

The constancy of decay is fundamental to all dating methods based on radioactive decay. Since radioactive decay is a nuclear process, it is not affected by the chemical or physical environment, which involves the electrons surrounding the nucleus. Decay by electron capture, however, involves an interaction between the nucleus and an orbital electron, therefore, differences in the electron density caused by different environments could result in different rates of decay. The electron capture decay of ^{7}Be has been shown to be slightly affected by chemical environment (27), but such an effect has not been observed for ^{40}K (28).

The occurrence of excess argon in geologic materials does not seem to be a serious problem, since most of the ages obtained by this method agree with the results obtained by other geochronological methods. However, several reported anomalous ages have been attributed to excess ^{40}Ar. The loss of radiogenic argon from samples can be a serious problem in potassium-argon dating, but can usually be avoided by careful sample selection. More will be said later about both excess argon and argon loss.

4. Argon Extraction, Purification, and Measurement

Two methods have been used to quantitatively remove argon from the sample to be dated. With both methods, the sample is placed inside a vacuum line, so that the gas released can be collected and purified. The first method employs a flux, which is mixed with the sample to be melted.

Frequently used fluxes include sodium hydroxide, sodium peroxide, sodium tetraborate, and mixtures of these. The principal advantage of this technique is that it allows the sample to be melted at a temperature of 1000°C or less, thus an inexpensive, external heater may be employed. The major disadvantage of this technique is that degassing of the flux liberates large amounts of active gases which must be removed, and also increases the amount of air argon contamination. Other disadvantages to the flux method are reaction between the flux and the sample container, and incomplete removal of argon from the sample. This method was widely used until the advent of radio-frequency induction heating in the mid-1950's. Among the first to investigate induction heating were Carr and Kulp (29); their work showed that argon could be quantitatively removed from a sample without the use of a flux. The main advantage of the induction heating technique is that it results in a "cleaner" extraction, since no foreign materials are added to the sample. This is especially important for geologically young materials, where the amount of atmospheric argon must be kept to a minimum. The principle disadvantage of this method is the high cost of radio-frequency induction heaters. Temperatures in excess of 1800°C can be achieved with induction heating. This temperature is sufficient to completely melt most minerals, but for very high melting materials, such as zircon, induction heating combined with the use of a flux has been employed to insure complete gas removal (30).

The gases released from a sample during melting are chiefly active gases such as water, carbon dioxide, nitrogen, oxygen, etc.; argon usually constitutes only a small percent of the total gas content of the sample. Before the amount of argon can be measured, it is necessary to separate or remove these active gases. This is usually accomplished by the formation of stable compounds of the active gases with metals at elevated temperatures. The gas purification systems used in various laboratories have been reported in the literature (28,31,32,33), and are all basically the same. The fundamental components and procedures will be briefly reviewed here. During melting, the gases evolved are usually collected on activated charcoal at liquid nitrogen temperatures; this allows a low pressure to be maintained in the vacuum system, preventing a glow discharge which could drive some argon into the walls of the oven when radio-frequency heating is used. After melting, the gases are exposed to a CuO getter, maintained at a temperature of 450°C to 550°C. Hydrogen reacts with the CuO to form water, while hydrocarbons are oxidized to water and carbon dioxide. Both water and carbon dioxide are then adsorbed by a molecular sieve trap. After this initial cleanup, the remaining gases are moved to a second part of the purification system and exposed to a second getter to remove the remaining active gases. This second getter is usually titanium metal at a temperature of about 800°C, although other metals such as calcium and

barium have been used (31). The titanium and copper oxide getters must be separated, since water formed by the oxidation of hydrogen at the CuO getter will be reduced by the titanium getter to form more hydrogen. After chemical cleanup by the hot titanium, only the noble gases remain. Argon is then collected on activated charcoal at liquid nitrogen temperatures, and analyzed by one of the procedures described below.

The most common method of determining the amount of radiogenic argon in a sample is by mass spectrometry, using ^{38}Ar as an isotopic diluent. A precisely known amount of ^{38}Ar is admitted to the vacuum system just prior to melting the sample. With this method, it is not necessary to quantitatively collect and analyze the argon extracted from the sample: only a representative fraction is needed. The mass spectrometric analysis may be performed in either a static or dynamic mode. In the static method, the spectrometer is isolated from its pumping system, and the gas sample is introduced into the mass spectrometer tube. The analysis is performed by alternately scanning mass-40, mass-38, and mass-36. From the known amount of ^{38}Ar in the sample, the relative amounts of ^{36}Ar and ^{40}Ar can be calculated, and the amount of ^{40}Ar which is from atmospheric contamination can be determined from the measured amount of ^{36}Ar. If the dynamic method is used, the sample is slowly leaked into the mass spectrometer, and after passing through the

ionization chamber, is pumped out the opposite end of the tube. The isotopic analysis is determined in the same manner as is used for the static method, but often a correction is necessary to account for isotopic fractionation of the gas while passing through the leak. The static method of analysis is usually preferred because of its greater sensitivity.

Four types of mass spectrometers are used for argon analysis. The "Reynolds-type" mass spectrometer is a 4½ inch radius, 60 degree instrument usually constructed of pyrex glass. This spectrometer was first designed by J.H. Reynolds (34) in 1956. The "Nier-type" mass spectrometer is a 6 inch radius, 60 degree instrument usually constructed of stainless steel. Currently used instruments are modifications of the design developed by Nier (35) in 1947. The third type of instrument used is the MS-10 mass spectrometer, which utilizes a 180 degree magnetic deflection and a 2 inch radius of curvature. The design of this instrument is similar to that proposed by Dempster (36) in 1918. This spectrometer has an advantage of being less expensive than the Reynolds- or Nier-type instruments, but its resolution is only about one half that of the other two types. The omagatron mass spectrometer is more closely related to the cyclotron than to the magnetic deflection instruments described above. Ions produced in a magnetic field are spiraled with a unique cyclotron frequency dependent upon the magnetic field and the mass/charge ratio. When an external radio-frequency field is applied at the

cyclotron frequency, the ions with the correct m/e ratio are spiraled outward to a collector. This instrument is smaller and less expensive than the magnetic deflection instruments, but its resolution for argon isotopes is even less than that of the MS-10 mass spectrometer. The omagatron has never gained much popularity for potassium-argon age studies, but is potentially useful for this type of work (37).

Direct volumetric measurement of the extracted argon has been used for age determinations, but with the current availability of mass spectrometers and pure ^{38}Ar tracers, this method has become basically of historical interest. This method requires that the argon be quantitatively collected and completely separated from all other gases, including the other noble gases. The argon is then expanded into a precisely known volume, and the pressure determined. The pressure can be determined precisely only with a McLeod gauge (38), and must be greater than 10^{-4} cm^3 to insure accurate measurement. Unless the amount of air argon contamination is extremely small, mass spectrometric analysis is still needed to determine the amount of radiogenic argon present.

Neutron-activation analysis has also been used for argon determinations (39,40,41). When ^{40}Ar and ^{36}Ar are irradiated with thermal neutrons, the radioactive nuclides ^{41}Ar and ^{37}Ar are produced according to the following reactions:

$$^{40}Ar\ (n,\nu)\ ^{41}Ar \xrightarrow[\beta^-]{1.82\ hr.}\ ^{41}K$$

$$^{36}Ar\ (n,\nu)\ ^{37}Ar \xrightarrow[e.c.]{35\ days}\ ^{37}Cl$$

Since neutron reactions with calcium and potassium produce appreciable amounts of ^{41}Ar and ^{37}Ar, the argon must be separated from the sample before irradiation. Because of the short half life of ^{41}Ar, counting of the beta activity of this isotope must be conducted soon after irradiation.

5. Factors Affecting Accuracy and Precision

The factors which affect the accuracy and precision of potassium-argon age determinations can be divided into three major categories: a) atmospheric argon contamination, b) instrumental limitations, and c) sample selection and preparation.

a) Atmospheric argon contamination

Atmospheric argon, which contains 99.6 percent argon-40, is incorporated on or in the samples analysed by the potassium-argon method. This atmospheric argon contamination is frequently in the range of 10^{-6} to 10^{-7} std. cm^3 per gram of sample. For young, low potassium rocks, this air argon may amount to 90 percent or more of the total argon.

One might intuitively suspect that the air argon is absorbed on the surface of the rock or in microcracks and would, therefore, be easily removed by vacuum baking, chemical etching, or mechanical removal of the surface layer. Experimental evidence, however, indicates that the problem is not

this simple. Some workers report that most of the air argon originates from adsorption on the surface of the sample during and after crushing (33,42). Others have reported an order of magnitude reduction in the air argon contamination by chemical etching with 10 percent hydrofluoric acid (32). In a more recent study (43) samples were surface etched with hydrofluoric acid or had the surface layers removed with a diamond saw in an argon free atmosphere; other samples were placed in pure argon atmospheres. Analysis showed no significant differences in the amount of air argon contamination between the various pre-treated samples. Other studies indicate that the quantity of adsorbed air argon varies with mineral type (33,44).

Correction for the air argon contamination is made from the mass spectrometric data. Since the $^{40}Ar/^{36}Ar$ ratio of atmospheric argon is known, the fraction of ^{40}Ar that is atmospheric can be determined from the measured amount of ^{36}Ar. As the percentage of air argon increases, the precision in measuring the amount of radiogenic argon decreases, due to the effect of subtracting one large number from another.

b) Instrumental limitations

Because the concentration of ^{36}Ar in atmospheric argon is quite small, the amount of this isotope released from a sample is frequently less than $1x10^{-9}$ std cc/gm. This amount of gas produces a signal of only a few millivolts. Background instrumental noise can amount to several tenths of a

millivolt, thus producing an unfavorable signal/noise ratio for ^{36}Ar measurements. If the air argon constitutes 95 percent of the total argon, a 1 percent error in the measurement of ^{36}Ar will produce approximately a 20 percent error in the radiogenic argon measurement. Thus for geologically young materials, the signal/noise ratio for the measurement of ^{36}Ar is often the most important source of error for potassium-argon age determinations.

The detector used on most mass spectrometers is the cage-type (Faraday cup), amplified by a vibrating-reed electrometer. The electrometer has different scales to accept a wide range of input signals. Since the different isotopes are measured on different scales, it is necessary that each scale be accurate relative to the others. For example, a 10 mv signal into the electrometer should read exactly 10 mv on all scales. If this is not the case, a correction must be made to the recorder data.

Because of slight physical differences in the isotopes and characteristics of the instrument, the mass spectrometer may not give the true ratio of the isotopes in the tube. This isotopic bias is usually determined using samples of air argon. From the known absolute $^{40}Ar/^{36}Ar$ ratio of air argon, and the ratio measured by the mass spectrometer, a correction factor can be calculated which must be applied to all argon isotopic determinations. This bias correction must be determined accurately, since a

1 percent error in the measured air $^{40}Ar/^{36}Ar$ ratio will result in an error of about 15 percent in the calculated radiogenic argon content for samples that contain 95 percent atmospheric argon contamination.

c) Sample selection and preparation

The ultimate accuracy of a potassium-argon age is strongly dependent on sample selection. Since one of the components measured is a gas, metamorphism, alteration or secondary heating of the sample may result in argon loss, thus producing a potassium-argon age which is considerably younger than the true geologic age. Loss of radiogenic argon from high temperature diffusion was noted very early in the history of potassium-argon dating (14). Subsequent studies have indicated that some minerals may lose significant amounts of radiogenic argon even at room temperatures. Orthoclase and microcline have been shown to lose argon quite readily (45), and are therefore considered unsuitable for potassium-argon dating. The exact reason for the lack of argon retentivity in these feldspars is not known, since the measured diffusions constants are not large enough to account for the observed loss (42,46). However, it has been shown that the amount of argon loss from microcline is proportional to the degree of perthitization (47). In contrast, other feldspars such as sanidine and anorthoclase appear to be quite suitable for potassium-argon dating (48,49). High temperature

plagioclase, found in volcanic rocks, retains argon completely (50), but low temperature plagioclase in plutonic and metamorphic rock is subject to argon loss (51). Micas usually give ages which are in agreement with other geochronological methods (52), however, biotite apparently loses argon rapidly when heated above a few hundred degrees centigrade (53). Amphiboles seem to be quite suitable for potassium-argon dating (54), hornblende being especially resistant to argon loss even at elevated temperatures (55). Argon determinations on whole-rock samples have become increasingly popular in recent years, especially for the dating of young basalts (33,56). This technique has been successfully applied to lavas in the Hawaiian Islands (57,58). Much of the potassium in basalts is found in the last components to solidify, which are usually the interstitial glass or fine grained feldspars (28). Therefore, whole rock samples should be carefully scrutinized for evidence of alteration of the interstitial material. Alteration of minerals which contain negligible amounts of potassium, such as olivine and pyroxene, should not effect the calculated age.

Frequently it is desirable to separate individual minerals for dating. If the mineral grain size is large enough, hand-picking may be used. Further separations can be made by taking advantage of differences in magnetic

susceptibility and specific gravity. Cleanliness is extremely important during crushing and separation of mineral fractions, since foreign materials, incorporated from the crushing equipment, etc., may seriously affect the final age determination.

6. Argon Diffusion in Minerals

Diffusion is an irreversible process which tends to eliminate concentration differences in a system by the random motion of diffusing molecules. For a completely isotropic material, the process of diffusion can be described by Fick's first law:

$$J = -D \frac{\partial C}{\partial X}$$

where J is the diffusion current, $\partial C/\partial X$ is the concentration gradient, and D is the diffusion coefficient. The change in concentration with time is described by Fick's second law:

$$\frac{\partial C}{\partial t} = D \frac{\partial^2 C}{\partial X^2}$$

These equations are quite generalized. Therefore, in order to use them, it is necessary to state certain restrictions and boundary conditions which describe the physical system under investigation. Because of the extreme complexity of geologic materials, exact solutions to Fick's laws are quite

difficult, if not impossible to obtain at the present time. However, approximate solutions can be obtained through the use of certain simplifying assumptions. The restrictions and assumptions generally used to describe diffusion in minerals are:

a) The mechanism of diffusion can be described by Fick's laws.

b) The mineral grains under investigation are spherical.

c) The diffusion will be isotropic: that is, independent of direction.

d) The diffusing material is homogenously distributed throughout the mineral.

e) The concentration of the diffusing material outside the mineral grain is always zero, or no back diffusion into the grain takes place.

f) The diffusion coefficient is dependent only on the temperature.

For these restrictions, the following solution to Fick's laws has been derived by Carslaw and Jaeger (59).

$$F = 1 - \frac{6}{\pi^2} \sum_{n=1}^{\infty} \frac{1}{n^2} e^{-Dn^2\pi^2tR^{-2}}$$

where R is the radius of the sphere, and F is the fractional loss in time t.

This equation is of limited usefulness, however, since the infinite series only converges at high losses. For low and moderate losses, the following approximate equations have been derived (59):

For $F \leq 10\%$

$$F = \frac{6}{\pi 3/2} \quad (Bt) \qquad \text{where } B = \frac{\pi^2}{R^2} \; D$$

and for $F < 90\%$

$$F = \frac{6}{\pi 3/2} \quad (Bt)^{\frac{1}{2}} - \frac{3}{\pi 2} \; Bt$$

Because of the possibility of diffusional loss of argon from minerals to be dated, much effort has been devoted to determining the diffusion characteristics of argon in rock forming minerals. Difficulties arise in relating laboratory experiments to geologic conditions because very small low temperature losses, which can add up to a sizable total loss over a several million year period, can not be measured in the laboratory. Diffusion studies must be conducted at temperatures of several hundred degrees centigrade, and the data then extrapolated to room temperature. Most minerals are not isotropic with respect to argon diffusion, and thus several diffusion coefficients are observed. In addition, phase transitions of the crystal lattice and lattice imperfections cause the measured diffusion to deviate from the ideal model.

7. Excess Radiogenic Argon

One of the fundamental assumptions of the potassium-argon method is that no radiogenic argon is contained in the sample at the time of formation: any radiogenic argon incorporated into the sample during formation will produce a potassium-argon age which is older than the true geologic age.

The number of reported occurrences of excess radiogenic argon is not sufficient to cast doubt on the general validity of the potassium-argon method, however, the possibility of such an excess should be considered when samples are selected. Excess ^{40}Ar has been reported in many rock-forming minerals: examples include, feldspars, micas, pyroxenes, amphiboles, olivine, and whole-rock basalt. Only those occurrences of excess ^{40}Ar relating to Hawaiian geology will be discussed here. The first anomalous age resulting from excess radiogenic argon in a Hawaiian basalt was reported by McDougall (57), who obtained an age of 8.36 million years from biotite in a rhyodacite from the Waianae Range on Oahu. This age was several million years older than other ages obtained on the lavas from the same range. Subsequent investigations of the rhyodacite by Funkhouser (60,61), showed that the anomalous age was the result of excess radiogenic argon trapped in fluid inclusions, present in grains of biotite

and hornblende. A recent analysis of lava from the 1800-1801 A.D. eruption of Hualalai Volcano on the island of Hawaii, produced an apparent age of over one million years (62).

Ultramafic inclusions in lavas of the alkalic and nephelinic suites in Hawaii have been extensively investigated because of their apparent excess of radiogenic argon. Lovering and Richards (63) dated a clinopyroxene from a pyroxenite (eclogite) xenolith erupted at Salt Lake Crater, Oahu, and obtained a potassium-argon age of 1.4 billion years. This work was confirmed by Funkhouser and Naughton (64) who obtained ages ranging from 3 million years to 3 billion years on several samples of olivine and pyroxene in the Salt Lake xenoliths. Measurement of the helium content of the minerals also produced uranium-helium ages of several million years (64). Salt Lake Crater is less than 500 thousand years old (this research). Funkhouser and Naughton (64) also reported analysis of olivine and pyroxene from dunite xenoliths, which are prevalent in the 1800-1801 Kaupulehu flow of Hualalai Volcano. Potassium-argon ages of these minerals also were as old as 3 billion years. Vacuum crushing of these minerals has been shown to release large amounts of argon and helium (60,65), believed to be held within fluid inclusions in these minerals.

8. Potassium Analysis

Accurate potassium analysis is as important to the potassium-argon method as is argon analysis, and in the case of older samples, may be more difficult than the argon analysis. Several techniques have been employed for potassium analysis as related to the potassium-argon dating method. These are reviewed below.

a) Gravimetric methods

The classical gravimetric methods of postassium analysis have been reviewed in detail by Muller (66). With the perfection of sophisticated instrumental techniques, the gravimetric methods have lost popularity, primarily because they require very careful technique by an experienced analyst. An additional limitation is the requirement of large sample sizes for minerals that are low in potassium. All of the gravimetric methods depend on the quantitative precipitation of an insoluble salt of potassium. Insoluble salts frequently employed include: potassium perchlorate ($KClO_4$), potassium hexachloroplatinate (K_2PtCl_6), potassium silvercobaltinitrite [$K_2Ag(Co(NO_2)_6)$], and potassium tetrephenylboron [$(C_6H_5)_4BK$]. In all of these techniques, rubidium and cesium are coprecipitated with potassium. Unless the concentrations of these elements are insignificant, they must be analyzed by other techniques, or they may be removed by methods such as ion exchange chromatography, prior to precipitation of the potassium salt.

b) Instrumental methods

Flame photometry is the method most frequently used for potassium analysis in laboratories engaged in potassium-argon dating. This method is more convenient than the various gravimetric methods, but is subject to numerous interferences. Other cations, such as sodium, iron, and magnesium can affect the emission intensity, frequently enhancing the potassium emission. Anions such as phosphate and aluminate are known to suppress the potassium emission. Various solution properties such as surface tension and viscosity may also affect the observed emission intensities. These interferences can be reduced by carefully matching the chemical and physical properties of the standards and unknown. However, this is frequently impracticable, since the complete chemical composition of the sample is seldom known. The method of standard addition is also useful in reducing interferences, however, this method greatly increases the time and effort required for an analysis.

The relatively new technique of atomic absorption spectrometry is being used in some laboratories for potassium analysis. When atomic absorption instruments first became commercially available, it was felt that this technique would be relatively free of interferences. Subsequent study has shown, however, that this technique is plagued with many of the same interference problems

associated with flame photometry. The sensitivity of the two methods is about the same for instruments of equal quality, and there is no general agreement as to which method is superior for potassium analysis.

Solid sample, thermal ionization mass spectrometry, using isotopic dilution with ^{41}K, is occasionally used for potassium analysis. The precision of this method depends on the sample matrix, the method of applying the sample to the filament, and even the composition of the filament. This technique is capable of detecting amounts of potassium as small as 10^{-11} grams (66).

Thermal neutron irradiation of ^{41}K produces ^{42}K, which decays to ^{42}Ca with a half-life of 12.4 hours. Measurement of the gamma radiation from ^{42}K provides an extremely sensitive method of analysis. This technique has been successfully applied to the determination of very low concentrations of potassium in silicate rocks (67).

X-ray fluorescence analysis is potentially useful, but infrequently used for potassium analysis. To minimize interferences from other elements, standards which closely match the chemical composition of the unknown are required. Sample homogeneity is an extremely important factor in obtaining good precision.

B. Statement of the Problem

The purpose of this research was to improve the instrumentation and gas extraction system available in this laboratory in order to provide more rapid and precise analysis. These improvements were then applied to the dating of the young volcanic lavas of the Honolulu Volcanic Series, Oahu, Hawaii. These eruptions are believed to range in age from just under a million years to only a few thousand years. It was hoped that lavas under 100 thousand years could be dated with sufficient precision to allow overlap between the potassium-argon method and the carbon-14 method of geochronology. One of the eruptions of this series, Salt Lake Crater, is the source of the ultramafic xenoliths mentioned previously. Since the noble gas content of these xenoliths has been studied by other workers in this laboratory (60,65), this line of investigation was continued in an attempt to provide further information on the possible origin of these materials.

C. Background of the Problem

1. Young potassium-argon age determinations

Until quite recently, one million years was generally considered to be the lower limit for obtaining reasonable precision with the potassium-argon method.

During the past few years, improved instrumentation and techniques have allowed some laboratories to extend their analysis to samples as young as 100 thousand years. Recently McDougall et al. (56) have reported ages younger than 50 thousand years, but these were based on a single argon analysis so the precision is difficult to evaluate. These ages are not in agreement with ^{14}C analysis of wood buried in the lava. The age differences were attributed to excess radiogenic argon in the lava. Samples used by these workers ranged in size from 35-45 grams of solid basalt. Samples of this size are difficult to handle in the extraction system, but more important, the use of such large chunks of lava may produce significant sampling errors.

2. The Honolulu Series

The Honolulu Series comprises about 30 separate eruptions of nepheline basanite, nepheline basalt and melilite nephelinite basalt, which occurred in the south-eastern end of the Koolau Range on Oahu. Geochronological evidence indicates that activity of the Koolau volcano subsided about 2.5 million years ago (57). After an erosional period of over 1.5 million years, secondary eruptions occurred along several rift zones. The locations of the vents and lavas of the Honolulu Series are given in

Figure 2 and Table 2, based on the mapping of these eruptions by Stearns (68).

In the absence of radiometric ages for the Honolulu Series, attempts have been made to group these eruptions between the levels of ancient shore lines in Hawaii during Pleistocene time (69,70). Several different levels of the ocean have been observed in the Hawaiian islands (71,72,73), as a result of advances and retreats of the polar ice caps. Some of these levels may be due to isostatic adjustments of the crust in response to the weight of the Koolau and Waianae Ranges (70). The relative relation of the glacio-eustatic sea levels and ancient shore lines in Hawaii has recently been published by Lum and Stearns (74), and is reproduced in Figure 3. The relations between the various stands of the ocean and the Honolulu Series eruptions, as reported by Winchell (70), are listed in Table 3. A detailed description of the petrology and petrography of the Honolulu Series lavas has been published by Winchell (70).

3. Salt Lake ultramafic xenoliths

Inclusions of garnet peridotite (lherzolite) and garnet pyroxenite (eclogite), present in the tuff at Salt Lake Crater, have been investigated by numerous researchers, most recently by White (75), Jackson (76), and Green (77).

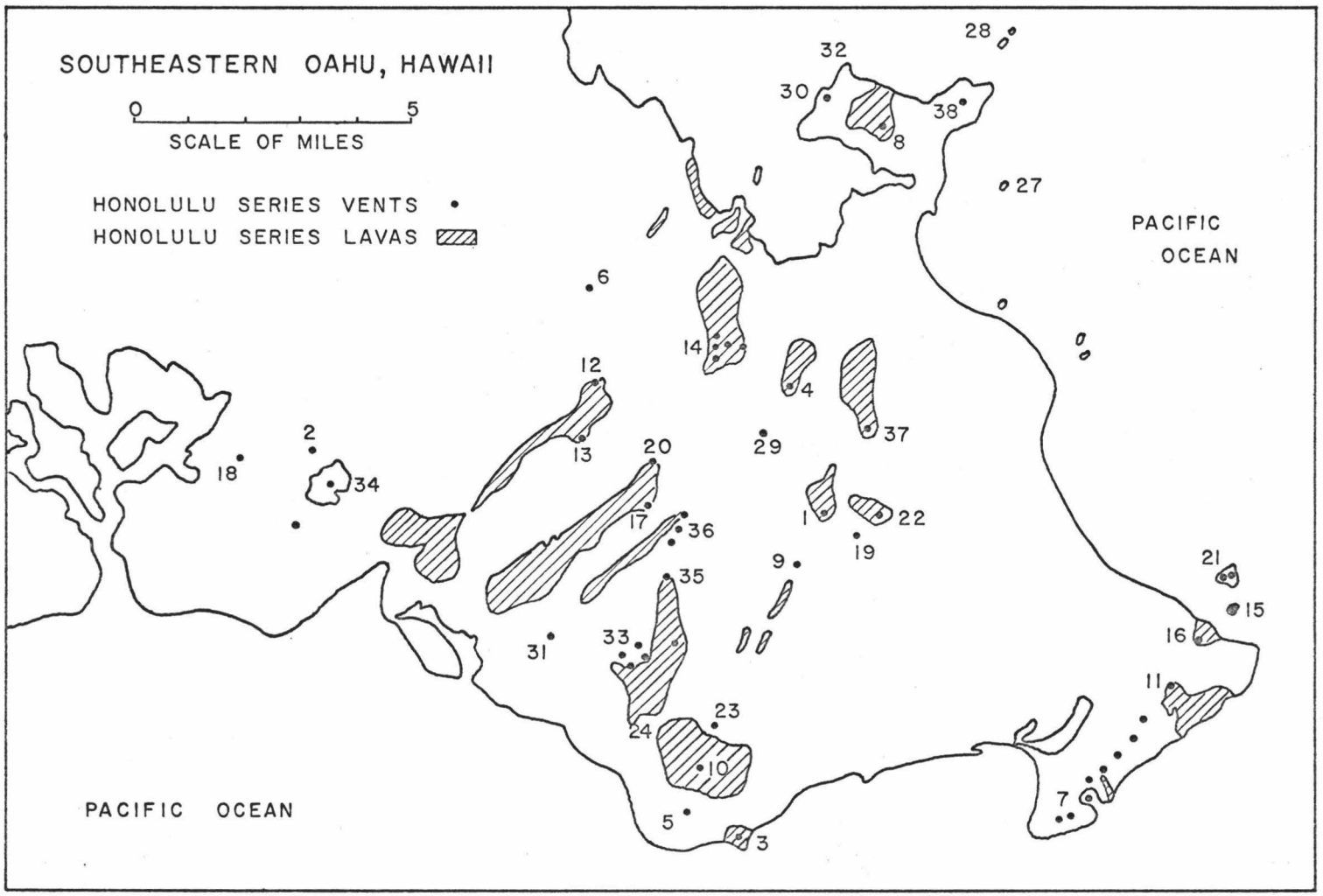

Figure 2: Location of Vents and Lavas of the Honolulu Volcanic Series

Table 2

Vents and Lavas of the Honolulu Series

1. Ainoni
2. Aliamanu
3. Black Point (Kupikipikio)
4. Castle
5. Diamond Head
6. Haiku
7. Hanauma Bay
8. Hawaiiloa
9. Kaau
10. Kaimuki
11. Kalama
12. Kalihi
13. Kamanaiki
14. Kaneohe
15. Kaohikaipu
16. Kaupo
17. Luakaha (south Nuuanu vent)
18. Makalapa
19. Makawao (possibly Koolau)
20. Makuku (north Nuuanu vent)
21. Manana (Rabbit) Island
22. Maunawilli
23. Mauumae
24. Moiliili Quarry
25. Mokapu (north outcrop)
26. Mokapu (south outcrop)
27. Mokolea
28. Moko Manu
29. Pali
30. Pali Kilo
31. Punchbowl
32. Pyramid Rock
33. Rocky Hill
34. Salt Lake Crater (Aliapaakai)
35. Sugar Loaf (Puu Kakea)
36. Tantalus
37. Training School
38. Ulupau Crater

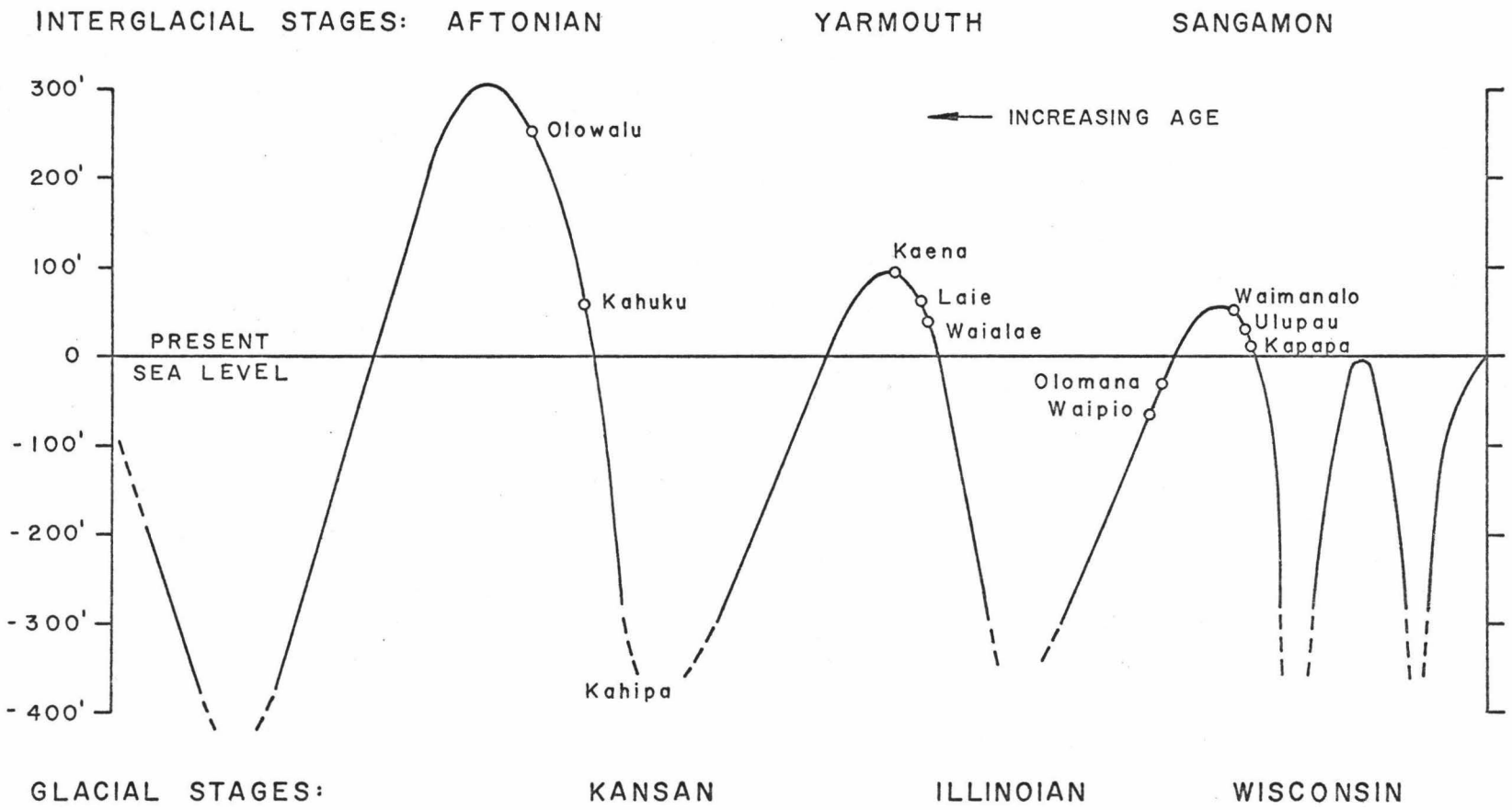

Figure 3 : Relation of Glacio-eustatic Sea Levels and Ancient Shorelines in Hawaii

Table 3

Relationship of the Honolulu Series Eruptions to Ancient Shore Lines in Hawaii

Shore Line	Eruption
Kahipa stand (-300 feet)	Hawaiiloa Pali Kilo Pyramid Rock Moku Manu Ulupau Mokolea
Kaena stand (95 feet)	Kalihi Haiku Rocky Hill Aliamanu Kaneohe Luakaha Makuku Pali Makawao Kaau
Laie stand (70 feet)	Mauumae
Waipio stand (-60 feet)	Salt Lake Makalapa Ainoni Castle Maunawili Training School Diamond Head Kaimuki Black Point Kamanaiki Punchbowl
Kapapa stand (5 feet) and Modern stand	Koko group Tantalus group

The inclusions are predominantly of two types. The lherzolite consists of about 75 percent olivine, 15 percent orthopyroxene, and 10 percent clinopyroxene: the eclogite contains about 75 percent clinopyroxene, 15 percent garnet, and 10 percent olivine (76). However, all gradations occur between the two types. Attempts to explain the origin of these inclusions have led to sharply conflicting opinions: several hypotheses are listed below:

a) The inclusions are clusters of phenocrysts formed within the basaltic magma.

b) The inclusions are fragments of primary mantle material.

c) The inclusions are the infusible residue of primary mantle material, and are therefore not representative of the mantle composition.

Although there seems to be general agreement that these xenoliths are of deep seated origin, the depth and mode of formation has not been unequivocally established. White (75) has proposed a compositional relationship between the xenoliths and their host rock, and has suggested multiple origins for these inclusions. The gradation between the two types of xenoliths, reported by Jackson (76) indicates that the origin of these two types may be inseparable. Roedder (78) has measured the pressure of carbon

dioxide present in the fluid inclusions in Hawaiian xenoliths. He concluded that the gas was trapped in these minerals at depths of 8-16 km. However, it would appear that diffusional losses have reduced the pressure in these fluid inclusions (this research), so the depths calculated by Roedder are too shallow.

II. EXPERIMENTAL

A. Description of the Mass Spectrometer

The mass spectrometer used in this research was a "Reynolds type" single focusing instrument, utilizing a 60 degree magnetic deflection and a 4.5 inch radius of curvature. The tube, magnet, and magnet regulator were purchased from Nuclide Corporation, State College, Pennsylvania. An accelerating voltage of 2KV was supplied by a Fluke Model 412B DC Power Supply (John Fluke Mfg. Co., Inc., Seattle, Washington). The ion collector was a "Faraday cup" type collector, amplified by a Cary Model 31 Vibrating Reed Electrometer (Applied Physics Corporation, Monrovia, California). An ultra high vacuum was maintained in the mass spectrometer tube with an 8 liter/sec. VacIon pump (Varian Associates, Palo Alto, California), which could be isolated from the tube through an all metal, bakable valve (type C, Granville-Phillips, Co., Boulder, Colorado). A more complete description of this instrument, including photographs, has been given by Funkhouser (60).

B. Modifications to the Mass Spectrometer

As mentioned in the introduction, accurate ^{36}Ar measurements require that the instrumental noise be reduced to the lowest level possible. Much of the noise is generated at the friction contact between the Faraday cup and

the electrometer preamplifier, and from variations in the line voltage which affect the output of both the emission regulator and electrometer (79). A brass plug connects the Faraday cup to the pressure contact of the electrometer. This plug was electrolytically silver plated from a silver cyanide bath, to improve electrical conductivity. The entire area surrounding the contact was enclosed in an airtight case constructed of rubber and polyethylene, and filled with dry silica gel. Replacing the silica gel about once a month was sufficient to keep the contact dry. Line voltage regulation was accomplished through the use of a Sorensen Model 1001 Voltage regulator (Raytheon Co., Norwalk, Connecticut) with a regulation accuracy of ± 0.01 percent and response time of 0.1 seconds. The electrometer and emission regulator were operated through this voltage regulator; all other instrumentation was supplied through a constant voltage transformer. These modifications, together with other minor changes, greatly improved the signal to noise ratio of the instrument. Funkhouser (60) reported a noise level of approximately 2 mv, producing a sensitivity (signal to noise ratio of 1:1) of about 7×10^{-10} std cc for argon analysis on this instrument. After the above modifications, the noise level was reduced to about 0.1 mv, producing a sensitivity of 5×10^{-11} std cc of argon.

The major contribution to improving the precision of analysis with this instrument was the installation of a new recorder. The recorder is a Leeds and Northrup Model G Speedomax 10 inch recorder, which was rebuilt and modified at the Analytical Mass Spectrometry Section, Analytical Chemistry Division, National Bureau of Standards. Modifications included the incorporation of an expanded scale circuit which allows any 10 percent segment of the chart to be expanded full scale. With this circuit the operator may expand that 10 percent portion of the chart containing the top of the mass spectral peak to full scale, thus allowing four significant figures to be read directly from the chart.

C. Construction and Description of the Gas Extraction System

1. Limitations of conventional systems

The gas extraction systems used previously in this laboratory, and still used in most laboratories conducting potassium-argon age studies are constructed of pyrex glass tubing, usually 10mm to 15mm in diameter. A vacuum is maintained through the use of an oil or mercury diffusion pump. When helium is analyzed, pyrex glass is undesirable because of its high helium permeability. Practical considerations usually limit the size of the glass tubing to 20mm or less. The weight of larger tubing, unless properly

supported, may produce strains which can lead to breakage, but more important, glass blowing and properly annealing large diameter tubing requires skills possessed by few amateur glass blowers. The length and diameter of the tubing is extremely important in determining the pumping and gettering speed of the vacuum system, especially at low pressures, where the mean free path for collision between molecules is larger than the tubing dimensions. Dushman (80) has derived the following approximate equation for calculating the conductance for molecular flow of a gas through a cylindrical tube:

$$F = \frac{3.64\pi r^2}{1+3/8(L/r)} \left[\frac{T}{M}\right]^{\frac{1}{2}} \text{ liters sec}^{-1}$$

where F is the conductance, L and r are the tubing length and radius in cm, T the temperature in degrees Kelvin, and M the molecular weight of the gas in grams per mole. For a cylindrical tube 1 cm in diameter and 100 cm long, the calculated conductance for air at 25°C is 0.12 liters/sec. If the tube diameter is increased to 4 cm, the conductance is increased to 7 liters/sec. Therefore, increasing the tubing diameter by a factor of four increases the conductance, and thus the pumping speed, by a factor of about 60.

As mentioned in the introduction, gettering of the active gases is usually accomplished in two steps. After one gettering step is completed, the gases are moved to a

second portion of the vacuum system to complete the removal of active gases. This multistep cleanup can take as long as 20 hours (60), part of this time being required to move the gases from one part of the vacuum system to another through small diameter tubing. Some laboratories have been able to reduce this time to about 4 hours for some samples (81). Lengthy gas purification times not only reduce the number of samples which can be analyzed, but also can increase the air argon contamination, entering the system through small leaks, present to some extent in nearly all vacuum systems.

Most laboratories use oil or mercury diffusion pumps to maintain a high vacuum in the extraction system. These pumps require cold traps, usually filled with liquid nitrogen, to keep the oil or mercury from backing up into the extraction system. Power failures, or absent-minded failure to fill the cold traps can result in contamination to the extraction system which is often difficult to remove, even with a high temperature baking of the system.

2. General design and construction of new extraction system

Part of this research involved the design and construction of a gas extraction system which would overcome many of the disadvantages inherent in the more conventional systems. To reduce the blank for helium analysis,

the system was constructed entirely of type 304 stainless steel, except for the cold fingers and ionization gauges, which were quartz and nonex respectively. This system is shown schematically in Figure 4 and is photographed in Figure 5. The heart of the extraction system is a 50 liter per second titanium sublimation pump purchased from Varian Associates, which replaces the CuO and titanium getters employed in other extraction systems. The pump operated by thermally subliming titanium from filaments heated by a current of 40-50 amperes. The freshly sublimed titanium forms a film on the walls of the pump chamber. Active gas molecules impinging on the walls of the pump react with the film to form stable titanium compounds. Since the walls of the pump are water cooled, re-emission of the gases, especially hydrogen, are substantially reduced. Because of the high pumping speed for hydrogen (equal to the pumping rate for nitrogen), the need for a copper oxide getter is eliminated. The high temperature required to sublime the titanium should be sufficient to "crack" any hydrocarbons. A 400 liter molecular sieve trap (Linde 13-X molecular sieve) was placed between the sample melting oven and the sublimation pump to remove water vapor and heavy hydrocarbons. The capacity of the trap (400 L) is defined as the number of liters of air at 50 percent relative humidity which can be pumped from atmospheric pressure through the trap before the system is

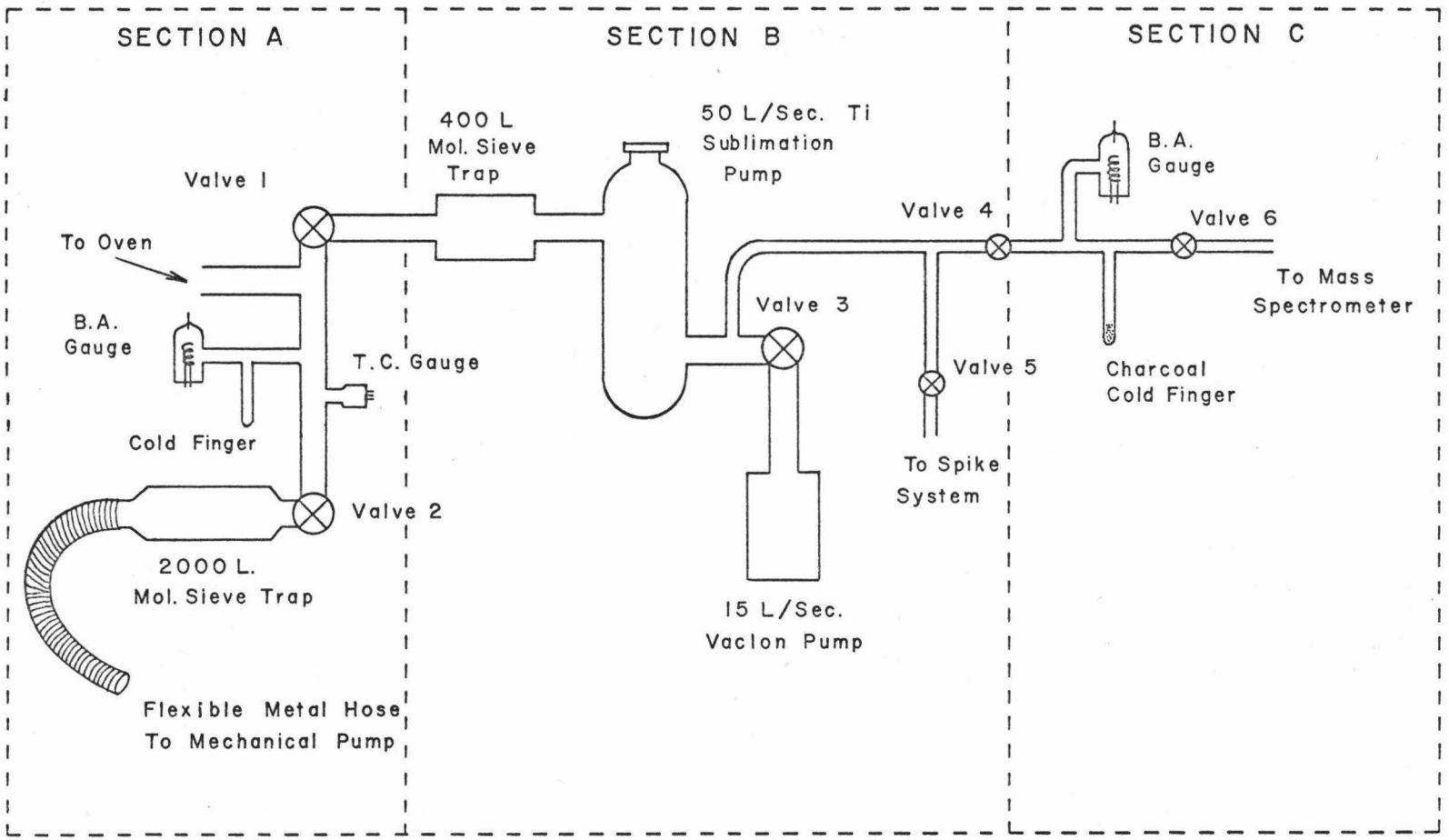

Figure 4: Gas Extraction and Purification System

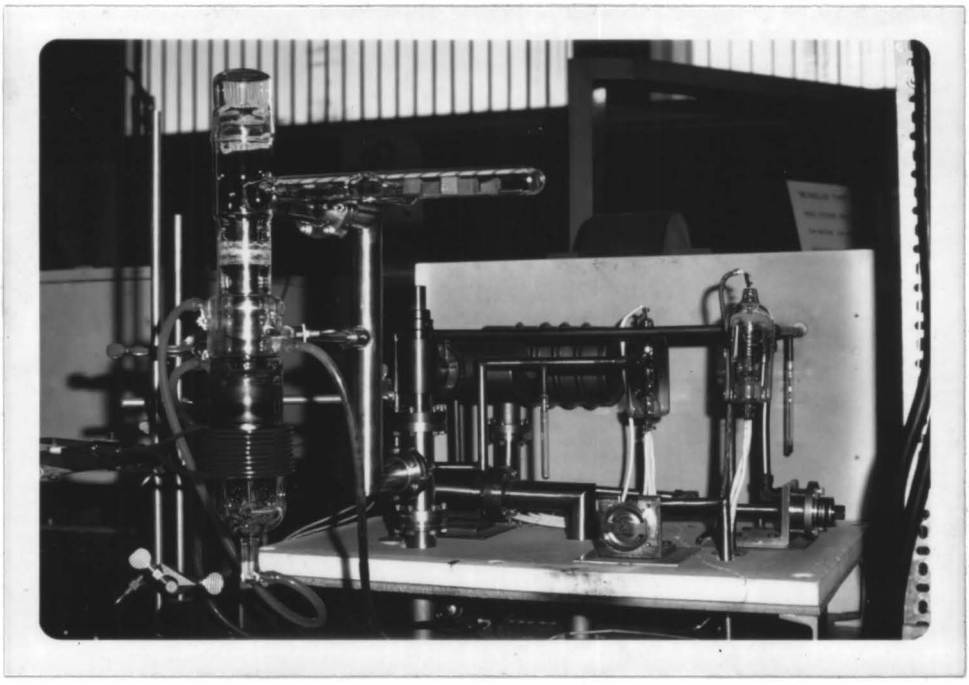

Figure 5

Gas Extraction and Purification System

limited to a base pressure equal to or exceeding 1.5×10^{-3} torr. Rough pumping was accomplished through a 2000 liter molecular sieve trap connected to a mechanical pump by way of a flexible metal hose. This rough pumping system was capable of pumping the extraction system from atmospheric pressure to 1×10^{-5} torr without baking the system, and to a pressure of less than 1×10^{-6} torr after an overnight bakeout at 250°C-300°C. After rough pumping, a 15 liter per second VacIon pump (Varian Associates) reduced the pressure in the extraction system to below 1×10^{-8} torr. Several components were commercially purchased and were connected by high vacuum flanges sealed with copper gaskets. Other components were fabricated in the laboratory from 1½ inch and 5/8 inch seamless stainless steel tubing. Laboratory fabricated components were joined with a "silver brazing type" silver solder (EutecSil 1020FC, Eutectic Welding Alloys, Corp., Flushing, N.Y.). This silver solder has a tensile strength of 85,000 PSI, and a melting point of 565°C. Whenever possible, soldered joints were cleaned by the following procedure:

a) Removal of loose oxidation with wire brush or emery paper.

b) Degrease with trichlorotrifluoroethylene.

c) Hydrochloric acid dip:solution of 1:1 HCl in water at 70°C.

d) Tap water rinse: copious amounts of water to remove all traces of hydrochloric acid.

e) De-ionized water rinse.

f) Methanol rinse: reagent grade.

g) Air drying at 130°C.

For those instances where the above cleaning procedure could not be used, the tubing was purged with oxygen free helium during soldering to reduce oxidation. The extraction system was mounted on a sheet of magnesite "Maranite" insulation (Johns Manville & Co.) and was fitted with a removable cover of the same material. Four 500 watt quartz infra-red heating lamps (General Electric Co.) were mounted inside the cover to allow the extraction system to be baked at temperatures up to 450°C.

3. Advantages of the new system

The extensive use of stainless steel has allowed the use of 1½ inch diameter tubing throughout the pumping sections of the extraction system. This has resulted in faster pumping and gettering rates, and a lower base pressure, which reduces the air argon contribution from the extraction system.

When the fusion oven is opened to the atmosphere to change samples, valve 1 (Figure 4) can be closed, thus keeping sections B and C of the extraction system under

high vacuum. The fusion oven (section A) can then be rough pumped through valve 2 to a pressure of 10^{-5} torr in about an hour. The combination of 1½ inch diameter tubing, large molecular sieve trap, and leak-free metal hose to the mechanical pump, provide an extremely fast pump-down time as shown in Figure 6. Preliminary rough pumping of section A before opening this section to the remainder of the extraction system provides maximum cleanliness to the system. Sections B and C are exposed to the atmosphere only when the sublimation pump filaments are changed (every one or two months). As a result of minimum exposure to the atmosphere, a vacuum of less than $1x10^{-8}$ torr, and often as low as $1x10^{-9}$ torr could be maintained in these sections. The atmospheric argon contribution from these two sections was about $5x10^{-10}$ std cc, only about 0.1 percent of the total atmospheric argon present in a typical sample analysis. The extraction system was sufficiently leak free as to show a pressure increase of less than $2x10^{-8}$ torr per hour when isolated from the pumps.

When large samples or rock are melted, copious amounts of gas may be released, especially during the early stages of melting. Unless this gas is quickly removed from the sample area, the high localized pressure may induce gas ionization caused by the radio frequency

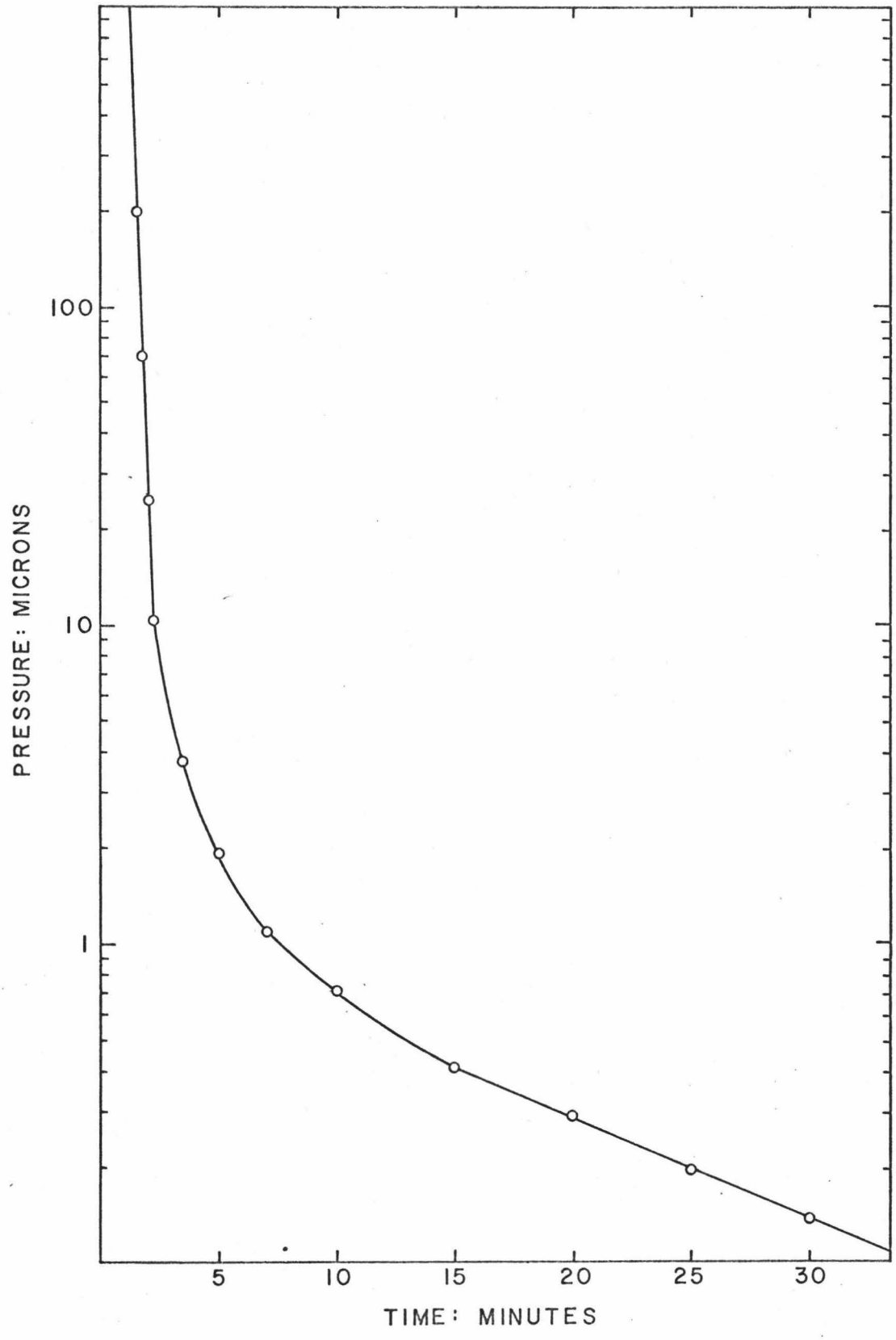

Figure 6: Pumping Speed of Section-A of the Extraction System

field generated by the induction heater. Such "glow-discharges" have been a problem with extraction systems used previously in this laboratory (82). In addition to being inconvenient, these discharges may irreversibly drive some of the radiogenic argon into the walls of the oven. The large diameter tubing from the sample oven to the sublimation pump, which is operated continually during sample melting, has completely eliminated the problem of gas discharges.

Conventional constant temperature getters are limited to a constant gettering rate, usually limited by the rate at which the gas can diffuse to the gettering material. The sublimation pump is more versatile, since the rate of titanium sublimation can be varied: sublimation rates as high as $1x10^{18}$ atoms of titanium per second can be obtained. This allows the operator to increase the rate of sublimation when large amounts of active gases are present in the extraction system. For pure mineral separations, and relatively clean whole-rock samples, the total time required for gettering with this extraction system is often less than 30 minutes. Even samples containing considerable amounts of active gases seldom require more than an hour of gettering. The total time for argon extraction and purification is usually less than two hours, only one tenth of the time required for the same operation on extraction systems previously used in the laboratory.

D. Preparation and Calibration of the Argon and Helium Spikes

Isotopic dilution mass spectrometry requires that a precisely known amount of a pure isotope be added to the sample prior to analysis. In the case of gas analysis, this isotopic tracer is usually dispensed through a pipet of known volume attached to a reservoir filled with the tracer gas. Usually the reservoir is a glass bulb and the pipet is constructed from two glass stopcocks (83). The possibility of breakage and of atmospheric gases diffusing into the reservoir are disadvantages to this spike system. These two disadvantages were eliminated in this research by constructing the spike system entirely of stainless steel. The gas pipets were constructed from two stainless steel Nupro SS-4H bellows valves, welded together in a back-to-back configuration to contain a volume of slightly less than one cm^3. These valves are bakable open to 350°C and closed to 250°C. A photograph of the spike system is shown in Figure 7.

Each time a spike is removed from the reservoir, the amount of gas in the bulb is depleted by an amount δ, called the depletion constant. The depletion constant is given by:

$$\delta = \frac{V_p}{V_p + V_r}$$

Figure 7

Argon and Helium Spike System

where V_p and V_r are the volumes of the pipet and reservoir respectively. If these volumes are known, then the amount of gas in any spike can be calculated from the following equation:

$$T = T_o e^{-\delta X}$$

where X is the tracer number and T_o is a constant dependent on the pressure of the gas in the reservoir. The value of T_o can be calculated either from direct pressure measurements or from comparison with a rock of known radiogenic argon content. The latter method was used in this research.

1. Argon-38 Spike calibration

The argon-38 spike pipet was calibrated by the following procedure. The pipet was attached to a vacuum system of accurately known volume (62.73 ± 0.06 Cm^3) which was equipped with a quartz fiber, precision pressure guage (Texas Instruments Co.). The pipet was filled with carbon dioxide at atmospheric pressure and then expanded into the vacuum system. From the known volume of the system, and the atmospheric pressure as read on a mercury barometer, the volume of the pipet could be calculated. The average of eight determinations gave a pipet volume of 0.855 ± 0.001 cm^3 (this and all other errors reported in this paper are for the 68 percent confidence level). The

volume of the reservoir was determined gravimetrically with water to be 1711.5 ± 0.4 cm^3. The value of T_o was calculated from comparison with the gas content of U.S.G.S. inter laboratory standard muscovite, P-207. The argon content of this standard has been determined to be $2.824 \pm 0.054 \times 10^{-5}$ std cc/gm, based on 118 analyses from over 20 laboratories (84). The average of eight determinations with P-207 gave a value for T_o of $3.968 \pm 0.045 \times 10^{-7}$. These determinations are listed in Table 4. Based on the measured parameters of the ^{38}Ar spike system, the standard volume of any spike can be expressed by the following equation:

$$^{38}Ar = (3.968 \times 10^{-7}) e^{-(4.993 \times 10^{-4})X} \text{ std cc}$$

where X is the number of the spike being removed.

The spike reservoir was attached to a vacuum system and pumped to a pressure of less than 1×10^{-7} torr, a sample of ^{38}Ar was then admitted to the vacuum system and allowed to equilibrate with the reservoir: The pipet valves were then closed and the pressure in the vacuum system measured with a McLeod gauge. The sample of ^{38}Ar was originally purchased from The Institute of Physical Chemistry, University of Zurich, Switzerland. The original sample was divided into six aliquots and sealed in glass tubes by Funkhouser (60): One of these aliquots was used

Table 4

Argon-38 Spike Calibration with P-207

measured ^{38}Ar std cc	spike number	calculated T_o
3.891×10^{-7}	16	3.922×10^{-7}
3.915×10^{-7}	25	3.964×10^{-7}
3.849×10^{-7}	62	3.970×10^{-7}
3.833×10^{-7}	63	3.956×10^{-7}
3.775×10^{-7}	76	3.921×10^{-7}
3.756×10^{-7}	102	3.952×10^{-7}
3.805×10^{-7}	103	4.006×10^{-7}
3.734×10^{-7}	164	4.052×10^{-7}

TABLE 5

Helium-3 Spike Calibration with R-1659

measured ^{3}He std cc	spike number	calculated T_o
4.80×10^{-7}	18	4.82×10^{-7}
4.65×10^{-7}	27	4.67×10^{-7}
5.07×10^{-7}	28	5.09×10^{-7}
4.84×10^{-7}	54	4.89×10^{-7}
4.64×10^{-7}	55	4.69×10^{-7}
4.82×10^{-7}	83	4.89×10^{-7}
4.60×10^{-7}	84	4.67×10^{-7}

to fill the ^{38}Ar reservoir. The original assay of the sample, determined at The University of Zurich, was reported as:

$$0.01^{5}\ \%\ ^{40}Ar$$
$$99.98^{2}\ \%\ ^{38}Ar$$
$$0.00^{3}\ \%\ ^{36}Ar$$

Analysis of the contents of the ^{38}Ar spikes from the reservoir gave the following assay:

$$0.09^{2}\ \%\ ^{40}Ar$$
$$99.90^{7}\ \%\ ^{38}Ar$$
$$0.00^{1}\ \%\ ^{36}Ar$$

The slight increase in ^{40}Ar is understandable considering that the sample has been expanded into a vacuum system at least twice, and has been standing in a glass tube for several years. A correction of 4×10^{-10} std cc of ^{40}Ar was applied to all argon measurements to account for the excess of this isotope in the spike.

2. Helium-3 spike calibration

The procedures used to determine the volume of the ^{3}He pipet and reservoir were identical to those used for the ^{38}Ar spike system. The volume of the ^{3}He pipet was calculated to be 0.859 ± 0.002 cm^3; the reservoir contained a volume of 4714 ± 0.5 cm^3. The value of T_o for this spike

system was determined from comparison with samples of M.I.T. Standard Zircon R-1659. The helium content of the zircon was assumed to be $9.62 \pm 0.33 \times 10^{-3}$ std cc/gm as reported by Damon (30). Because of the high melting point of zircon (ca. 2500°C) the sample could not be melted with the radio-frequency heater. It was found that if a few grams of rock were melted in the crucible prior to analysis of the zircon, the silicate melt acted as a flux to dissolve the sample. Heating the zircon and silicate melt for 15 minutes at a temperature of 1800°C was sufficient to remove all of the helium. Repetition of this heating schedule produced no further release of helium. The large amount of helium in this standard is a major disadvantage to its use. To keep the amount of gas within the limits of the mass spectrometer, sample sizes could be no larger than 100mg. The zircon crystals were about 1 mm in diameter, so only a few grains were used for each analysis. Sample inhomogeneity is probably the cause of the relatively larger standard deviation (± 3%) for calibration of the ^{3}He spike. Calibration of this spike with the zircon yields an average value for T_o of $4.82 \pm 0.14 \times 10^{-7}$. These determinations are listed in Table 5. From the measured parameters of the ^{3}He spike system, the amount of gas in any spike can be expressed by the following equation:

$$^{3}He = (4.82 \times 10^{-7}) e^{-(1.822 \times 10^{-4})X} \text{ std cc}$$

where X is the number of the spike being removed.

The spike reservoir was filled by the same method used for filling the ^{38}Ar spike system. The sample of helium-3 was purchased from The Monsanto Research Corporation and was assayed to contain:

$$99.99\ \%\ ^{3}He$$
$$0.01\ \%\ ^{4}He$$

Analysis of the contents of the ^{3}He spikes from the reservoir gave the following assay:

$$99.8 \pm 0.1\ \%\ ^{3}He$$
$$0.2 \pm 0.1\ \%\ ^{4}He$$

The increase in ^{4}He is probably the result of contamination of the sample during filling of the reservoir from the glass vacuum system.

3. Air argon spike calibration

A spike of air argon was prepared to allow calibration of the mass spectrometer for isotopic bias. The spike reservoir was filled by the same procedure used for filling the other spike systems. The air argon was a reagent grade sample obtained from Air Reduction Company. The $^{40}Ar/^{36}Ar$ ratios of spikes taken from the air argon reservoir were identical to the ratios obtained by analyzing a portion of air admitted to the extraction system from the room.

E. Sample Preparation

1. Sample collection

Most of the samples analyzed in this research were collected by the author. Some samples were obtained from faculty members of the Geology Department, University of Hawaii, and one sample (Punchbowl) was obtained from the Honolulu Board of Water Supply. All samples used in this research are described in Appendix B.

Fresh samples of many of the Honolulu Series lavas were extremely difficult to locate. Many of the lavas are either covered with dense vegetation, or with housing developments. Exposures in stream beds or road cuts were often highly weathered, and thus unsuitable for dating. Although the progress of man has destroyed many potential sampling sites, this same progress provided several samples from sewer and building excavations.

The suitability of each sample for potassium-argon analysis was determined from petrographic examination of a thin section. Samples which showed extensive alteration were discarded. All of the melilite nephelinite lavas examined contained some zeolites, usually between 1 percent and 3 percent by volume. During excavations for a new engineering building on The University of Hawaii Campus, the author had the opportunity to examine several tons of

rock from the Sugar Loaf flow. In spite of a persistent and thorough search, no lava could be found that was completely zeolite free. Those portions of the samples collected which contained the minimum amount of zeolites were used for analysis.

2. Preparation of whole-rock samples

Because of the young ages of the samples analyzed, whole-rock samples were used for argon analysis to minimize surface adsorbed air argon contamination. Sampling errors, as a result of inhomogeneous distribution of potassium in the lava, are a serious disadvantage to using solid blocks of whole-rock basalt. However, it was felt that if the samples were crushed to a size that would assure sample homogeneity, the analytical errors resulting from the increased air argon contamination would be much larger than the sampling errors expected from the use of blocks of lava.

A block of lava approximately 2cm x 2 cm x 12 cm was usually cut from the center of a large piece of lava with a diamond saw. This block was then subdivided into cubes approximately 2cm on a side. The first, third, and fifth cubes were saved for argon analysis. The second and fourth cubes were combined for potassium analysis, and the sixth cube was used for the preparation of a thin section.

Samples used for argon and potassium analysis were cleaned with distilled-deionized water in an untrasonic cleaner. Ultrasonic cleaning was repeated until the water remained clear: This usually required three to four 2 minute cleaning periods. The samples were then dried in air at 130°C for about 1 hour. The two samples for potassium analysis were then crushed to less than 100 microns, thoroughly mixed, and placed in a bottle for future analysis.

3. Mineral separations

Mineral separations were conducted only on the ultramafic xenoliths from Salt Lake. Minerals from these nodules were hand picked to obtain maximum purity. Additional purification, when necessary, was made on a Franz Isodynamic Magnetic Separator. By careful hand picking, several grams of olivine, enstatite, chrome diopside, augite, and pyrope were separated with a purity of 99 percent or greater. Purity is especially important for the helium and argon analysis of olivine from these xenoliths. The pyroxenes contain about three orders of magnitude more argon and helium than does olivine. Therefore, analysis of an olivine sample containing 0.1 percent pyroxene contamination will give an apparent noble gas content of twice the true amount.

4. Particle size separations

The minerals from the Salt Lake xenoliths were crushed and separated according to grain size by use of sieves of varying pore size (Tyler series sieves). The minerals were grouped into ranges of -40+60 mesh, -60+80 mesh, -80+100 mesh, etc., down to 400 mesh (38 microns). Particle sizes less than 38 microns were separated according to their rate of settling in water. Fractions sieved between -150+200 mesh, -200+250 mesh, -250+325 mesh, and -325+400 mesh were allowed to settle in a 80 cm column of distilled water. The time required for the first and last groups of particles to reach the bottom of the tube was measured with a stop watch. From this data, a linear log-log plot was constructed for the settling rate vs. particle size. An extrapolation of this plot was used to calculate the settling time for particles in the ranges of 30 to 40 microns, 20 to 30 microns, 10 to 20 microns, and 1 to 10 microns. Particles of augite were separated into these ranges for a study to be reported later in this paper.

F. Potassium Analysis

1. Sample preparation

The methods previously used to decompose rock samples in this laboratory involved the reaction of the

sample with a mixture of hydrofluoric and sulfuric acids (60), or hydrofluoric and perchloric acids (65). The sample and acids were placed in a platinum crucible and heated overnight on a hot plate. In addition to the lengthy time required for decomposition, the possibility of contamination from air-borne material entering the crucible, and potassium loss from volatilization and spattering were disadvantages of these methods. In addition, the high salt concentrations, produced by relatively large quantities of concentrated acid needed to decompose the samples, produced several matrix effects including signal suppression and instability.

A new method for sample decomposition has been used in this research. The techniques used are almost identical to those proposed by Bernas (85). The sample for potassium analysis, which had been previously ground to less than 100 microns (see section E2), was split with a mechanical sample splitter to obtain four samples of 100-150 mg size. Each sample was placed in a Teflon lined stainless steel "pressure cooker" type container. The sample was moistened with distilled deionized water and 3 ml of hydrofluoric acid (48%) was added. The decomposition vessel was sealed with a screw cap containing a Teflon sealing disk and placed in an oven at about 110°C. The sample was usually decomposed within 30 minutes, but one hour was allowed to

insure complete decomposition. The pressure build-up within the airtight reaction vessel apparently accelerates the rate of decomposition, and the closed container eliminates the possibility of sample loss or contamination. After decomposition, the reaction vessel was allowed to cool to ambient temperature before being opened. The decomposed sample was diluted with 4-6 ml of distilled deionized water followed by the addition of 2.8 grams of boric acid. After stirring to dissolve the boric acid, an additional 5-10 ml of distilled deionized water was added; at this stage, all precipitated fluorosilicates and metal fluorides should dissolve. The solution was then quantitatively transferred to a 100 ml polyethylene volumetric flask, and diluted to volume with distilled deionized water.

2. Sample analysis

Samples were analyzed with a Perkin-Elmer Model 303 atomic absorption spectrophotometer, using an air-acetylene flame. It was found, contrary to the report by Bernas (85), that the hydrofluoric acid-boric acid matrix caused some suppression of the potassium absorption when samples were run directly from the solutions prepared above. To eliminate this, two dilutions were prepared from the original solutions in the following manner. Pairs of

solutions were prepared by pipeting 5 ml aliquots of the original solution into each of two 50ml volumetric flasks. An aliquot containing 3 mg of lithium was added to each flask to enhance the potassium absorbtivity. To one of the flasks, an additional 10 micrograms of potassium was added. Both flasks were then diluted to volume with distilled deionized water. The unknown sample and unknown sample plus standard addition were then analyzed by atomic absorption spectrophotometry. The potassium content was then calculated by standard procedures, described in several instrumental analysis textbooks (86). To insure proper instrumental response, a set of controls were run daily. The composition of the controls were as follows:

1. blank containing $HF-H_3BO_3$.
2. blank plus 10 micrograms of K.
3. blank plus 40 micrograms of K.
4. blank plus 50 micrograms of K.

G. Argon Analysis

1. Procedure for argon extraction

Samples to be analyzed were placed in the side arm of a quartz and pyrex water cooled oven. This oven is shown in Figure 8. The lower portion of the oven was equipped with two water cooling jackets to reduce the diffusion of helium into the extraction system. Ovens

Figure 8

Gas Extraction Oven

with single water jackets have been used previously in this laboratory (65), but since quartz conducts heat along its length, the quartz above the water jacket often reached a temperature of about 60°C during fusion of the sample. It was found that by adding a second, independent water jacket above the first, this problem was eliminated and the helium blank was reduced by about 25 percent. The water flow to the jackets was connected in series, flowing first through the upper jacket and then through the lower jacket at a rate of about 2 liters per minute. A molybdenum crucible supported on a molybdenum rod was placed in the oven at a level even with the center of the lower water jacket. Samples could be pushed one at a time from the side arm into the crucible, being directed by a molybdenum funnel suspended above the crucible. Movement of the samples in the side arm was accomplished by placing a small bar magnet inside the side arm with the samples. This small magnet was used to push the samples by using a second magnet external to the vacuum system.

As mentioned previously, the pumping system was capable of producing a high vacuum in a relatively short time. However, because of the need for an extremely low air argon background, the samples and oven were baked overnight at about 200°C. Even though the pressure could be reduced to below 1×10^{-8} torr in less than two hours

after pumping was started, degassing of air argon from the samples and walls of the oven produced an extremely high air argon background. After overnight baking, the load coil of a 5 KW radiofrequency induction heater (Model T-5-3-KC-L-S, Lepel High Frequency Laboratories) was placed around the oven to allow degassing of the molybdenum crucible.

Before melting each sample, a blank was run, duplicating all procedures used during an actual analysis except for admitting a ^{38}Ar spike into the extraction system. The blank served a dual purpose: to determine the air argon contamination contributed by the extraction system, and to make sure that no excess of either ^{36}Ar or ^{40}Ar was present. The air argon present in a blank determination was usually in the range of $1x10^{-8}$ std cc. Larger amounts of air argon indicated that either a small leak was present in the vacuum system, or that additional baking of the samples and oven was needed. Since very small amounts of radiogenic argon were released from the samples analyzed, it was extremely important that no excess of any of the argon isotopes were present in the extraction system. If the blank determination proved satisfactory, a sample was dropped from the side arm of the oven into the molybdenum crucible. Valve #3 to the VacIon pump (Figure 4) was closed, a ^{38}Ar spike was admitted

to the extraction system, and liquid nitrogen was placed on both cold fingers. The cold finger in section A was used to collect carbon dioxide and water. The cold finger in section C contained activated charcoal to collect argon and the active gases.

The sample was heated with the radio frequency induction heater, starting at a low temperature to allow surface absorbed gases to be removed and pumped away before the sample started to melt. The heating schedule was somewhat variable, depending upon the particular sample, but was generally as follows:

1. 70% of maximum power - on 1 min, off 30 sec.
2. 80% of maximum power - on 1 min, off 30 sec.
3. 90% of maximum power - on 1 min, off 30 sec.
4. 95% of maximum power - on continuously.

The heating time at 95 percent power was dependent on the particular sample and on the total amount of rock in the crucible. Usually the sample started to melt after about 1 min of heating at 95 percent power; complete melting was accomplished in about 5 min. The progress of melting could be observed through the top of the oven with the aid of a mirror. When the sample showed no further signs of degassing, an additional five minutes of heating was allowed to insure complete gas removal. During melting of the sample, gases were collected continuously

on the cold fingers, and the sublimation pump was operated continuously at a current of 45 amps. From Figure 4, it can be seen that the active gases had to pass through the sublimation pump before reaching the charcoal finger. Thus, much of the gettering was accomplished during the gas extraction process. Studies on solidifying rock melts (87) have indicated that noble gases may be incorporated into the melt during solidification: The amount of incorporation being dependent on the partial pressure of the gas over the melt. Calculations based on the maximum argon partial pressure to be expected in the extraction system, show that gas losses from the mechanism would be insignificant (less than 10^{-12} std cc). However, to eliminate this as a possible source of argon loss, the crucible was allowed to cool to below 600°C before the gases were expanded back into the extraction system for gettering.

Two sizes of ovens were used during this research. A large oven containing a 1.5 inch diameter crucible was used for analysis of the Honolulu Series lavas, and was capable of obtaining a temperature of 1500-1600°C as measured with an optical pyrometer. An identical but smaller oven, containing a 3/4 inch diameter crucible was used for analysis of the minerals in the Salt Lake xenoliths. The smaller oven allowed samples to be heated

to over 1800°C; this higher temperature was required to melt olivine.

2. Procedure for diffusion studies

In order to study the diffusion characteristics of argon and helium in the minerals from the Salt Lake xenoliths a nickel oven was constructed. The oven consisted of a nickel tube 1½ inch in diameter and 12 inches long. A nickel plate was welded to the bottom of the tube and a Kovar to pyrex seal was silver soldered to the top. Copper water cooling coils were soldered to the upper portion of the nickel to keep the nickel to Kovar and Kovar to pyrex seals cool. The pyrex portion of the oven contained a side arm similar to that present on the fusion ovens described previously. The sample was wrapped in nickel foil and attached to a bar magnet in the side arm by means of a 14 inch piece of 24 gauge nicrome wire. With this arrangement, the sample could be lowered into the oven and quickly pulled out of the oven by activating the bar magnet with a second magnet external to the vacuum system. The nickel oven was heated with a nicrome wire furnace at a temperature of 1100°C. The temperature was measured with a chromel-alumel thermocouple attached to the outside of the nickel tube. The thermocouple was calibrated to within ± 3°C with a platinum versus platinum + 10 percent rhodium thermocouple, measured at

The National Bureau of Standards to produce an E.M.F. of 10.743 mv (reference junction: 0°C) at 1100°C. During heating of the sample, the temperature was maintained to within ± 10°C of 1100°C. A blank determination was run before each sample analysis, primarily to determine the helium blank which must be subtracted from the total helium found from the sample heating. If the blank was satisfactory, the oven was allowed to stabilize at 1100°C, and the sample was lowered into the nickel oven. At the end of 60 minutes, the sample was quickly pulled out of the oven. The procedures used for gettering, collection, and analysis of the gases was identical to those used for the sample fusion experiments.

3. Procedure for gas purification

After extraction of the gases from the sample, the liquid nitrogen was removed from the charcoal cold finger (Figure 4, Section C) allowing the collected gases to expand back into the extraction system. The time required to getter the system free of active gases was quite variable, depending on the particular sample. It was necessary to getter the pressure in the extraction system to below 5×10^{-7} torr, and preferably to 1×10^{-7} torr, if a good mass spectrometric analysis was to be obtained. The minerals from the ultramafic xenoliths were quite clean

with respect to active gases, and could be gettered to a pressure of $1x10^{-7}$ torr in about one-half hour. Some of the Honolulu Series lavas, particularly those from the Koko rift zone, were also quite clean and could be gettered to a low pressure in a short period of time. However, many of the Honolulu Series lavas, especially the melilite nephelinite lavas, contained large amounts of active gases. Ten gram samples of these lavas were sufficient to raise the initial pressure in the extraction system to above 10^{-3} torr. At pressures this high, the gases adsorb on the walls of the extraction system. As the gases in the system are removed by gettering, the materials adsorbed on the walls slowly desorb, thus preventing a low pressure from being obtained. Such samples often required 1 to 3 hours of gettering before a pressure of $5x10^{-7}$ torr could be reached. The large amount of active gases present in some samples may be due to incorporation of atmospheric gases in microscopic cavities in the lava at the time formation took place. This is based on the observation that large amounts of active gases were often accompanied by large quantities of air argon, and the amount of both active gases and air argon was quite variable among different samples of the same specimen of lava. For some flows, as many as four samples were melted before one was found to be clean enough to warrant an age calculation.

After gettering to a sufficiently low pressure, liquid nitrogen was again placed on the charcoal finger to collect the argon. It was found that argon could be quantitatively collected on the charcoal in 30 minutes: 40 minutes was allowed to insure complete collection. Studies using tracers of ^{38}Ar and ^{3}He showed that no loss of argon or helium occurred during any of the above gettering or collection steps.

4. Mass spectrometric analysis

Mass spectrometric analysis and interpretation of the spectral data is the most crucial step in the potassium-argon age determination of geologically young materials. Obtaining accurate isotopic ratio measurements has been the source of much frustration to previous workers using this instrument (65). Once the gases are admitted to the mass spectrometer, the magnitude of the output signal for the various isotopes varies with time. Part of this change is due to the "memory effect" of the mass spectrometer: a combination of pumping as a result of ions being driven into the walls of the tube, and re-emission of previously pumped gases. The amount of pumping is dependent upon the partial pressure of the gas being ionized, while the amount of re-emission is dependent not only on the total pressure in the tube but also on the past history of the tube, that is, the amount of gas previously analyzed and the length of

time since the last sample was in the tube. This pumping and re-emission occurs with all gases in the mass spectrometer tube, but only the behavior of argon is of interest here. The re-emission of argon in the mass spectrometer tube is shown in Figures 9 and 10. Figure 9 shows the effect of pumping time on the re-emission of ^{40}Ar after a large sample of air argon had been analyzed in the tube.

Noble (65) found that the change in isotopic intensities with time produced a very erratic pattern which was almost impossible to extrapolate to time zero. He was able to improve this condition by not turning on the accelerating voltage until the start of the analysis. However, the techniques developed by Noble were not sufficiently accurate to obtain the precise isotopic ratio measurements required to date very young samples. Further investigation of this problem has shown that the erratic behavior of the spectra was the result of the presence of active gases in the mass spectrometer tube. It was found that if the pressure in the mass spectrometer tube was kept below 5×10^{-7} torr during analysis, this problem was almost completely eliminated; the resulting change in isotopic intensities with time were nearly, but not exactly linear. However, if the mass spectrometer "memory" contribution to the peak intensities are subtracted from

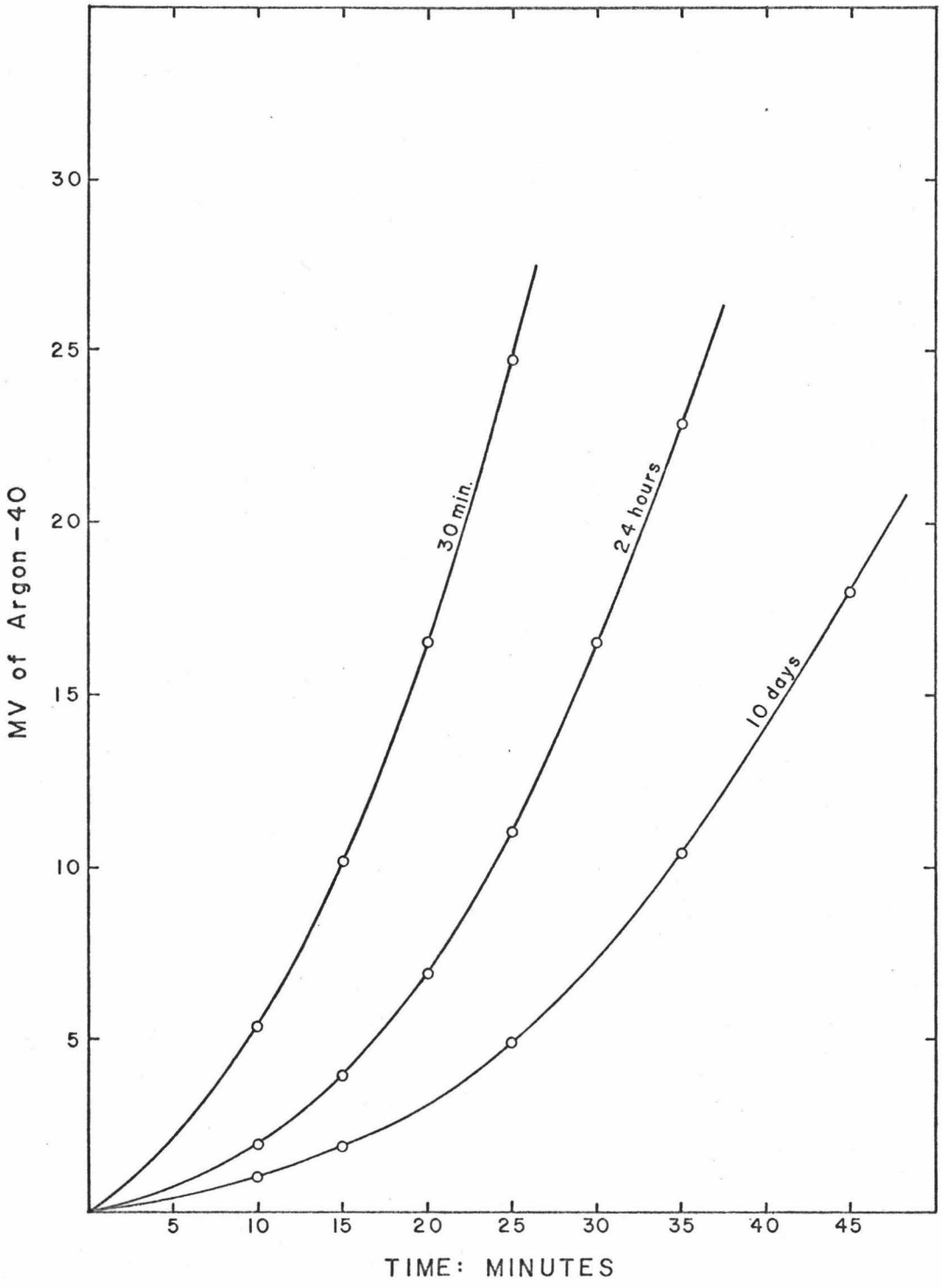

Figure 9 : Mass Spectrometer Memory for Argon-40

each isotopic peak, plots of the resulting $^{40}Ar/^{38}Ar$ and $^{38}Ar/^{36}Ar$ ratios are linear with time. Since the "memory" of the mass spectrometer is dependent on the tube's previous history, the memory correction must be determined just prior to the analysis of the sample. The following steps summarize the procedure necessary to obtain precise mass spectra data:

a) During collection of argon on the charcoal finger, a background of the mass spectrometer tube is run to determine the memory correction to be applied to the data. The tube is isolated from the VacIon pump and the accelerating voltage and chart are turned on simultaneously. Mass 36, 38, and 40 are scanned repetitively for 30 minutes. Argon-40 and argon-38 will show an exponential increase with time. Argon-36 usually shows very little change with time but may increase by a few hundredths of a mv during the 30 minutes. There is always a slight excess of mass-36 in the mass spectrometer tube, therefore this mass must be measured very carefully so that it can be subtracted from the sample analysis. The amount of mass-36 in the tube ranges from 0.03mv to 0.05mv. Figure 10 shows a typical memory correction for ^{40}Ar and ^{38}Ar. After completion of the memory determination, the valve between the tube and the VacIon pump was opened to allow the re-emitted gases to be pumped from the tube.

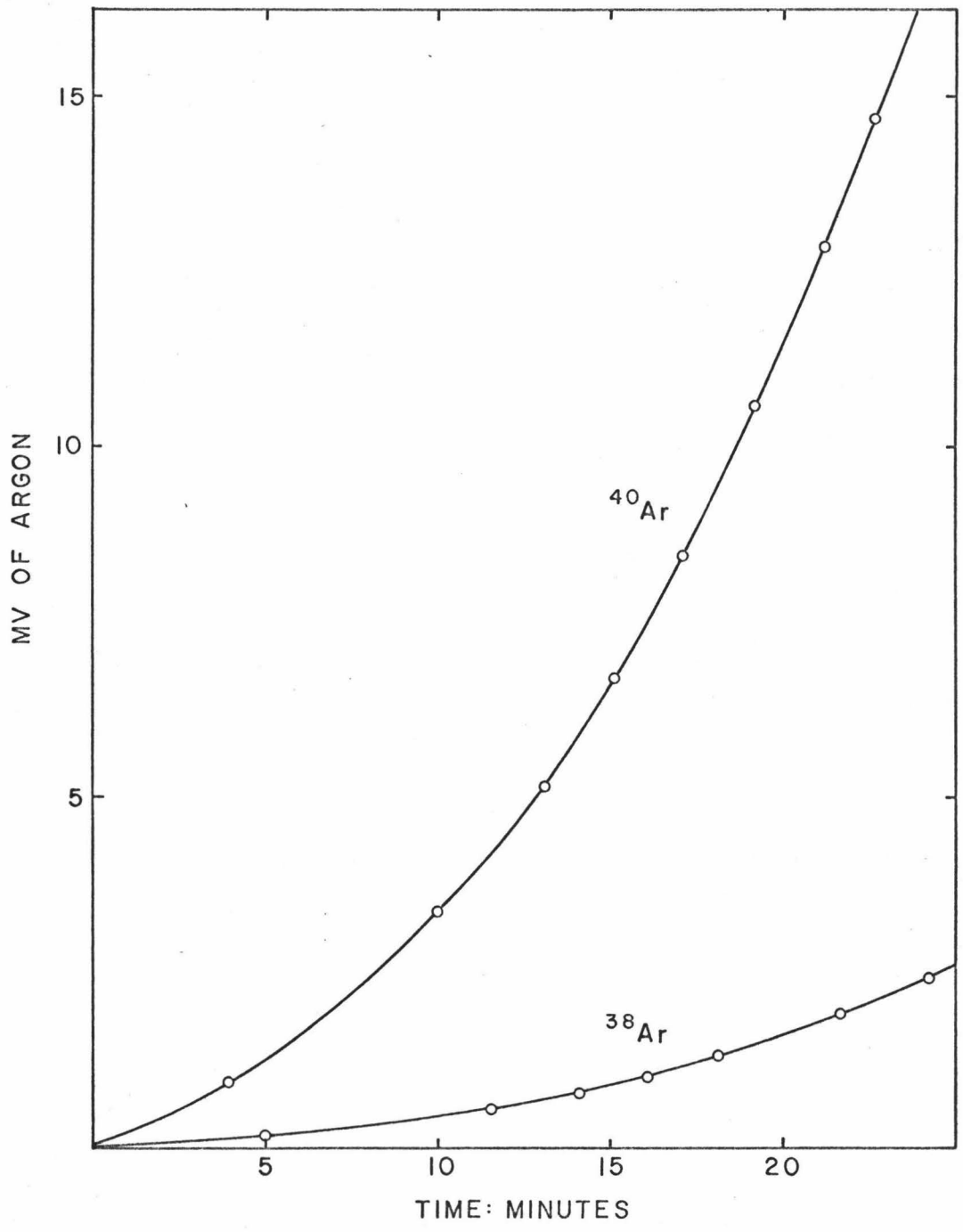

Figure 10: Typical Mass Spectrometer Memory Correction

b) After the argon from the extraction system had been collected on the charcoal finger, valve 4 of the extraction system was closed and the liquid nitrogen was removed from the finger. When the finger had warmed to near ambient temperature, the mass spectrometer tube was isolated from its pump and the valve between the tube and the extraction system (valve 6) was opened. Five minutes was allowed for the argon to equilibrate with the mass spectrometer after which valve 6 was closed. The magnetic field was adjusted to 4.00 kilogauss, and the parameters of the emission regulator were adjusted to the following values:

filament current	3.4 amps
trap current	30 microamps
case voltage	50 volts
trap voltage	147 volts

These conditions were found to give the maximum sensitivity and resolution for argon analysis, and could be adjusted with two potentiometers which directly controlled the filament current and case voltage. The recorder chart and accelerating voltage were turned on simultaneously, and the magnetic field was swept downward to mass-40 (3.95 KG). When the top of the mass-40 peak was located, the recorder was switched to the

expanded scale circuit, and the peak was monitored for about 30 seconds. The magnetic field was then scanned down to mass-38 (3.75 KG) and the procedure used to measure the mass-40 peak was repeated for mass-38. Between mass-40 and mass-38 the recorder was momentarily switched to the expanded scale circuit to allow the base line to be checked. After measurement of the mass-38 peak, the magnetic field was decreased to about 3.60 KG, and then allowed to slowly decrease to the mass-36 peak (3.55 KG). This established a base line about one-half inch long for the mass-36 peak. Because the amount of ^{36}Ar was relatively small, it was found that the peak height could be determined more accurately by slowly scanning over the peak, than by trying to sit on the top. Therefore, the ^{36}Ar peak was slowly scanned three times, after which an additional one-half inch base line was recorded. The magnetic field was then increased to bring mass-40 into focus and the above procedure was repeated. Measurement of the three argon isotopes required about 5 minutes, therefore six sets of peaks could be recorded in a 30 minute period. After recording six sets of peaks, the accelerating voltage was turned off and the gases were pumped from the tube. A portion of a typical spectra is shown in Figure 11.

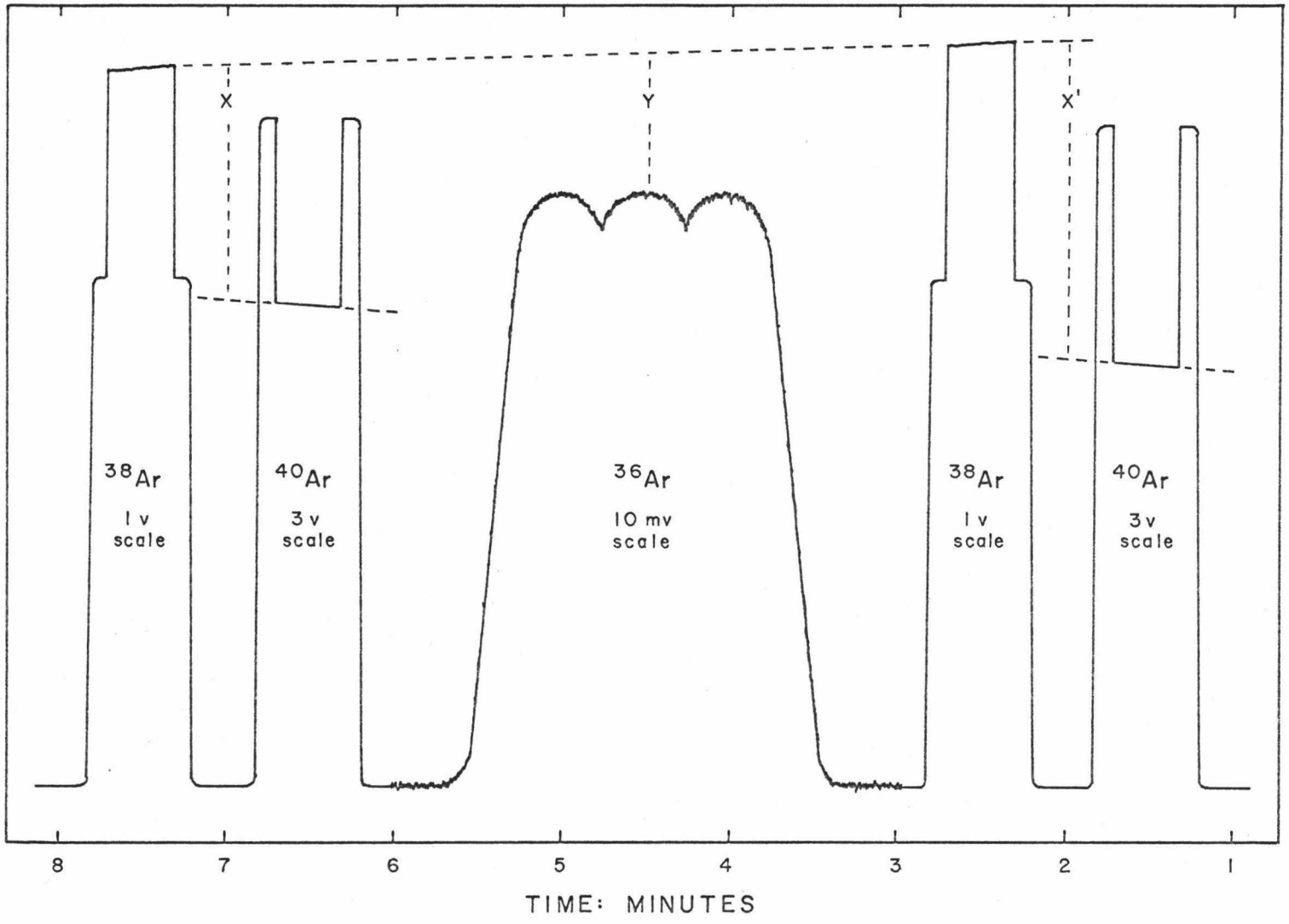

Figure II : A Portion of a Mass Spectrometer Chart for Argon Analysis

5. Interpretation of mass spectral data

After analysis the chart was removed from the recorder and the appropriate mass spectrometer memory correction was subtracted from each of the argon isotopic peaks. The $^{40}Ar/^{38}Ar$ and $^{38}Ar/^{36}Ar$ ratios were then measured at various time intervals along the chart. The $^{40}Ar/^{38}Ar$ ratio was measured at a point intermediate between the ^{40}Ar and ^{38}Ar peaks. (X and X' of Figure 11). The $^{38}Ar/^{36}Ar$ ratio was measured near the center of the ^{36}Ar peak (Y of Figure 11). For purposes of simplification, the mass spectrometer memory correction was not subtracted from Figure 11. The time-zero isotopic ratios were then calculated by a least squares regression analysis. The least squares analysis calculated the best fit of the data points to the line:

$$Y = a + bX$$

In addition to determining the time-zero intercept, the scatter of the data points about the regression line, called the standard error of estimate of Y on X, was calculated. The standard error estimate is given by:

$$S_{y.x} = \left[\frac{\Sigma Y^2 - a\Sigma Y - b\Sigma XY}{N} \right]^{\frac{1}{2}}$$

Where N is the number of data points. This estimate has properties analogous to those of the standard deviation: if N is large enough, 68 percent of the data points would be

within $\pm S_{y.x}$ of the least squares lines. The values of $S_{y.x}$ calculated for the $^{40}Ar/^{38}Ar$ and the $^{38}Ar/^{36}Ar$ ratios were used as the standard deviations of these ratios for the purpose of calculating an error on the final age determination. The values of $S_{y.x}$ were usually between 0.05 percent and 0.10 percent for the $^{40}Ar/^{38}Ar$ ratios, and between 0.08 percent and 0.20 percent for the $^{38}Ar/^{36}Ar$ ratios.

6. Age calculations and precision of analysis

A sample age calculation for one of the Honolulu Series lavas is shown in detail in Appendix C. All other ages reported in this paper were calculated in the same manner.

Because of the time and expense required to make even a single argon analysis, few laboratories conduct multiple determinations. Therefore, it is necessary to have some systematic method of estimating the precision of a single age determination. The following formula for estimating the standard deviation of a single potassium-argon age determination has been derived by Cox and Dalrymple (88):

$$\sigma = \left[(\sigma_k)^2 + (\sigma_x)^2 + (\sigma^{40/38})^2 \left(\frac{1}{r}\right)^2 + (\sigma^{38/36})^2 \left(\frac{1-r}{r}\right)^2 \right]^{\frac{1}{2}}$$

where σ_k = the standard deviation of the potassium analysis.

σ_x = the standard deviation of the spike calibration.

$\sigma^{40/38}$ = the standard deviation of the ratio $^{40}Ar/^{38}Ar$.

$\sigma^{38/36}$ = the standard deviation of the ratio $^{38}Ar/^{36}Ar$.

r = the fraction of ^{40}Ar that is radiogenic.

This equation was used to calculate the standard deviation of the potassium-argon ages reported in this paper. For this research:

$\sigma_x = 1\%$.

$\sigma^{40/38} = S_{y.x}$ for the $^{40}Ar/^{38}Ar$ ratio.

$\sigma^{38/36} = S_{y.x}$ for the $^{38}Ar/^{36}Ar$ ratio.

It should be noted that the above equation does not take into consideration errors resulting from sample inhomogeneity or systemic errors in interpreting the data from the recorder chart. Thus, standard deviations calculated in this manner should be regarded as instrumental errors. If the sample is reasonably homogenous and extreme care is exercised to eliminate errors in interpreting the spectral data, the calculated error should approximate the true error of the analysis.

Most workers who use this equation base their errors for the isotopic ratios on the precision obtained from multiple analyses of a standard sample or of air argon, the errors calculated from the standard being applied to all subsequent analyses. The author has found that the precision of isotopic ratio measurements can be quite variable from one sample to the next. For example, analyses run at night are generally more precise than those run during the day, because of a lower background noise level. In addition, the size of standard samples and samples of pure air argon are usually chosen to give optimum conditions for analysis, a situation seldom obtained in the analysis of an unknown sample. The favorable signal to noise ratios and sample cleanliness provided by these standards generally produce greater precision than is obtained for an average analysis. It is felt that the use of $S_{y.x}$, for calculation of the error of the isotopic ratio measurements, produces a more realistic estimate of the precision of the age determination than the methods used by other workers.

For young samples, where the air argon contamination is 90 percent or more, precise isotopic ratio measurements are a necessity if meaningful ages are to be obtained. Figure 12 shows the effect of high air argon concentrations on the standard deviation of a potassium-argon age determination. The two curves shown are calculated from the equation

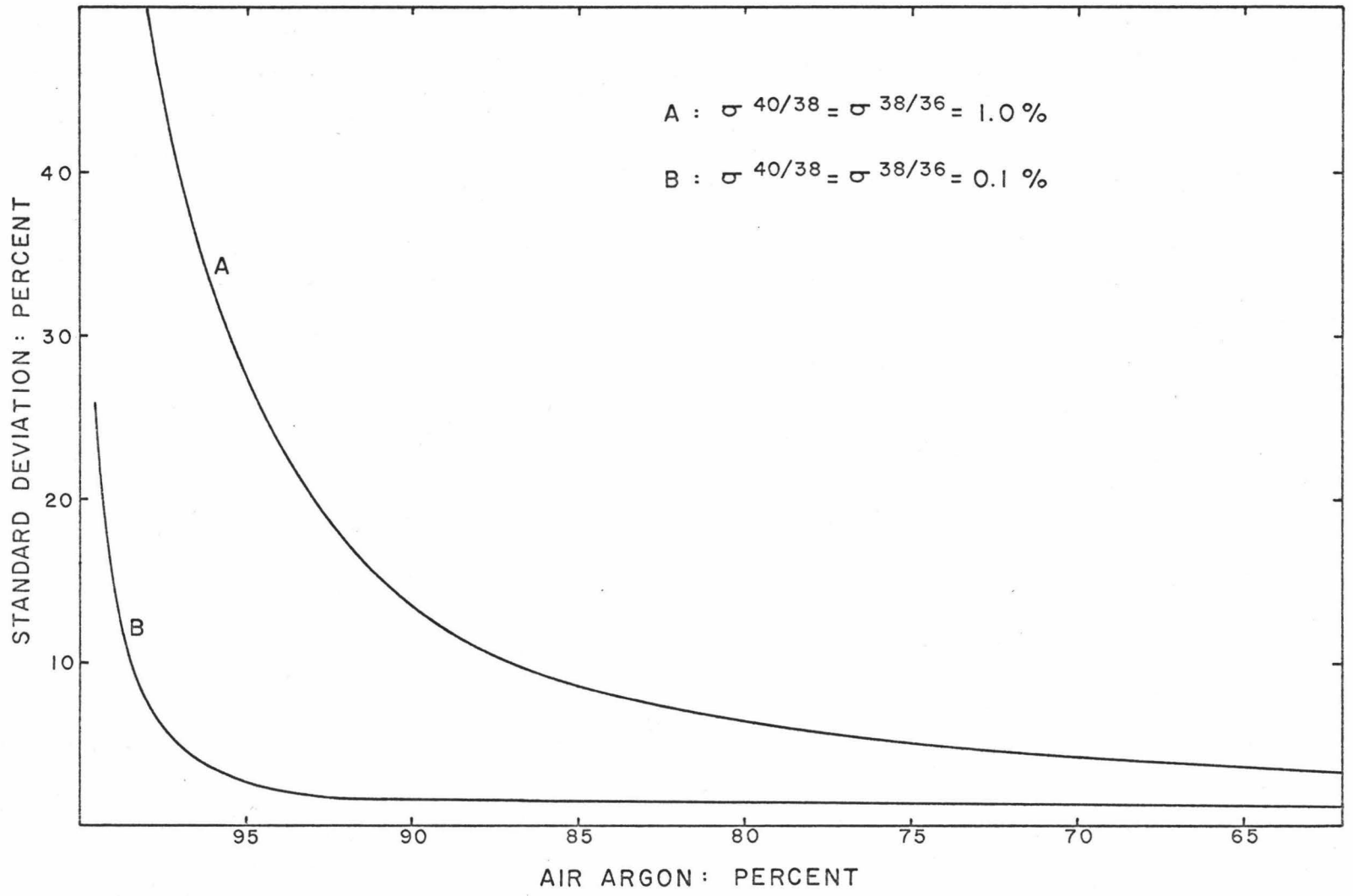

Figure 12: Error in K–Ar Age as a Function of the Amount of Air Argon

derived by Cox and Dalrymple, and assume that both σ_x and σ_k are ± 1 percent. Curve A is calculated for a ± 1 percent error in the isotopic ratio measurements, while curve B is for a ± 0.1 percent error in these ratios. It can be seen that for a sample containing 98 percent air argon, the error in the age determination from curve A is greater than ± 50 percent. By improving the isotopic ratio measurements to ± 0.1 percent, the error in the age is reduced to less than ± 8 percent.

The accuracy of a potassium-argon age determination is much more difficult to determine than the precision, since the true age of the material being dated is seldom known. Even though several argon determinations may show good precision, the measured value may differ considerably from the true value because of systematic errors in the ^{38}Ar spike calibration, techniques of analysis, data interpretation, etc. In the absence of a standard sample of exactly known radiogenic argon content, the best method of estimating the accuracy of argon determinations is by comparison with the results obtained at other laboratories on an identical sample. Such a sample (BCR-2) was supplied by J. H. Reynolds at the University of California at Berkley. Three determinations in this laboratory gave a radiogenic argon content of $8.98 \pm 0.04 \times 10^{-7}$ std cc/gm. After the results of these analyses were sent back to Reynolds, he reported that seven analyses of this sample

by G. H. Curtis, at the geochronology laboratory of the University of California, gave a radiogenic argon content of $8.92 \pm 0.12 \times 10^{-7}$ std cc/gm (89). The close agreement between the results obtained in two independent laboratories is a strong indication that the argon determinations reported in this paper are not subject to any large systematic errors.

7. Mass spectrometer isotopic bias determinations

Due to a variety of factors, the mass spectrometer may not show the true isotopic ratio of gases in the tube. The true $^{40}Ar/^{36}Ar$ ratio of air argon is 295.5, however, the mass spectrometer may give a ratio that is a few percent different from this. This difference or isotopic bias is usually determined by analyzing a sample of air argon and measuring the $^{40}Ar/^{36}Ar$ ratio. This measured ratio is then used to determine the air argon correction to be applied to a sample analysis. For young samples that contain a high percentage of air argon, precise measurement of the isotopic bias is extremely important; a 0.1 percent error in the bias determination may cause an error of several percent in the radiogenic argon measurement. This problem is further complicated by the fact that the bias on the instrument used in this research is extremely sensitive to changes in the environment near the tube. Pieces of metal, apparently affecting the magnetic field, have the

most serious effect on the bias: a screw driver placed on the mass spectrometer table, or a gas cylinder placed 3 feet from the table can change the bias by several percent. Other factors, such as vibration of the table from building construction outside the lab, and the activities of other workers in the lab also effect the bias. Because of the possibility of variations, the bias must be determined several times a week when young samples are being dated. Table 6 shows the results obtained for the isotopic bias during a one month period when the value did not change significantly. The errors listed for the $^{40}Ar/^{38}Ar$ and $^{38}Ar/^{36}Ar$ ratios are the values of $S_{y.x}$. The errors reported for the calculated $^{40}Ar/^{36}Ar$ ratios are determined from the following equations:

$$\sigma = N_1 N_2 \left[\frac{(S_{y.x})_1^2}{N_1} + \frac{(S_{y.x})_2^2}{N_2} \right]^{\frac{1}{2}}$$

where N_1 and N_2 refer to the listed values for $^{40}Ar/^{38}Ar$ and $^{38}Ar/^{36}Ar$. The fact that the agreement among replicate analyses is better than the calculated precision of the individual analyses may just be random "good luck," or it may indicate that the actual precision is greater than that calculated from $S_{y.x}$.

Table 6

Isotopic Bias Determinations with Air Argon

$^{40}Ar/^{38}Ar$	$^{38}Ar/^{36}Ar$	Air $^{40}Ar/^{36}Ar$
3.6105 ± 0.0009	83.94 ± 0.03	303.07 ± 0.13
3.7190 ± 0.0002	81.49 ± 0.16	303.06 ± 0.59
3.7436 ± 0.0036	80.91 ± 0.07	302.89 ± 0.39
3.7135 ± 0.0007	81.57 ± 0.25	302.91 ± 0.93
3.7743 ± 0.0001	80.26 ± 0.04	302.93 ± 0.15
3.7790 ± 0.0035	80.20 ± 0.01	303.08 ± 0.28
3.8318 ± 0.0002	79.04 ± 0.15	302.87 ± 0.57
3.7774 ± 0.0037	80.23 ± 0.07	303.06 ± 0.40
3.7713 ± 0.0013	80.38 ± 0.10	303.11 ± 0.39
±.04%	±0.12%	± 0.14%

H. Helium Analysis

1. Procedure for helium extraction

Helium was extracted from the samples at the same time that the argon was released. When helium analysis was desired, the helium content of the blank was carefully measured. A ^{3}He spike was expanded into the extraction system at the same time that the ^{38}Ar spike was admitted. After gettering of the sample and collection of the argon on the charcoal finger, the mass spectrometer was opened to the extraction system to allow the helium to expand into the tube.

2. Mass spectrometric analysis

After allowing 5 minutes for equilibration, the valve between the extraction system and the mass spectrometer was closed. The accelerating voltage and recorder chart were started simultaneously and mass-3 and mass-4 were scanned alternately for 20 to 30 minutes. The top of each mass peak was monitored for about 30 seconds. After completion of the analysis, the helium was pumped out of the tube by the VacIon pump connected to the mass spectrometer before the argon was expanded into the tube for analysis. The change in peak heights with time for both isotopes was quite linear, so the time-zero $^{4}He/^{3}He$ ratio was determined by extrapolation of the peaks with a

straight edge placed on the chart. The amount of ^4He found in the blank was subtracted from the amount measured from the sample.

III. RESULTS AND DISCUSSION

A. Potassium-Argon Ages of the Honolulu Series Lavas

1. The Koko rift zone

A line of tuff cones along the southeastern end of the island of Oahu mark the Koko rift zone, one of the two major rifts of the Honolulu Series. These eruptions are the youngest on the island. The tuff overlies marine deposits of the 25 foot Waimanalo stand of the sea (70). Radiometric ages on corals from the Waimanalo stand average about 120 thousand years (90), therefore, the Koko eruptions are younger than this age. The relative lack of weathering of the range, and the absence of any extensive reef development are further indications that these eruptions are geologically quite young. The relative ages of the Koko rift eruptions are not known with any certainty. The Koko Crater tuff overlies the pyroclastics of Kalama Crater, but lava flowing from Kalama Crater was deflected by material from Koko Crater (70). Thus Koko Crater erupted before as well as after Kalama Crater.

Most of the materials which erupted along the Koko rift are pyroclastics, however, some lava flows are present. One small flow originated from a fissure on the southwest flank of Koko Crater. This flow crosses the highway between the Kahauloa Crater rifle range and the

"Blow-Hole." A second, more extensive flow originated from Kalama Crater and flowed to the sea along the area now known as Sandy Beach. A third flow originated from a fissure on the side of the cliff behind what is now Sea Life Park. All three of these lavas are characterized by abundant olivine phenocrysts and a groundmass containing much feldspar and opaque minerals. These lavas have been classified as linosaite by Winchell (70).

The potassium-argon ages obtained for these three flows are reported in Table 7. The good agreement obtained for the six analyses is quite convincing evidence that the potassium-argon dating method can be extended to lavas 30 thousand years old or less, while still preserving a reasonable degree of precision. It must be pointed out, however, that these lavas were relatively clean with respect to both active gases and air argon. Melilite nephelinite lavas of this age could probably not be dated with the same precision. The samples used for the argon analyses of the Koko rift lavas ranged in size from 10-15 grams. Better single analysis precision could have been obtained by the use of larger samples, but one of the objectives of this research was to show that reliable ages could be obtained from sample sizes that could be conveniently handled in a vacuum system.

The lavas dated in this research are probably late stage eruptions of the Koko rift, but the analytical

Table 7

K-Ar Ages of Lavas From the Koko Rift Zone

sample number	location	potassium % K	radiogenic argon: std cc/gm	air argon: %	age: thousand years
HK204	Koko	0.936 ± 0.070	$1.37 \pm 0.03 \times 10^{-9}$	93.1	36.8 ± 1.0
			$1.12 \pm 0.06 \times 10^{-9}$	93.5	30.1 ± 2.2
HK213	Kaupo	0.601 ± 0.010	$7.3 \pm 1.1 \times 10^{-10}$	98.5	30 ± 5
			$7.8 \pm 0.8 \times 10^{-10}$	98.5	32 ± 3
HK216	Kalama	0.880 ± 0.015	$1.14 \pm 0.19 \times 10^{-9}$	98.8	32.4 ± 5.4
			$1.27 \pm 0.13 \times 10^{-9}$	98.3	36.1 ± 3.6

data is not able to distinguish any age differences. The eruptions may have been simultaneous or they may have occurred a few thousand years apart. It has been thought that the Kaupo flow might be considerably younger than the rest of the Koko range: perhaps only about 10 thousand years old (91,92). However, this research indicates that there is no significant difference between the Kaupo flow and the other late stage Koko rift eruptions.

2. The Kaimuki rift zone

The Kaimuki rift zone, also referred to as the Kaau rift zone in some literature, is the second major rift of the Honolulu Series. Activity along this rift built four volcanic cones on the Honolulu side of the Koolau Range: Kaau Crater, Mauumae cinder cone, Kaimuki lava dome, and the world's most famous tuff cone, Diamond Head. An eruption southeast of Diamond Head produced the Black Point lava flow which can be considered as part of the Kaimuki rift. On the windward side of the Koolau Range, the vents of the Maunawili and Training School eruptions are on a line with the Kaimuki rift vents, and may be part of the same rift zone.

The age of the Kaau eruption has not been known, but Wentworth suggested that it may have erupted during the Kaena or Laie stands of the sea (70). Diamond Head tuff overlayed the Mauumae lava in the old Kapahulu quarry.

The top of the tuff is baked at the contact with overlying Kaimuki lava. The apparent conformity between the Diamond Head tuff and the Kaimuki lava suggests that very little time elapsed between the Diamond Head and Kaimuki eruptions (70). A similar relationship exists between the tuff and the Black Point lava. Diamond Head tuff is exposed overlying a reef from the 95 foot Kaena stand which is dated at 320 thousand years or older (93). Evidence of cuts in the Diamond Head tuff resulting from the 25 foot Waimanalo stand (94) bracket the age of Diamond Head, and presumably also Black Point and Kaimuki, between 120 thousand years and about 320 thousand years.

The potassium-argon ages obtained for three eruptions from the Kaimuki rift zone are listed in Table 8. The ages obtained for Kaimuki and Black Point show no significant difference between the time of these eruptions. These results combined with the nearly identical petrography of the two lavas support the possibility that they may have been simultaneous vents of the same eruption. The nearly identical ages obtained from four samples of different potassium concentrations is evidence that the ages obtained represent the true geologic age of the lavas.

Mineralogically, lava from Kaau Crater is considerably different from the lavas of the Kaimuki and Black Point vents. The Kaau lava is a melilite nephelinite basalt with a groundmass of much nepheline and no labradorite.

Table 8

K-Ar Ages of Lavas From the Kaimuki Rift Zone

sample number	location	potassium: % K	radiogenic argon: std cc/gm	air argon: %	age: thousand years
HK203	Kaimuki	0.484 ± 0.007	$5.59 \pm 0.07 \times 10^{-9}$	83.3	289 ± 7
			$5.26 \pm 0.17 \times 10^{-9}$	86.7	272 ± 10
HK210	Kaimuki	0.639 ± 0.007	$7.43 \pm 0.31 \times 10^{-9}$	92.9	290 ± 12
			$7.32 \pm 0.48 \times 10^{-9}$	94.7	286 ± 19
HK215	Black Point	0.617 ± 0.010	$7.72 \pm 0.11 \times 10^{-9}$	86.6	313 ± 8
HK219	Black Point	0.829 ± 0.023	$9.56 \pm 0.13 \times 10^{-9}$	84.5	288 ± 9
			$1.05 \pm 0.01 \times 10^{-8}$	87.2	316 ± 10
HK220	Kaau	0.888 ± 0.009	$2.37 \pm 0.07 \times 10^{-8}$	94.3	677 ± 23
			$2.19 \pm 0.02 \times 10^{-8}$	64.3	617 ± 9

In contrast the Kaimuki and Black Point lavas contain a considerable amount of labradorite in the groundmass, but only small amounts of nepheline. These lavas have been classified by Winchell (70) as nepheline basanites. The considerably older age obtained for Kaau Crater combined with the mineralogical differences, indicates that there may be no genetic relation between the Kaau eruption and the Kaimuki and Black Point eruptions. The fact that Kaau Crater lies on a line through the Diamond Head, Kaimuki, and Mauumae vents may be only coincidental.

3. Other lavas of the Honolulu Series

The remaining lavas of the Honolulu Series, which were dated, are all nephelinite or melilite nephelinite lavas. Several other possible rift lines have been proposed based on field studies and petrographic and geographic evidence. Since evidence for these rifts is not as strong as for the Koko and Kaimuki rifts, the remaining lavas discussed here will not be grouped with any particular rift. The potassium-argon ages found for the melilite nephelinite and nephelinite lavas are listed in Tables 9 and 10 respectively.

The melilite nephelinite lavas from Salt Lake Crater and Kalihi, and the nephelinite lava from Nuuanu give similar potassium-argon ages. From the ages found in this research, it would appear that the Kalihi eruption is

Table 9

K-Ar Ages of the Melilite Nephelinite Lavas of the Honolulu Series

sample number	location	potassium: % K	radiogenic argon: std cc/gm	air argon: %	age: thousand years
HK201	Salt Lake	1.47 ± 0.06	$2.53 \pm 0.11 \times 10^{-8}$	91.4	430 ± 25
			$2.62 \pm 0.07 \times 10^{-8}$	88.3	446 ± 21
			$2.46 \pm 0.04 \times 10^{-8}$	82.8	418 ± 18
HK202	Sugar Loaf	1.33 ± 0.05	$3.05 \pm 0.17 \times 10^{-9}$	97.7	57.3 ± 3.4
			$2.96 \pm 0.14 \times 10^{-9}$	98.2	55.6 ± 3.2
HK212	Castle	0.812 ± 0.002	$2.66 \pm 0.03 \times 10^{-8}$	71.7	819 ± 8
			$2.70 \pm 0.03 \times 10^{-8}$	69.8	831 ± 10
HK217	Kalihi	0.958 ± 0.019	$1.75 \pm 0.02 \times 10^{-8}$	83.3	457 ± 11
			$1.78 \pm 0.07 \times 10^{-8}$	90.6	464 ± 22

Table 10

K-Ar Ages of the Nephelinite Lavas of the Honolulu Series

sample number	location	potassium: % K	radiogenic argon: std cc/gm	air argon: %	age: thousand years
HK207	Nuuanu	0.832 ± 0.011	$1.40 \pm 0.03 \times 10^{-8}$	89.3	421 ± 10
			$1.42 \pm 0.04 \times 10^{-8}$	90.0	427 ± 13
HK222	Punchbowl	0.881 ± 0.010	$1.05 \pm 0.02 \times 10^{-8}$	91.6	297 ± 6
			$1.04 \pm 0.03 \times 10^{-8}$	95.4	296 ± 10

slightly older than the other two, but the age difference is too small to establish the order of these eruptions with certainty. The Kalihi and Nuuanu eruptions have been assigned to the Kaena 95 foot stand of the sea, while the Salt Lake Crater eruption has been placed with the more recent 60 foot Waipio stand (70). Based on this research it would appear that the three eruptions occurred during the same stand.

The nephelinite lava dated from Punchbowl Crater places this eruption at about the same time as Diamond Head. It is interesting that Honolulu's two most famous landmarks are indistinguishably identical in age. Both of these eruptions have been placed with the 60 foot Waipio stand of the sea.

The Castle flow, on the Kailua side of the Koolau Range provides a possible conflict between the potassium-argon age and geological evidence. The late eruptions of the Koolau volcano have been dated by McDougall (57) who obtained ages of about 2.5 million years. This has been confirmed by the author, who obtained ages of 2.50 million years and 2.46 million years on two Koolau lavas that were accidentally collected as Honolulu Series samples. The eruptive center of the Koolau volcano was on the Kailua side of the Nuuanu-Pali cliffs, covering approximately the area from Waimanalo to Kaneohe (95). Thus approximately one half of the Koolau volcano has been eroded away. The

Castle flow is at the base of the Nuuanu-Pali cliffs and must have erupted after this side of the Koolau volcano had eroded down to nearly sea level. The potassium-argon age of over 800 thousand years, obtained for the Castle flow, implies that the erosion of the Koolau volcano was nearly completed in just a little over 1.5 million years. The author is satisfied that the age obtained for the Castle flow is the true potassium-argon age, and can find no evidence to indicate that the sample analyzed would not give the true geologic age.

The Sugar Loaf flow is an example of the difficulties involved in dating many of the melilite nephelinite lavas of the Honolulu Series. The two dates reported are the result of nearly a dozen attempts to obtain an argon analysis on this sample. The sample was extremely difficult to melt. The lava contains a large amount of gas and is very viscous in the molten state. As a result the sample would form a foam instead of releasing the gas. This foam would be pushed upward in the crucible as a result of additional gas being released from the sample. The resulting overflow of the crucible would invalidate the analysis because of the possibility of incomplete sample melting. In addition, the large amount of active gases and air argon released from the sample caused difficulties in obtaining a good mass spectrometric analysis. Several criteria have been established to decide whether an argon

analysis should be accepted or rejected. Four argon analyses were obtained, but two were rejected because they failed to meet all of the specifications of a good analysis. These discarded results produced ages of about 170 thousand years, much older than the two accepted analyses. Analyses obtained from samples that are not sufficiently clean with respect to active gases often produce ages that are too old. The two analyses reported in Table 9 were judged to be satisfactory, and should represent the true age of the Sugar Loaf flow. The potassium-argon age obtained for the Sugar Loaf flow (ca. 60 thousand years) is older than geologic estimates (91,92), but the difference is not sufficient to constitute a major discrepancy between the radiometric age and the geologic predictions.

A sample of lava from the Pali eruption provided an example of one of the possible interferences to the potassium-argon method: excess radiogenic argon. The Pali lava flow contains numerous ultramafic xenoliths, similar to those present at Salt Lake Crater. The minerals in these xenoliths are known to contain an excess of radiogenic argon. A whole rock sample of Pali lava was dated at over 2 million years. Close investigation of the sample showed that small xenolithic fragments were dispersed throughout the lava. A sample of the lava was crushed to -40+60 mesh and all crystals of olivine and pyroxene,

suspected of being of xenolithic origin, were hand picked from the lava. The remaining lava then gave an apparent age of 1.3 million years. The decrease of one million years in the age by removing a few grains of olivine and pyroxene is proof that the excess radiogenic argon is in these xenolithic fragments. One could probably reduce the age further by additional removal of the grains, but the true age could only be approached and not determined with certainty. Stearns (69) has placed the age of the Pali flow between the Nuuanu eruption and the Salt Lake Crater eruption, based on the observation that Pali rocks lie over the Nuuanu lava but cinders from the Pali eruption are under Salt Lake Crater. If this is true then the age of the Pali eruption can be deduced from the measured ages of Nuuanu and Salt Lake Crater. The Pali eruption would then be about 430 ± 20 thousand years old.

It is interesting to compare these results obtained from the Pali lava with the results obtained by Dalrymple (62) on three recent eruptions which gave anomalously old ages. Lava from Hualalai, Hawaii (eruption: 1801 A.D.) gave an apparent age of 1.1 million years, lava from Sunset Crater, Arizona (eruption: 1065 A.D.) gave an age of 0.22 million years, and lava from Mt. Etna, Sicily (eruption: 1792 A.D.) gave an age of 0.15 million years. All three of these eruptions produced ultramafic xenoliths similar to those found in the Pali lava. It seems very likely that

the anomalous ages obtained by Dalrymple were the result of xenolithic fragments present in the block samples analyzed.

In general, the potassium-argon ages obtained from this research are in good agreement with geologic expectations, but more important, it has been demonstrated that the potassium-argon method can be used to accurately date volcanic lavas younger than 50 thousand years old. Thus, the potassium-argon and carbon-14 methods can be applied to the same eruptions, providing a cross-check on both methods. It is felt by the author, that with additional instrumental modifications, careful techniques, and favorable samples, the potassium-argon method can be used to date volcanic rocks less than 15 thousand years old with a precision of ± 20 percent or less.

4. Secondary minerals in the Honolulu Series lavas

Zeolites were found in all melilite nephelinite lavas collected by the author. They could not be separated from the lava without grinding the sample to at least -80+100 mesh. The increased air argon resulting from increasing the surface area by grinding would prohibit accurate age determinations. Therefore, the zeolites were not removed from the lava, but samples were chosen for analysis which appeared to contain the least amount of zeolites.

Zeolites from the Sugar Loaf flow, reported to be chabazite and phillipsite (70), were dated to be over 2 million years old. Subsequent analyses failed to reproduce this age and gave very erratic results. Some samples showed an excess of radiogenic argon, some showed no radiogenic argon, and others showed an extremely large amount of air argon. Amounts of air argon up to 10^{-3} std cc/gm were measured. It was found that those samples which showed an apparent excess of radiogenic argon were in the side arm of the oven while samples containing a large amount of radiogenic argon were melted. The zeolites apparently adsorbed radiogenic argon from the vacuum system, even at very low partial pressures. The samples exhibiting a large amount of air argon were not baked in the vacuum system: overnight baking at 200°C was found sufficient to remove the air argon. Samples not baked showed an increase in the active gases, but the increase did not seem to be proportional to the amount of air argon. Therefore, the zeolites appear to be somewhat selective in their affinity for argon. This phenomenon was not felt to be a problem in the analysis of the Honolulu Series samples, since the amount of zeolites exposed on the surface of the samples were quite small, and the amount of radiogenic argon in the extraction system during analysis of other samples was several orders of magnitude less than the amount present when the adsorption phenomenon was observed.

B. Ultramafic Xenoliths from Salt Lake Crater

The presence of ultramafic inclusions in the tuff of Salt Lake Crater has been known for over 70 years (96). Interest in these inclusions has been recently stimulated by numerous papers which have indicated that these materials represent fragments of rocks that formed at considerable depths in the earth's mantle. Nodules of peridotite and related rocks are common in the alkalic and nephelinic lavas in Hawaii, and are found in several locations throughout the world. The inclusions found at Salt Lake Crater are the only known oceanic source of garnet-bearing xenoliths.

1. Argon-40 and helium-4 content of the Salt Lake xenoliths

The radiogenic argon and helium content of the minerals in the Salt Lake xenoliths have been investigated by several workers (63,64,65). In all cases, the potassium-argon and uranium-helium ages calculated for these minerals were considerably older than the expected age of the Salt Lake eruption. Additional studies of the noble gas content of these minerals were conducted in this research. Three samples were investigated: Two of the samples (SL201 and SL203) were composed of about 75 percent olivine, 15 percent enstatite, and 10 percent chrome

diopside. A small amount of spinel was present in one of the samples (SL201), as well as a trace of garnet and biotite. These two samples will be referred to as "lherzolite" in this paper. The third sample (HK139) contained about 80 percent augite, 20 percent pyrope, and a trace of olivine. This sample will be referred to as an "eclogite." The two types of samples studied here represent the two extremes, one being nearly free of garnet and the other being nearly free of olivine. However, all gradations occur between these two types (76). The argon, helium, and potassium analyses on the minerals from these three samples are listed in Tables 11 and 12. Biotite from a fourth sample (SL200) was also investigated with respect to its argon and potassium content. It is the author's opinion that the argon and helium content of these minerals bears no relation to the geologic age, and for that reason the apparent potassium-argon ages of these minerals has not been included in this paper. It is sufficient to say that all of the minerals studied produced apparent K-Ar ages in excess of one million years.

The following important conclusions can be deduced from the data presented in Table 11. First, the argon and helium content of the minerals is dependent upon the particle size being studied. Second, the $^{4}He/^{40}Ar$ ratio decreases as the particle size is decreased. And third, the $^{4}He/^{40}Ar$ ratio for all of the minerals is

Table 11

Argon-40 and Helium-4 Content of Minerals From the Salt Lake Xenoliths

sample number	mineral	mesh range	helium-4: std cc/gm	argon-40: std cc/gm	air argon: %
SL201	Chrome Diopside	-60+100	5.05×10^{-7}	2.39×10^{-6}	8.3
		-60+100	4.98×10^{-7}	2.32×10^{-6}	4.5
		-400	2.88×10^{-7}	8.58×10^{-7}	76
		-400	2.80×10^{-7}	8.40×10^{-7}	75
SL203	Chrome Diopside	-60+80	4.81×10^{-7}	2.00×10^{-6}	13.4
SL201	Enstatite	-42+60	3.30×10^{-7}	1.22×10^{-6}	13.3
		-42+60	3.30×10^{-7}	1.19×10^{-6}	13.6
SL203	Enstatite	-60+100	9.07×10^{-8}	5.76×10^{-7}	24.5
		-60+100	1.03×10^{-7}	5.58×10^{-7}	24
		-150+250	8.28×10^{-8}	5.75×10^{-7}	40.5
		-250+325	7.58×10^{-8}	5.33×10^{-7}	42.5
		-400	4.50×10^{-7}	3.02×10^{-7}	85
SL201	Olivine	-60+100	1.20×10^{-7}	1.81×10^{-7}	57
		-60+100	1.10×10^{-7}	2.11×10^{-7}	51

Table 11 (Continued)

Argon-40 and Helium-4 Content of Minerals from the Salt Lake Xenoliths

sample number	mineral	mesh range	helium-4: std cc/gm	argon-40: std cc/gm	air argon: %
SL203	Olivine	-100+150	4.09×10^{-8}	3.88×10^{-8}	80
		-100+150	3.40×10^{-8}	3.83×10^{-8}	82
SL201	Spinel	-400	6.40×10^{-8}	2.18×10^{-5}	6.4
HK139	Spinel	-42+150	1.08×10^{-6}	5.64×10^{-6}	5
		-42+150	1.06×10^{-6}	5.40×10^{-6}	8.5
HK139	Pyrope	-100+325	5.45×10^{-7}	1.35×10^{-6}	29
		-100+325	4.40×10^{-7}	1.38×10^{-6}	21.5
		-400	1.10×10^{-7}	5.65×10^{-7}	78.4
SL200	Biotite			1.804×10^{-6}	21
				1.828×10^{-6}	20.5

Table 12

Potassium Content of the Minerals
from the Salt Lake Xenoliths

sample number	mineral	potassium: ppm
SL201	Olivine	96.1
SL203	Olivine	48.0
SL201	Enstatite	56.6
SL203	Enstatite	30.3
SL201	Chrome Diopside	48.8
SL203	Chrome Diopside	109
HK139	Augite	438
HK139	Pyrope	148
SL201	Spinel	0.205%
SL200	Biotite	7.77%

lower than the value expected from decay of potassium and uranium-thorium in these materials. The $^{4}He/^{40}Ar$ ratio of gas accumulated from radioactive decay of potassium, uranium, and thorium, can be approximated by the following equation (97):

$$^{4}He/^{40}Ar = U/K\ (3.0 + 0.72\ Th/U)\ x10^{4}$$

which is independent of time from the present back to about 100 million years. It can be seen that the $^{4}He/^{40}Ar$ ratio is not very sensitive to changes in the Th/U ratio, which can be assumed to be about 3. Recent determinations of the uranium content of lherzolites from Australia (98) give the following average concentrations: olivine = 0.0005 ppm U, clinopyroxene = 0.3 ppm U, and orthopyroxene = 0.003 ppm U. Using these values for the uranium content and the potassium concentrations from Table 12, the following approximate $^{4}He/^{40}Ar$ ratios of the Salt Lake minerals can be calculated from the above equation: olivine = 0.5, chrome diopside = 300, and enstatite = 3. Measurement of the $^{4}He/^{40}Ar$ ratio in the sample of lava from Salt Lake (HK201) produced a value of 3.4, more than an order of magnitude larger than the average values obtained for the xenoliths. The value of the Salt Lake lava is in good agreement with a $^{4}He/^{40}Ar$ ratio of 3.9, obtained from the Kaimuki lava (HK203). Therefore, the $^{4}He/^{40}Ar$ ratio in the xenoliths

is also lower than the value for the host rock. Volcanic gases released from New Zealand fumaroles were found to have $^{4}He/^{40}Ar$ ratios of 2 to 4 (99), in good agreement with the values found for the Honolulu Series lavas, but much larger than the ratios found in the xenoliths.

The low helium/argon ratios found in these minerals, together with the apparent further decrease in these values for small particle sizes prompted further investigation. The radiogenic helium and argon contents of samples of HK139 augite, ranging in average size from 300 microns down to 5 microns, were measured. The results are shown in Table 13 and Figure 13. The amount of helium and argon that is lost from the augite when the grains were crushed to small sizes was much larger than the amount expected to be released from the opening of the mineral lattice. Calculations indicate that the amount of gas released from the lattice by grinding should be significantly less than the observed release, even if one assumes that grinding releases all gases to a depth of 1000 unit cell dimensions into the grain. This is taken as proof that most of the helium and argon is held in the fluid inclusions, which are prevalent in all of the minerals from the Salt Lake xenoliths. Since most of these fluid inclusions lie along planes in the minerals, it would be expected that crushing would cause preferential breakage along these planes of weakness. The augite data also shows a decrease in the

Table 13

Argon-40 and Helium-4 Content of HK 139 Augite

mesh size	ave. size: microns	radiogenic argon: std cc/gm	helium std cc/gm
-42 + 60	300	9.10×10^{-6}	1.67×10^{-6}
-42 + 60	300	8.95×10^{-6}	1.60×10^{-6}
-42 + 150	227	8.56×10^{-6}	1.66×10^{-6}
-80 + 100	161	8.46×10^{-6}	1.45×10^{-6}
-100 + 150	125	8.08×10^{-6}	1.33×10^{-6}
-150 + 250	80	7.38×10^{-6}	1.29×10^{-6}
-250 + 325	50	6.00×10^{-6}	9.74×10^{-7}
-400	-38	3.14×10^{-6}	5.42×10^{-7}
-400	-38	3.03×10^{-6}	4.85×10^{-7}
30-40 μ	35	3.91×10^{-6}	4.87×10^{-7}
20-30 μ	25	3.31×10^{-6}	4.83×10^{-7}
20-30 μ	25	3.39×10^{-6}	4.44×10^{-7}
10-20 μ	15	2.62×10^{-6}	3.80×10^{-7}
10-20 μ	15	2.93×10^{-6}	3.70×10^{-7}
1-10 μ	5	1.13×10^{-6}	1.72×10^{-7}
1-10 μ	5	1.30×10^{-6}	1.72×10^{-7}

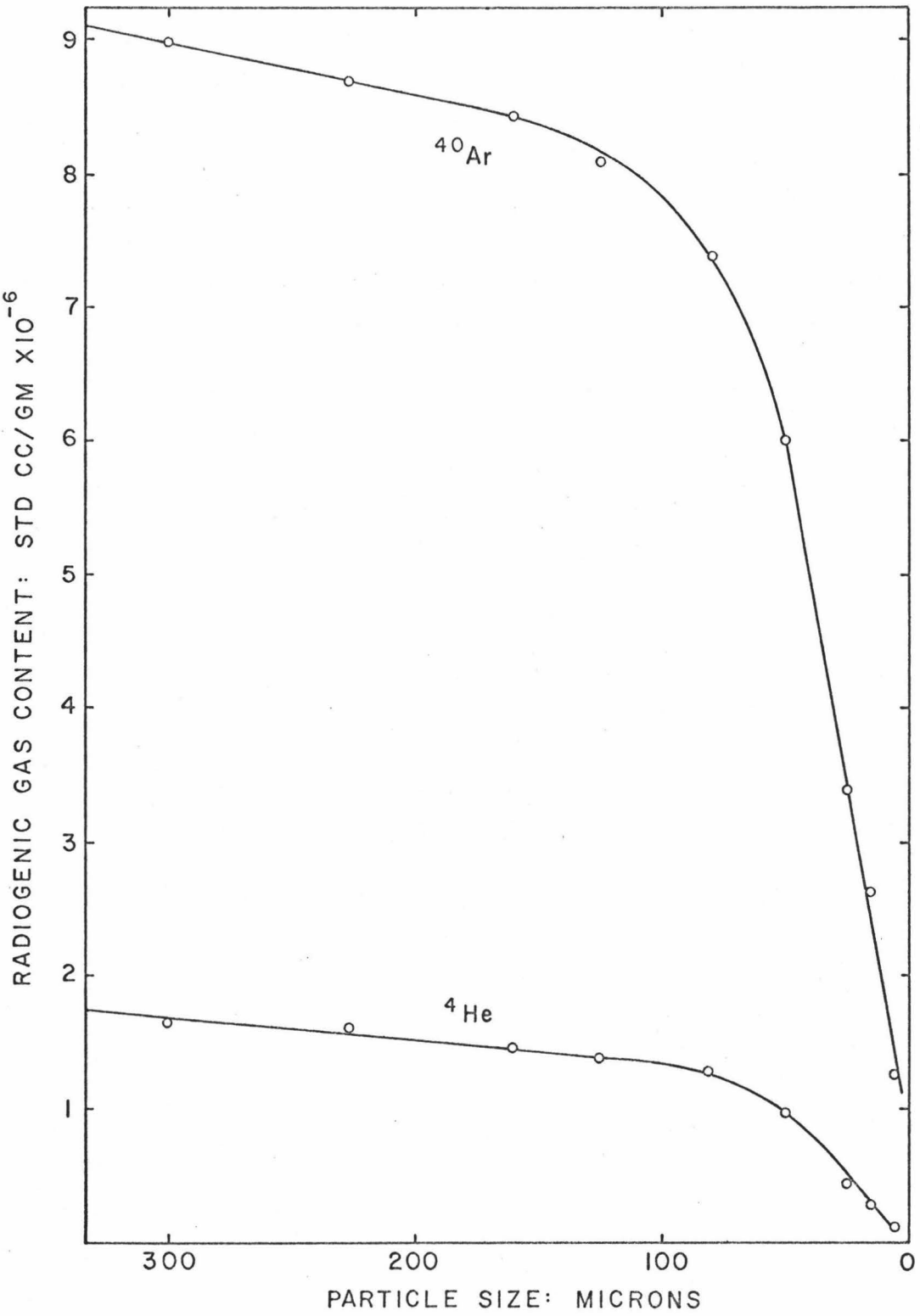

Figure 13: Radiogenic Gas Content vs. Particle Size for HK139 Augite

$^{4}He/^{40}Ar$ ratio of the gases remaining in the sample, as the sample size is decreased. If crushing preferentially releases helium and argon trapped in the fluid inclusions, then the gases remaining at small particle sizes should approach the gas content of the mineral lattice. Gases produced by radioactive decay of potassium, thorium, and uranium in the lattice would be expected to produce a $^{4}He/^{40}Ar$ ratio higher than the value found in the fluid inclusions; instead the $^{4}He/^{40}Ar$ ratio of lattice gases appears to be considerably lower. This discrepancy can best be explained by a mass dependent loss mechanism, such as diffusion. Since these xenoliths have experienced a high temperature history during ascent to the surface with the molten lava, loss of gases by diffusion is not surprising.

2. Diffusion studies on the Salt Lake xenoliths

To test this hypothesis, the loss of argon and helium from the augite was measured during a 5 hour heating period at 1100°C. The results of this study are reported in Table 14. It can be seen that even during a relatively short heating period, a preferential loss of helium from the mineral causes a decrease in the $^{4}He/^{40}Ar$ ratio. Thus, the ratio found in these xenolithic minerals does not reflect the gas ratio of the environment at the time of formation of the fluid inclusions. If these

Table 14

Measured Diffusional Loss of Argon and Helium from HK139 Augite at 1100°C

Average grain size: 3.00×10^{-2} cm

total heating time: hours	argon remaining std cc/gm	helium remaining std cc/gm	$^4He/^{40}Ar$
0	6.76×10^{-6}	9.96×10^{-7}	0.147
1	6.45×10^{-6}	6.70×10^{-7}	0.104
2	6.45×10^{-6}	5.80×10^{-7}	0.0902
3	6.45×10^{-6}	5.09×10^{-7}	0.0790
4	6.45×10^{-6}	4.60×10^{-7}	0.0715
5	6.45×10^{-6}	4.23×10^{-7}	0.0656

xenoliths are of mantle origin then the initial $^{4}He/^{40}Ar$ ratio trapped in the minerals should have been representative of the mantle environment.

It was felt that if sufficient information could be obtained on the diffusion characteristics of argon and helium in these minerals, it would be possible to extrapolate the $^{4}He/^{40}Ar$ ratios back in time to a point where all of the minerals contained the same $^{4}He/^{40}Ar$ ratio; this then would be the gas ratio of the environment from which the gases were trapped.

Any diffusion data collected on the separated minerals from the xenoliths must be corrected to the average grain size found in the xenoliths. Because of complex texture of the eclogite, an average grain size could not be determined for augite. However, the mineral grains in the lherzolite were readily discernible, and an average grain size (Tables 15-20) could be calculated. A photograph of a portion of one of the lherzolites is shown in Figure 14. The rate of diffusion of argon and helium, at a temperature of 1100°C, was measured for the three most prevalent minerals in the lherzolites. From the experimental data, the diffusion coefficients of the gases were calculated from the diffusion equations discussed on pages 20-22 of this paper. The average grain size in the lherzolites was determined from measurement of over a hundred random grains with a calibrated microscope. The

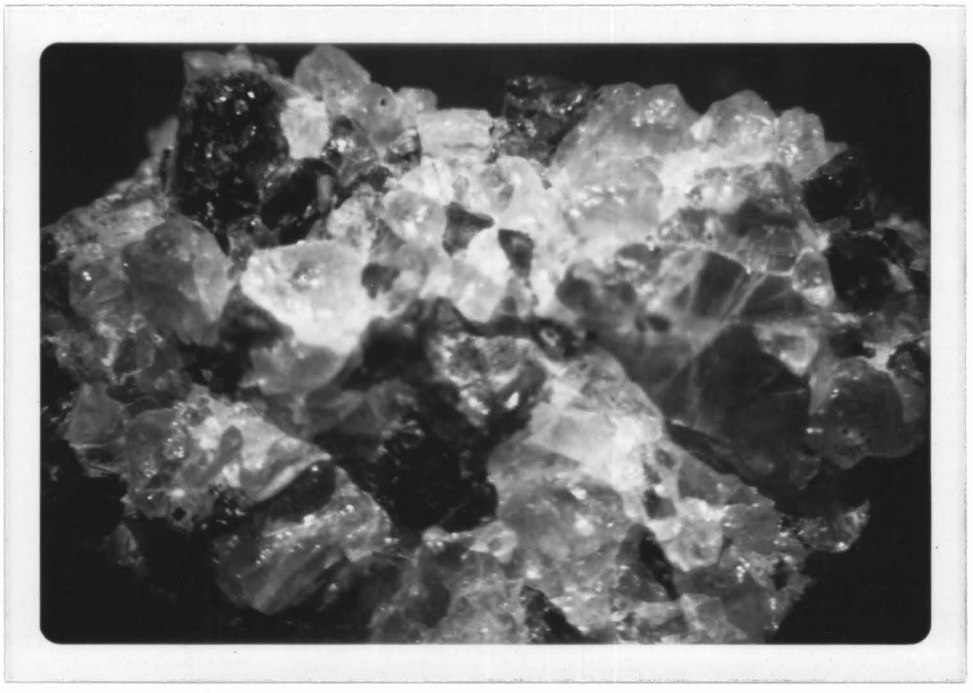

Figure 14

SL-203 Salt Lake Lherzolite

Table 15

Measured Diffusional Loss of Argon and Helium from SL 203 Olivine at 1100°C

Average grain size: 6.2×10^{-3} cm

total heating time: hours	argon remaining std.cc./gm	helium remaining std.cc./gm
0	3.840×10^{-8}	3.75×10^{-8}
1	3.758×10^{-8}	3.54×10^{-8}
2	3.758×10^{-8}	3.42×10^{-8}
3	3.758×10^{-8}	3.37×10^{-8}

Table 16

Calculated Diffusional Loss of Argon and Helium from SL 203 Olivine at 1100°C

Average grain size: 2.14×10^{-1} cm

total heating time: hours	argon remaining std.cc./gm	helium remaining std.cc./gm	$^4He/^{40}Ar$
0	3.840×10^{-8}	3.745×10^{-8}	0.9752
1	3.836×10^{-8}	3.733×10^{-8}	0.9734
2	3.836×10^{-8}	3.726×10^{-8}	0.9713
3	3.836×10^{-8}	3.723×10^{-8}	0.9708

Table 17

Measured Diffusional Loss of Argon and Helium from SL 201 Enstatite at 1100°C

Average grain size: 3.0×10^{-2} cm

total heating time: hours	argon remaining std.cc./gm	helium remaining std.cc./gm
0	1.205×10^{-6}	3.300×10^{-7}
1	1.129×10^{-6}	2.664×10^{-7}
2.05	1.128×10^{-6}	2.457×10^{-7}
3	1.128×10^{-6}	2.356×10^{-7}
4	1.128×10^{-6}	2.255×10^{-7}

Table 18

Calculated Diffusional Loss of Argon and Helium from SL 201 Enstatite at 1100°C

Average grain size: 1.09×10^{-1} cm

total heating time: hours	argon remaining std.cc./gm	helium remaining std.cc./gm	$^4He/^{40}Ar$
0	1.205×10^{-6}	3.300×10^{-7}	0.2739
1	1.184×10^{-6}	3.113×10^{-7}	0.2629
2.05	1.184×10^{-6}	3.057×10^{-7}	0.2582
3	1.184×10^{-6}	3.028×10^{-7}	0.2557
4	1.184×10^{-6}	2.996×10^{-7}	0.2530

Table 19

Measured Diffusional Loss of Argon and Helium from SL 201 Chrome Diopside at 1100°C

Average grain size: 1.98×10^{-2} cm

total heating time: hours	argon remaining std.cc./gm	helium remaining std.cc./gm
0	2.355×10^{-6}	5.015×10^{-7}
1	2.148×10^{-6}	3.615×10^{-7}
2.03	2.148×10^{-6}	3.194×10^{-7}
3	2.148×10^{-6}	2.947×10^{-7}
4	2.148×10^{-6}	2.723×10^{-7}

Table 20

Calculated Diffusional Loss of Argon and Helium from SL 201 Chrome Diopside at 1100°C

Average grain size: 7.50×10^{-2} cm

total heating time: hours	argon remaining std.cc./gm	helium remaining std.cc./gm	$^{4}He/^{40}Ar$
0	2.355×10^{-6}	5.015×10^{-7}	0.2130
1	2.296×10^{-6}	4.627×10^{-7}	0.2015
2.03	2.296×10^{-6}	4.502×10^{-7}	0.1961
3	2.296×10^{-6}	4.415×10^{-7}	0.1923
4	2.296×10^{-6}	4.340×10^{-7}	0.1890

measured grain size and the diffusion coefficient were then used to calculate the expected argon and helium loss from the xenoliths. The results of this study are listed in Tables 15 through 20. Since for small gas losses, the fraction lost is a function of the square root of time, a plot of the $^4He/^{40}Ar$ ratio against $t^{\frac{1}{2}}$ is linear. Least squares analysis of the data gave the following lines of best fit for the change in $^4He/^{40}Ar$ ratio with time:

Olivine: $^4He/^{40}Ar = (0.9754 \pm 0.0004) - 0.002624(t^{\frac{1}{2}})$

Enstatite: $^4He/^{40}Ar = (0.2737 \pm 0.0003) - 0.01048(t^{\frac{1}{2}})$

Chrome Diopside:

$$^4He/^{40}Ar = (0.2132 \pm 0.0002) - 0.01201(t^{\frac{1}{2}})$$

where t is in hours. These least squares lines are shown in Figures 15 and 16. The extrapolation shown in Figure 16 is daring, to say the least, but unfortunately data points can not be obtained prior to the eruptions. The lines resulting from diffusion from the pyroxenes intercept the olivine line at times corresponding to about 6500 hours and 8000 hours. Calculations based on a magma viscosity of 3000 poises indicate that an ascending speed of at least 22 meters per hour would be necessary to carry a 6 inch xenolith 0.7 gm/cc denser than the molten lava to the surface (100). If it is assumed that the xenoliths were carried upward at an average speed of 22 meters per hour after coming in contact with the lava, the resulting depth of formation is between 140 and 180 Km. This depth is in

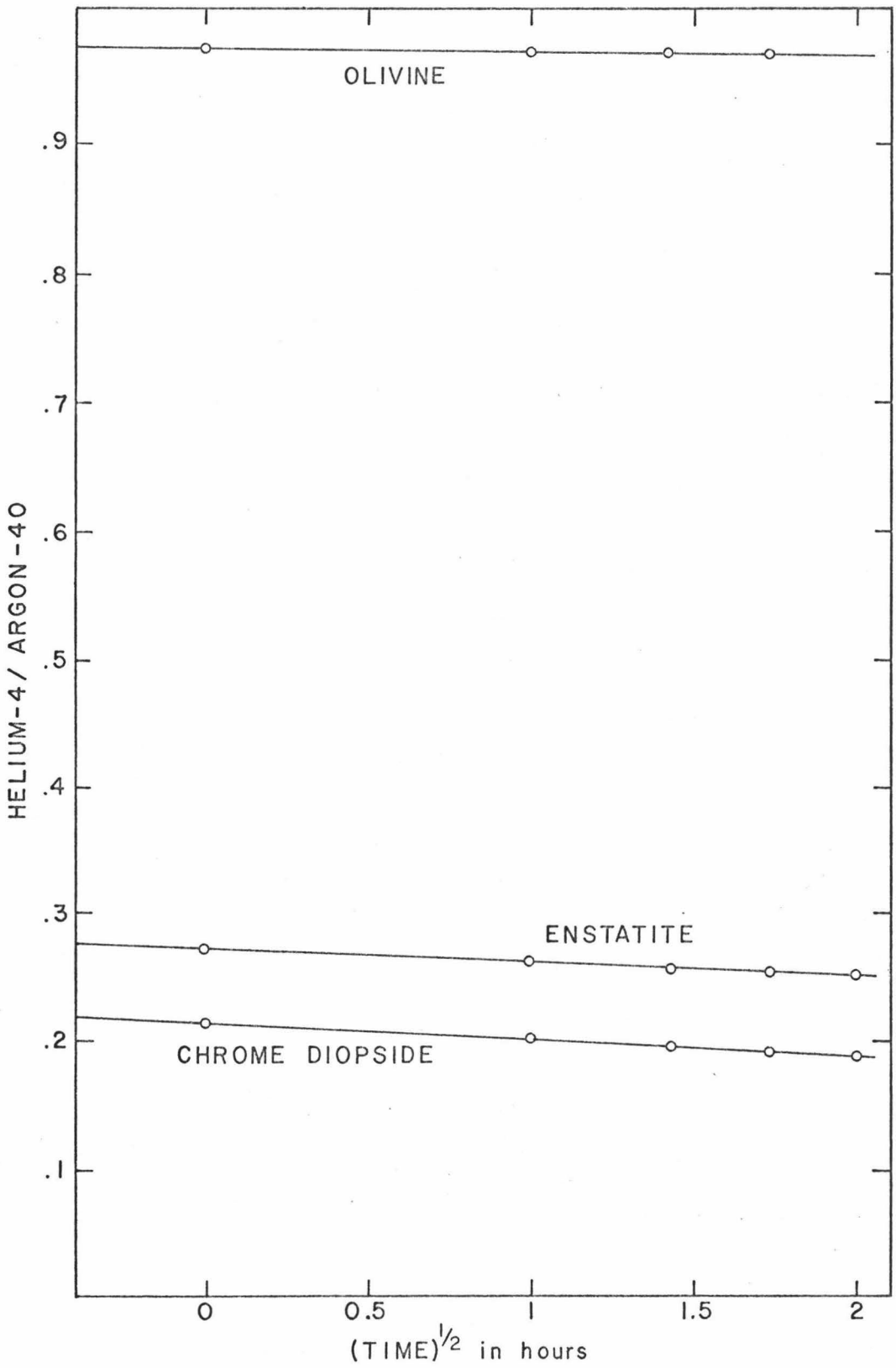

Figure 15: Change in $^{4}He/^{40}Ar$ Ratio with Time at 1100°C

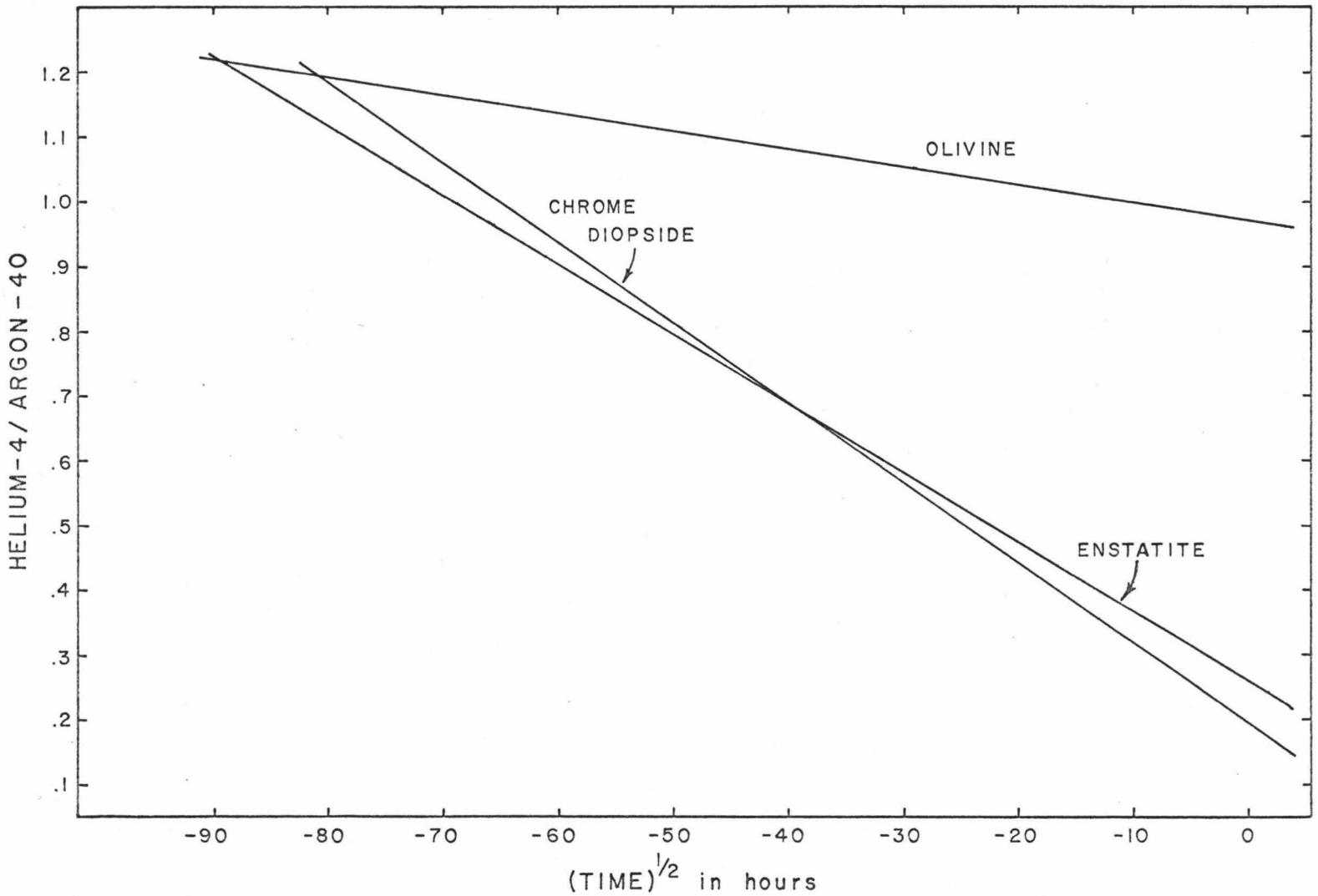

Figure 16: Extrapolated Change in $^{4}He/^{40}Ar$ Ratio with Time at 1100°C

good agreement with current geological predictions (92). Independent of the depth calculation, the $^{4}He/^{40}Ar$ ratio of the environment from which the xenoliths incorporated the gas is found to be about 1.2.

The general validity of this approach to the problem, and the conclusions drawn from the data are difficult to evaluate. Additional investigations of numerous xenoliths, not only from Salt Lake, but also from other parts of the world are needed before it can be said with any certainty that this approach is valid. Several assumptions were necessary to obtain the results reported in this study:

a) The restrictions and assumptions needed to obtain usable diffusion equations are reasonably valid. These conditions were listed on page 21 of this paper.

b) The temperature experienced by these minerals while in contact with the molten lava was near 1100°C.

c) The laboratory diffusion studies duplicated the conditions controlling diffusion from the minerals during their ascent with the molten lava.

d) The xenoliths were essentially quenched with respect to diffusion when they reached the surface, and that the laboratory studies continued the diffusional process from where it stopped at the time of quenching.

Examination of the restrictions and assumptions necessary to derive a useful diffusion equation shows that probably none of the assumptions are exactly valid. The mineral grains under investigation were not perfect spheres, but a variety of extremely complex geometric shapes. Microscopic examination showed no predominate shape, so a spherical model is probably as good as any other. The diffusion from the mineral grains is probably not isotropic, but the experimental data did not clearly indicate more than one activation energy. The diffusing gases are not homogenously distributed throughout the grains, but instead are trapped in the fluid inclusions. However, if the sample studied contained several hundred grains, the position of the bubbles in the grains should average out to produce a relatively homogenous distribution. An additional complication is the possibility that Fick's law of diffusion may not be the controlling factor in the loss of gases from these grains. Studies on the behavior of xenon in single crystals of uranium dioxide (101) indicate that gases trapped in voids or bubbles, analogous to the fluid inclusions, are reluctant to enter the lattice. Therefore, the rate determining step for loss of gases from these minerals may be the overcoming of a high potential barrier for gas particles entering the lattice from the fluid inclusions. However, comparison of the diffusion coefficients obtained for these minerals (Table 21) with

Table 21

Measured Diffusion Coefficients at 1100°C for Argon and Helium in the Salt Lake Lherzolites

mineral	D for ^{40}Ar: cm^2/sec	D for ^{4}He: cm^2/sec
Olivine	4.2×10^{-13}	$2.9\text{-}3.6 \times 10^{-12}$
Enstatite	2.2×10^{-11}	$1.6\text{-}2.2 \times 10^{-10}$
Chrome Diopside	1.7×10^{-11}	$1.7\text{-}2.1 \times 10^{-10}$

the fragmentary data available in the literature for other minerals at this temperature, indicates that these results are of the correct order of magnitude. The only reported work which can be directly related to this research is the study of a pyroxene of unreported composition by Amirkhanoff et al. (102). Contrary to this research, these workers found no difference in the diffusion rates of argon and helium. They reported diffusion coefficients of 8.0×10^{-13} cm^2/sec at 750°C and 8.0×10^{-11} cm^2/sec at 900°C for both argon and helium.

It is also assumed that there is no back diffusion of argon or helium into the grain. This is hard to justify since there is certainly some helium and argon in the volcanic gases and dissolved in the molten lava. It is hoped that the partial pressure of these gases is small enough, or that the potential barrier for diffusion back into the grain is large enough, so that back diffusion is not a serious problem. Fick's laws assume that the diffusion coefficient is dependent only on the temperature. The results obtained in this research showed a gradual decrease in the diffusion coefficient with time. This phenomenon has been observed from diffusion studies on Hawaiian basalts in this laboratory (103), and from other natural materials in other laboratories (104).

The diffusion studies conducted in the research were at a temperature of 1100°C, the maximum temperature that could be conveniently obtained with the equipment available. It is quite possible that the temperatures of the melilite nephelinite lavas of the Honolulu Series may have been closer to 1200-1300°C (92). Recalculation of the experimental data for these higher temperatures is difficult because of the lack of experimentally determined diffusion parameters for this temperature range. For an ideal diffusion model, the relation between the diffusion coefficient and the temperature can be expressed by the following equation (28):

$$D = D_o e^{-E/RT}$$

where D_o is a characteristic constant, E is the activation energy, R is the ideal gas constant, and T is the absolute temperature. If one assumes an activation energy of 74 Kcal/mole for the pyroxenes (104), then it is found that the diffusion coefficient is increased by about an order of magnitude if the temperature is increased from 1100°C to 1300°C. This would cause an increased rate of diffusion and thus an increase in the slopes of the least squares lines in figure 16. The $^4He/^{40}Ar$ ratio would not be greatly effected, increasing to about 1.4, however the time would be greatly decreased.

The resulting depth would be closer to 50 Km than to the 150 Km obtained for a temperature of 1100°C.

It is felt that the approach taken in this research to investigate the origin of the ultramafic xenoliths has opened a potentially useful path to obtaining further knowledge about the earth's interior. In spite of the many approximations and assumptions needed to obtain the values reported in this paper, it is felt that the lherzolites from Salt Lake had their origin at a depth of 50-150 Km, and that the $^{4}He/^{40}Ar$ ratio of the environment at this depth is between 1.0 and 1.5. However, this can only be confirmed by numerous additional studies.

If the $^{4}He/^{40}Ar$ ratio calculated above is representative of the mantle environment, then any proposed model for the mantle's composition must have a potassium, uranium, and thorium content capable of producing this $^{4}He/^{40}Ar$ ratio. For gas accumulation times of less than 1 billion years, no reasonable composition model will produce a $^{4}He/^{40}Ar$ ratio of 1 to 1.5. However, for gas accumulation times greater than 1 billion years, the resulting $^{4}He/^{40}Ar$ ratio decreases quite rapidly back to about 6 billion years. Figure 17 shows the $^{4}He/^{40}Ar$ that would be produced by various rock types as a function of the total time of accumulation of argon and helium. The curve for garnet pyroxenite is based on the uranium/potassium ratio determined by

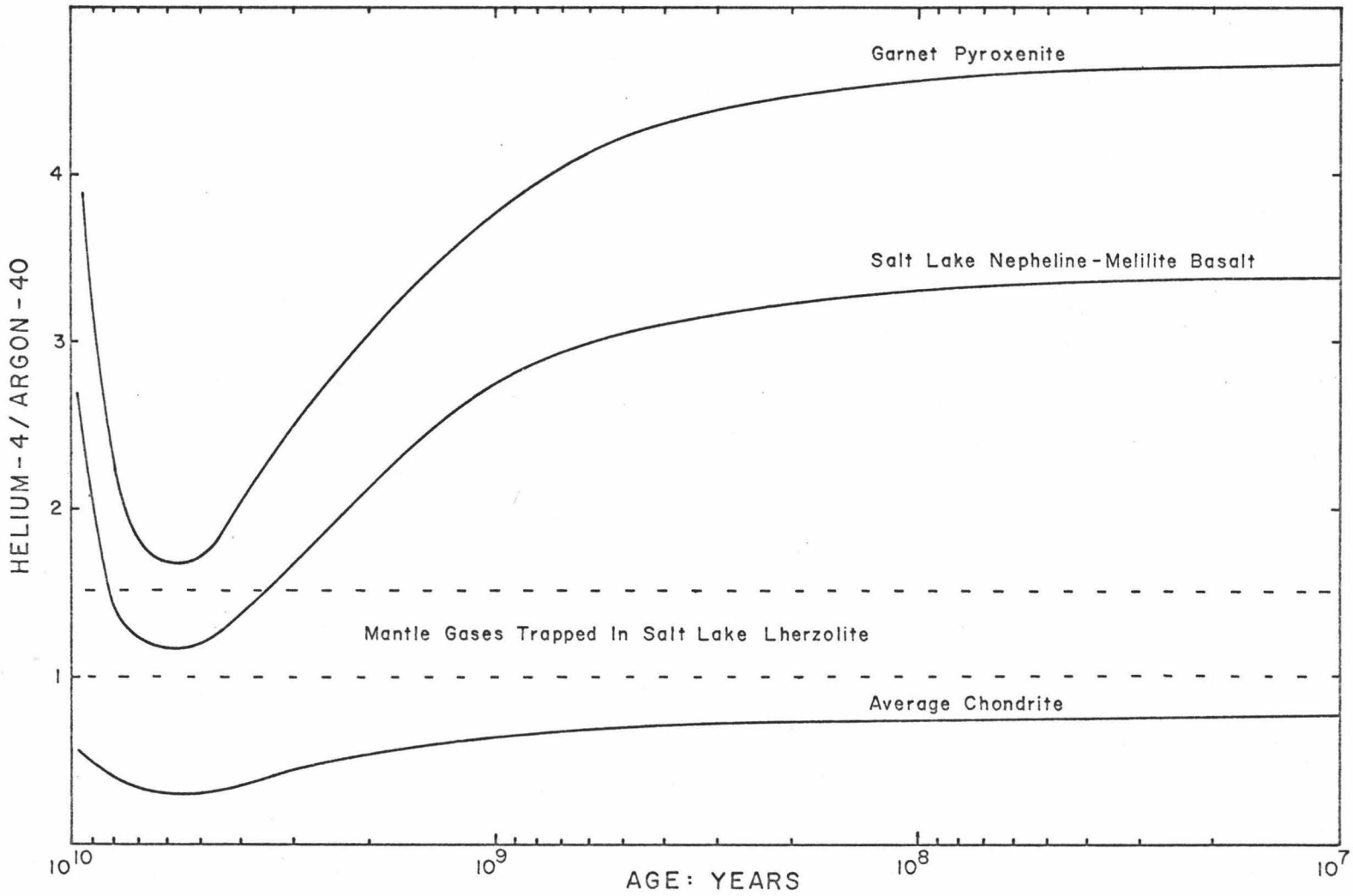

Figure 17: Change in the $^{4}He/^{40}Ar$ Ratio with Time

Tilton and Reed (105). The curve for the Salt Lake melilite nephelinite lava is based on the $^{4}He/^{40}Ar$ ratio measured in this research. The curve for an average chondrite is based on the uranium/potassium ratio obtained by Zahringer (106). It can be seen from figure 17, that if the helium and argon found in the lherzolite is the result of accumulation of these gases in the mantle for a period of at least 3.5 billion years, then the $^{4}He/^{40}Ar$ ratio in the mantle can be explained by a mantle composition containing the same relative amounts of potassium, uranium, and thorium as are found in the melilite nephelinite lava which brought these lherzolites to the surface. Based on the available data for the potassium and uranium content of the lherzolites, the minimum $^{4}He/^{40}Ar$ ratio which could be produced by this material is about 7. Therefore, it is felt that lherzolite is not primary mantle material, but perhaps the unfused residue of the mantle. The composition of garnet pyroxenite is capable of producing a $^{4}He/^{40}Ar$ ratio near the value of 1 to 1.5 (figure 17), if the gas accumulation time is about the estimated age of the earth (4-5 billion years). Garnet peroxenite seems to be a much more likely candidate for primary mantle material than the lherzolite. If one can not assume an extremely long gas accumulation time, then it is necessary

to develop a compositional model for the mantle which approaches the composition of chondritic meteorites.

C. Air Argon and the Surface Area of Samples

In spite of the problems caused by air argon contamination, little effort has been exerted toward finding the source of the air argon. It is generally felt that the amount of air argon is related in some way to the surface area. Unfortunately, no attempt has been made to back up these feelings with quantitative data. Some efforts have been made to correlate the amount of air argon with mineral type (33,44), but the results have been reported as the amount of air argon per gram of sample with no reference to the sample particle size being studied.

In this research a study was made to determine the relationship between the air argon contamination and the surface area of a sample of augite from one of the ultramafic xenoliths. Because of its deep-seated origin, this sample should have trapped no air argon in its lattice during formation, thus all air argon originating from the sample could be assumed to be of surface origin. The measured relation between particle size and surface area has been reported for several minerals (107); a log-log plot of surface area versus particle size is nearly linear. It was found that if the minerals

were normalized to the same specific gravity the particle size-surface area data for the different minerals were very close to a single line on a log-log plot. This normalized line was used to calculate the surface area for various sizes of augite grains. The specific gravity of augite was assumed to be 3.2 (108). The absolute surface area may be in error by as much as 10%, but relative to the other grain sizes the calculated surface area should be good to within 2%. It is difficult to measure the air argon from the samples accurately because the air argon contribution from the extraction system can only be determined by running a blank prior to the sample analysis. The sample sizes used in this study were only a few tenths of a gram each, so the extraction system contribution was quite significant. The data obtained is summarized in table 22. For a surface area change by a factor of over 50, the amount of air argon per cm^2 of surface area changes uniformly by a factor of about 6. The decrease in the amount of air argon per cm^2 with decreasing particle size is explained by adsorption of air argon in microcracks and surface imperfections which are more prevalent on the larger grains. These imperfections increase the effective surface area for argon adsorption. Crushing of the grains causes preferential breakage along these imperfections, thus reducing the surface area contribution of the

Table 22

Relation Between Air Argon Contamination and Mineral Surface Area for HK139 Augite

average size:	air argon: std cc/gm	approx. surface area: cm^2	air argon/area: std cc/cm^2
300	3.28×10^{-7}	138	2.5×10^{-9}
300	3.89×10^{-7}	138	2.8×10^{-9}
227	5.28×10^{-7}	178	2.9×10^{-9}
125	5.66×10^{-7}	295	1.9×10^{-9}
50	8.55×10^{-7}	680	1.3×10^{-9}
35	8.25×10^{-7}	930	8.9×10^{-10}
25	1.10×10^{-6}	1300	8.5×10^{-10}
25	8.57×10^{-7}	1300	6.6×10^{-10}
15	1.18×10^{-6}	2100	5.7×10^{-10}
15	1.44×10^{-6}	2100	6.8×10^{-10}
5	2.27×10^{-6}	5900	3.9×10^{-10}
5	2.67×10^{-6}	5900	4.3×10^{-10}
5	2.25×10^{-6}	5900	3.8×10^{-10}

imperfections as the grain size is decreased. The air argon measured in this study is very strongly bound to the surface and can not be removed to a significant extent, even by baking the sample for several hours at 200-300°C. An additional amount of air argon is physically adsorbed on the surface, and can be removed by placing the sample under vacuum. Measurement of the amount of argon being removed from the sample at various times after the sample is placed under vacuum indicates that the physically adsorbed air argon is removed at a first order rate. The rate of removal increases with increasing temperature. Thus the air argon, which is the major cause of errors in the dating of geologically young samples, is believed to originate primarily from the surface of the samples.

Surface adsorption is not the only source of air argon, however. It was found that many of the vesicular lavas of the Honolulu Series contained less air argon than the very dense lavas. In the case of one dense Koolau lava, a large block sample contained a considerable amount of air argon. Close examination of the sample revealed the presence of microscopic bubbles in the lava. Crushing the sample to -60+80 mesh reduced the air argon concentration to half the amount found in the large block. It is believed that the small bubbles contained atmospheric gases trapped at the time of formation of the lava.

IV. SUMMARY

A stainless steel gas purification system has been designed and constructed to provide more rapid and convenient purification of noble gases released from rocks. Instrumental improvement to a Reynolds-type mass spectrometer, together with the development of precise techniques for the collection and interpretation of mass spectral data, has allowed the measurement of argon isotopic ratios with a precision of ±0.1%. This improved precision in argon isotopic-ratio measurements has permitted the dating of whole-rock basalts containing potassium concentrations of 0.5-1%, and ages as recent as 30 thousand years old, with a precision of ±10%.

The potassium-argon dating method has been applied to determining the ages of the eruptions of the Honolulu Volcanic Series, Oahu, Hawaii. The measured ages range from 800 thousand years to about 30 thousand years.

Helium and argon determinations on minerals contained in ultramafic xenoliths from Salt Lake Crater, Oahu, Hawaii, indicate that excess radiogenic gases in these minerals are held in fluid inclusions in the grains, and the gas content of these minerals has been altered by diffusion during ascent with the erupting lava. Diffusion studies on these minerals indicate that they may have come from a depth of 50-150 Km. The $^{4}He/^{40}Ar$ ratio

of the environment at this depth is calculated to be between 1.0 and 1.5.

APPENDIX A

Derivation of the Potassium-Argon Age Equation

The basic equation of radioactive decay is:

$$N = N_o \, e^{-\lambda t} \qquad \text{(A-1)}$$

where N is the number of parent atoms remaining at time t, and N_o is the initial number of parent atoms. At any time the number of parent atoms remaining, N, plus the number of daughter atoms, D, equals the initial number of parent atoms, N_o:

$$N_o = N + D \qquad \text{(A-2)}$$

Substituting (A-2) into (A-1) yields:

$$D = N \, (e^{\lambda t} - 1) \qquad \text{(A-3)}$$

For branching decay with daughter products D_1 and D_2, equation (A-3) becomes:

$$D_1 + D_2 = N \left[e^{(\lambda_1 + \lambda_2)t} - 1 \right] \qquad \text{(A-4)}$$

For the specific case of the decay of ^{40}K, this can be written:

$$^{40}Ar + {}^{40}Ca = {}^{40}K \left[e^{(\lambda_\kappa + \lambda_\beta)t} - 1 \right] \qquad \text{(A-5)}$$

The fraction of ^{40}K atoms that decay to ^{40}Ar is:

$$\frac{^{40}Ar}{^{40}Ar + ^{40}Ca} = \frac{\lambda_\kappa}{\lambda_\kappa + \lambda_\beta} \qquad \text{(A-6)}$$

Substituting (A-6) into (A-5) yields:

$$^{40}Ar = ^{40}K \frac{\lambda_\kappa}{\lambda_\kappa + \lambda_\beta} \left[e^{(\lambda_\kappa + \lambda_\beta)t} - 1 \right] \qquad \text{(A-7)}$$

Solving (A-7) for t gives:

$$t = \frac{1}{\lambda_\kappa + \lambda_\beta} \ln \left[\frac{^{40}Ar}{^{40}K} \frac{\lambda_\kappa + \lambda_\beta}{\lambda_\kappa} + 1 \right] \qquad \text{(A-8)}$$

which is the potassium-argon age equation.

APPENDIX B

Description of Samples

HK201 Melilite nephelinite basalt from Salt Lake Crater. The sample was supplied by Dr. K.A. Pankiwskyj, Dept. of Geology, University of Hawaii. A dark gray, nearly black, nonvesicular sample with about 4% unaltered glass.

HK202 Melilite nephelinite basalt from the Sugar Loaf flow. The sample was collected about 10 feet below the surface during excavation for the engineering building, spring 1970, on the University of Hawaii campus. The sample is a dark gray, medium grain, nonvesicular basalt containing about 2% fine grained zeolites.

HK203 Nepheline basanite (70) or basanitoid (109) from the Kaimuki lava shield. The exact location of this sample is unknown. Petrographic examination identifies it as Black Point or Kaimuki lava. The sample was collected from a large pile of recently excavated rock, most probably from the sewer project on the southeastern side of the Kaimuki shield.

HK204 Linosaite from Koko Crater dike flow. Sample collected from a road cut between the Kahauloa Crater rifle range and the "Blow Hole". Sample is a dark gray, vesicular lava with abundant olivine phenocrysts.

HK206 Basanite from the Pali lava flow. Collected from small gorge at the end of the Old Pali Road, just past the Kailua side of the Pali tunnel. Sample is a dark gray nonvesicular basalt containing numerous small ultramafic xenoliths, similar to those found at Salt Lake. Small fragments of xenolithic material are intimately mixed with the lava. The sample is somewhat weathered, with much of the olivine being completely altered to iddingsite.

HK207 Nephelinite lava from the Nuuanu eruption, probably the northern (Makuku) vent. The sample was collected from the side of the stream bed where the Nuuanu Fresh Water Fish Preserve crosses the Old Pali Road. Sample shows slight weathering; much of the olivine is rimmed with iddingsite.

HK210 Basanitoid lava from Kaimuki shield. Collected at 18th Ave. and Kilauea Ave. Sample was donated

by Dr. G.A. Macdonald, Dept. of Geology, University of Hawaii. A chemical analysis has been published (109) as sample C-32.

HK212 Melilite nephelinite lava from the Castle flow, collected from the main face of Kapaa Quarry, near Kailua. Sample was donated by Dr. G.A. Macdonald. A chemical analysis has been published (110) as sample C-165.

HK213 Basanitoid from the Kaupo lava flow collected from a roadcut just east of the entrance to Makapuu Beach Park. Sample was donated by Dr. G.A. Macdonald and its chemical analysis has been published (110) as sample C-164. The lava is somewhat vesicular with abundant olivine phenocrysts.

HK215 Nepheline basanite from the Black Point lava flow, collected from a roadcut exposure on Black Point Road. The sample is similar to, but slightly more vesicular than HK219.

HK216 Nepheline basanite from the Kalama Crater flow collected from a roadcut on Kamehameha Highway between Koko Crater and Makapuu Head. The sample is a medium gray, vesicular lava with abundant olivine phenocrysts.

HK217 Melilite nephelinite lava from the Kalihi flow. Sample was collected from excavations for the Kalihi-Kai sewer project, on Kalihi Street between Umalu Place and the Honolulu Watershed Forest Reserve boundary. The sample is a dark gray, nonvesicular lava with about 2% fine grained zeolites.

HK219 Nepheline basanite from the Black Point lava flow, collected from an exposure at the end of Kaikoo Place on Black Point. The sample was collected above the emerged reef from the 95 foot Kaena stand of the sea.

HK220 Melilite nephelinite lava from the Kaau Crater flow into Palolo Valley. Collected from the side of Pukeke Stream where the stream crosses under La-I Road. The sample is a dark gray, nonvesicular lava containing about 4% fine grained zeolites.

HK222 Nephelinite lava from Punchbowl Crater. The sample was collected by C.K. Wentworth (111) on April 14, 1939, from the basement of an excavation along Lisbon Street. The 100 gram hand specimen (B.W.S. sample #8207) was obtained from the Honolulu Board of Water Supply.

HK139 A composite of several garnet eclogites collected from Salt Lake Crater.

HK200 An eclogite containing a considerable amount of biotite. Collected from Salt Lake Crater.

SL201 A large lherzolite xenolith collected from Salt Lake Crater. The sample contains primarily olivine, chrome diopside, and enstatite. A small amount of spinel is present, as well as a trace of garnet.

SL203 A large lherzolite xenolith collected from Salt Lake Crater. The sample is very similar in composition and grain size to SL201.

APPENDIX C

Sample Age Calculation

Sample: HK204 Koko Crater

Sample weight: 10.5120 gm

^{38}Ar Spike #160: 3.663×10^{-7} std cc

Measured $^{40}Ar/^{36}Ar$ ratio of air argon: 303.0

Mass spectral data:

time: min	$^{40}Ar/^{38}Ar$	time: min	$^{38}Ar/^{36}Ar$
2	0.5944	4	543.2
7	0.6022	9	533.6
18	0.6170	15	523.4
24	0.6250	21	513.7
30	0.6337	26	506.3

Least squares analysis:

initial $^{40}Ar/^{38}Ar$ ratio: 0.5920 ± 0.0003

initial $^{38}Ar/^{36}Ar$ ratio: 549.4 ± 0.6

Total ^{40}Ar: $(0.5920)\ 3.663 \times 10^{-7} = 2.168 \times 10^{-7}$

less ^{40}Ar from spike $= .004 \times 10^{-7}$

2.164×10^{-7}

Air argon: $\dfrac{(303.0)\,3.663 \times 10^{-7}}{549.4} = 2.020 \times 10^{-7}$

Radiogenic $^{40}Ar = 0.144 \times 10^{-7}$ cc/10.512 gm

$= 1.37 \times 10^{-9}$ std cc/gm

Potassium = 0.930%

$$^{40}Ar/^{40}K = 1463 \left[\frac{^{40}Ar: \text{ std cc/gm}}{K\%}\right] = 2.16 \times 10^{-6}$$

$$t = 1.709 \ (^{40}Ar/^{40}K) \times 10^{10} \text{ years}$$

$$t = 1.709 \ (2.16 \times 10^{-6}) \times 10^{10} \text{ years}$$

$$t = 36.8 \text{ thousand years}$$

BIBLIOGRAPHY

(1) R. W. Force, "The Origin of the Polynesians," Talk presented at the Pacific Area Meeting of the National Association of Soil and Water Conservation Districts, Honolulu, Hawaii, December 12, 1963.

(2) J. J. Thompson, "On the emission of negative corpuscles by the alkali metals," Phil. Mag. 10, 584-590 (1905).

(3) N. R. Campbell, A. Wood, "The radioactivity of the alkali metals," Proc. Cambridge Phil. Soc. 14, 15-21 (1906).

(4) F. W. Aston, "The mass spectra of the alkali metals," Phil. Mag. 42, 436-441 (1921).

(5) F. H. Newman, H. J. Walke, "The radioactivity of potassium and rubidium," Phil. Mag. 19, 767-773 (1935).

(6) O. Klemperer, "On the radioactivity of potassium and rubidium," Proc. Roy. Soc. London 148, 638-648 (1935).

(7) A. O. Nier, "Evidence for the existence of an isotope of potassium of mass 40," Phys. Rev. 48, 283-284 (1935).

(8) A. K. Brewer, "Further evidence for the existence of ^{40}K," Phys. Rev. 48, 640 (1935).

(9) W. R. Smythe, A. Hammendinger, "The radioactive isotope of potassium," Phy. Rev. 51, 178-182 (1937).

(10) C. F. Von Weizsäcker, "Uber die Möglichkeit eines dualen Zerfalls von Kalium," Physik Zeitschr. 38, 623-624 (1937).

(11) L. T. Aldrich, A. O. Nier, "Argon-40 in potassium minerals," Phys. Rev. 74, 876-877 (1948).

(12) M. J. Pahl, J. Hiby, F. Smits, W. Gentner, "Mass spectrometric determination of argon from potash salts," Z. Naturforsch. 5, 404 (1950).

(13) F. Smits, W. Gentner, "Argonbestimmungen an Kalium Mineralien I, Bestimmungen an Tertiären Kalisalzen," Geochim. Cosmochim. Acta 1, 22 (1950).

(14) W. Gentner, R. Präg, F. Smits, "Argonbestimmungen an Kalium Mineralien II, Das Alter eines Kalilagers im unteren Oligozän," Geochim. Cosmochim. Acta 4, 11 (1953).

(15) W. Gentner, K. Goebel, R. Präg, "Argonbestimmungen an Kaliummineralien III, Vergleichende Messungen nach der Kalium-Argon und Uran-Helium Methode," Geochim. Cosmochim. Acta 5, 124 (1945).

(16) A. O. Nier, "A redetermination of the relative abundances of the isotopes of carbon, nitrogen, oxygen, argon, and potassium," Phys. Rev. 77, 789-793 (1950).

(17) C. Reuterswärd, "The isotopic abundance of ^{40}K," Ark. Fys. 4, 203-205 (1952).

(18) C. Reuterswärd, "On the isotopic constitution of potassium," Ark. Fys. 11, 1-54 (1956).

(19) F. A. White, T. L. Collins, F. M. Rourke, "Search for possible naturally occurring isotopes of low abundance," Phy. Rev. 101, 1986-1991 (1956).

(20) P. E. Damon, "Potassium-argon dating of igneous and metamorphic rocks with applications to the Basin Ranges of Arizona and Sonora," In Radiometric Dating for Geologists (E.I. Hamilton, R.M. Farquhar, eds.), Interscience Publishers, New York, N.Y., 1968, pp. 1-72.

(21) P. M. Endt, J. C. Kluyver, "Energy levels of light nuclei (Z 11 to Z 20)," Rev. Mod. Phys. 26, 95-166 (1954).

(22) G. W. Wetherill, "Radioactivity of potassium and geologic time," Science 126, 545-549 (1957).

(23) A. McNair, R. N. Glover, H. W. Wilson, "The decay of potassium-40," Phil. Mag. 1, 199-211 (1956).

(24) R. E. Folinsbee, H. Baadsgaard, J. Lipson, "Potassium argon time scale," Int. Geol. Congr. 21, 7-17 (1960).

(25) L. V. Firsov, "On the choice of decay constants of ^{40}K for the determination of the ages of rocks by the ratio of ^{40}Ar to ^{40}K," Izv. Acad. Sci. U.S.S.R. 1960, 77-78 (1960).

(26) A. G. Smith, "Potassium-argon decay constants and age tables," Quart. J. Geol. Soc. Lond. 120, 129-141 (1964).

(27) J. J. Krausharr, E. D. Wilson, K. T. Bainbridge, "Comparison of the values of the disintegration constants of Be^7 in Be, BeO, and BeF_2," Phys. Rev. 90, 610-614 (1953).

(28) G. B. Dalrymple, M. A. Lanphere, Potassium-Argon Dating, W. H. Freeman & Co., San Francisco, Cal., 1969.

(29) D. R. Carr, J. L. Kulp, "Use of ^{37}Ar to determine argon behavior in vacuum systems," Rev. Sci. Instr. 26, 379-381 (1955).

(30) P. E. Damon, J. L. Kulp, "Determination of radiogenic helium in zircon by stable isotope dilution techniques," Tran. Am. Geophy. Union 38, 945-953 (1957).

(31) T. Kirsten, "Determination of radiogenic argon," In Potassium Argon Dating (O.A. Schaeffer, J. Zahringer, eds.), Springer-Verlag New York Inc., New York, N. Y., 1966, pp. 7-39.

(32) J. F. Evernden, G. H. Curtis, "Potassium-argon dating of late Cenozoic rocks in East Africa and Italy," Current Anthropology 6, 343-385 (1965).

(33) I. McDougall, "Precision methods of potassium-argon isotopic age determinations on young rocks," In Methods and Techniques in Geophysics, Interscience Publishers, New York, N. Y., 1966, pp. 279-304.

(34) J. H. Reynolds, "High sensitivity mass spectrometer for noble gas analysis," Rev. Sci. Inst. 27, 928-934 (1956).

(35) A. O. Nier, "A mass spectrometer for isotope and gas analysis," Rev. Sci. Inst. 18, 398-411 (1947).

(36) A. J. Dempster, "A new method of positive ray analysis," Phys. Rev. 11, 316-325 (1918).

(37) R. L. Grasty, J. A. Miller, "The omegatron: a useful tool for argon isotope investigation," Nature 207, 1146-1148 (1965).

(38) P. Rosenberg, "A method for diminishing the sticking of mercury in capillaries," Rev. Sci. Inst. 9, 258 (1938).

(39) A. Moljk, R. W. P. Drever, S. C. Curran, "Trace quality analysis: neutron activation applied to potassium-mineral dating," Nucleonics 13, 44-46 (1955).

(40) R. L. Armstrong, "Potassium-argon dating of silicates using neutron activation for argon determination," Geol. Soc. Am. Bull. 70, 1563 (1959).

(41) R. L. Armstrong, "K-Ar dating using neutron activation for Ar analysis: granitic plutons of the eastern Great Basin, Nevada and Utah," Geochim. Cosmechim. Acta 30, 565-600 (1966).

(42) J. F. Evernden, G. H. Curtis, R. W. Kistler, J. Obradovich, "Argon diffusion in glauconite, microcline, sanidine, leucite, and phlogopite," Amer. J. Sci. 258, 583-604 (1960).

(43) A. E. Mussett, G. B. Dalrymple, "An investigation of the source of air argon contamination in K-Ar dating," Earth Planet. Sci. Letters 4, 422-426 (1968).

(44) A. W. Laughlin, Ph.D. dissertation, Department of Geology, University of Arizona, 1969, pp. 162-165.

(45) G. W. Wetherill, L. T. Aldrich, G. L. Davis, "Ar^{40}/K^{40} ratio of feldspars and micas from the same rock," Geochim. Cosmochim. Acta 8, 171-172 (1955).

(46) H. Baadsgaard, J. Lipson, R. E. Folinsbee, "The leakage of radiogenic argon from sanidine," Geochim. Cosmochim. Acta 25, 147-157 (1961).

(47) S. S. Sardarov, "Retention of radiogenic argon in microcline," Geochemistry 3, 233-237 (1957).

(48) J. F. Evernden, G. T. James, "Potassium-argon dates and the Tertiary floras of North America," Amer. J. Sci. 262, 945-974 (1964).

(49) J. F. Evernden, J. R. Richards, "Potassium-argon ages in eastern Australia," J. Geol. Soc. Australia 9, 1-50 (1962).

(50) R. E. Folinsbee, H. Baadsgaard, J. Lipson, "Potassium-argon dates of Upper Cretaceous ash falls, Alberta, Canada," Annals N. Y. Acad. Sci. 91, 352-363 (1961).

(51) G. J. Wasserburg, G. J. Hayden, K. J. Jensen, "Ar^{40}-K^{40} dating of igneous rocks and sediments," Geochim. Cosmochim. Acta 10, 153-165 (1956).

(52) J. L. Kulp, J. Engels, "Discordances in K-Ar and Rb-Sr isotopic ages," In Radioactive Dating, Vienna International Atomic Energy Agency, 1963, pp. 219-238.

(53) M. R. Westcott, "Loss of argon from biotite in a thermal metamorphism," Nature 210, 83-84 (1966).

(54) M. A. Lanphere, E. M. Mackevett, T. W. Stern, "Potassium-argon and lead-alpha ages of plutonic rocks, Bokan Mountain area, Alaska," Science 145, 705-707 (1964).

(55) G. N. Hanson, P. W. Gast, "Kinetic studies in contact metamorphic zones," Geochim. Cosmochim. Acta 31, 1119-1153 (1967).

(56) I. McDougall, H. A. Polach, J. J. Stipp, "Excess radiogenic argon in young subaerial basalts from the Auckland volcanic field, New Zealand," Geochim. Cosmochim. Acta 33, 1485-1520 (1969).

(57) I. McDougall, "Potassium-argon ages from lavas of the Hawaiian Islands," Geol. Soc. Am. Bull. 75, 107-128 (1964).

(58) I. McDougall, "Potassium-argon ages on lavas of Kohala Volcano, Hawaii," Geol. Soc. Am. Bull. 80, 2597-2600 (1969).

(59) H. S. Carslaw, J. C. Jaeger, Conduction of Heat in Solids, Oxford University Press, London, 1959.

(60) J. G. Funkhouser, "The determination of a series of ages of a Hawaiian volcano by the potassium-argon method," Ph.D. Dissertation, University of Hawaii, 1966.

(61) J. G. Funkhouser, I. L. Barnes, J. J. Naughton, "Problems in the dating of volcanic rocks by the potassium-argon method," Bull. Volcanol. 29, 709-718 (1966).

(62) G. B. Dalrymple, "$^{40}Ar^{36}Ar$ analysis of historic lava flows," Earth Planet. Sci. Letters 6, 47-55 (1969).

(63) J. F. Lovering, J. R. Richards, "Potassium-argon age study of possible lower-crust and upper-mantle inclusions in deep-seated intrusions," J. Geophys. Res. 69, 4895-4901 (1964).

(64) J. G. Funkhouser, J. J. Naughton, "Radiogenic helium and argon in ultramafic xenoliths from Hawaii," J. Geophys. Res. 73, 4601-4607 (1968).

(65) D. S. Noble, "Investigation of the inert gas content of Hawaiian inclusions that exhibit anomalous ages," Ph.D. Dissertation, University of Hawaii, 1969.

(66) O. Muller, "Potassium analysis," In Potassium-Argon Dating (O. A. Schaeffer, J. Zahringer, eds.), Springer-Verlag New York Inc., New York, N. Y., 1966, pp. 40-67.

(67) J. W. Morgan, A. D. T. Goode, "Potassium abundances in some ultrabasic and basic rocks," Earth Planet. Sci. Letters I, 110-112 (1966).

(68) H. T. Stearns, "Geologic map and guide of the island of Oahu, Hawaii," Terr. Hawaii, Div. Hydrog. Bull. 2, (1939).

(69) H. T. Stearns, K. N. Vaksvik, "Geology and ground-water resources of the island of Oahu, Hawaii," Terr. Hawaii, Div. Hydrog. Bull. I, (1935).

(70) H. Winchell, "Honolulu series, Oahu, Hawaii," Bull. Geol. Soc. Am. 58, 1-48 (1947).

(71) H. T. Stearns, "Shore benches on the island of Oahu, Hawaii," Geol. Soc. Am. Bull. 46, 1467-1482 (1935).

(72) H. T. Stearns, "Pleistocene shore lines on the islands of Oahu and Maui, Hawaii," Geol. Soc. Am. Bull. 46, 1927-1956 (1935).

(73) H. T. Stearns, "Ancient shore lines on the island of Lanai, Hawaii," Geol. Soc. Am. Bull. 49, 615-628 (1938).

(74) D. Lum, H. T. Stearns, "Pleistocene stratigraphy and eustatic history based on cores at Waimanalo, Oahu, Hawaii," Geol. Soc. Am. Bull. 81, 1-16 (1970).

(75) R. W. White, "Ultramafic inclusions in basaltic rocks from Hawaii," Contr. Mineral. Petrol. 12, 245-314 (1966).

(76) E. D. Jackson, "Eclogite in Hawaiian basalts," U.S. Geol. Survey Prof. Paper 550-D, D151-D157 (1966).

(77) D. H. Green, "The origin of the eclogites from Salt Lake Crater, Hawaii," Earth Planet. Sci. Letters I, 414-420 (1966).

(78) E. Roedder, "Liquid CO_2 inclusions in olivine-bearing nodules and phenocrysts from basalts," Am. Mineralogist 50, 1746-1782 (1965).

(79) I. L. Barnes, personal communication.

(80) S. Dushman, Scientific Foundations of Vacuum Technique, John Wiley & Sons, Inc., New York, N. Y., 1962.

(81) G. B. Dalrymple, personal communication.

(82) C. S. Noble, personal communication.

(83) M. A. Lanphere, G. B. Dalrymple, "Simplified bulb tracer system for argon analysis," Nature 209, 902-903 (1966).

(84) M. A. Lanphere, G. B. Dalrymple, "K-Ar and Rb-Sr measurements on p-207, the U.S.G.S. interlaboratory standard miscovite," Geochim. Cosmochim. Acta 31, 1091-1094 (1967).

(85) B. Bernas, "A new method for decomposition and comprehensive analysis of silicates by atomic absorption spectrometry," Anal. Chem. 40, 1682-1686 (1968).

(86) H. H. Willard, L. L. Merritt, J. A. Dean, Instrumental Methods of Analysis, D. Van Nostrand Co., Inc., New York, N. Y., 1965, p. 342.

(87) T. Kirsten, "Incorporation of rare gases in solidifying enstatite melts," J. Geophys. Res. 73, 2807-2810 (1968).

(88) A. Cox, G. B. Dalrymple, "Statistical analysis of geomagnetic reversal data and precision of potassium-argon dating," J. Geophys. Res. 72 2603-2614 (1967).

(89) J. H. Reynolds, Personal communication to J. J. Naughton.

(90) H. H. Veeh, "Th 230/U 238 and U 234/U 238 Ages of Pleistocene High Sea Level," J. Geophs. Res. 71, 3379-3386 (1966).

(91) H. T. Stearns, Geology of the State of Hawaii, Pacific Books, Palo Alto, California, 1966.

(92) G. A. Macdonald, personal communication.

(93) H. T. Stearns, personal communication.

(94) H. T. Stearns, "Age of dunes on Oahu, Hawaii," B. P. Bishop Museum, Occasional Papers XXIV, 49-72 (1970).

(95) G. A. Macdonald, W. Kyselka, Anatomy of an Island, A Geological History of Oahu, Bishop Museum Press, Honolulu, Hawaii.

(96) C. H. Hitchcock, "Geology of Oahu," Geol. Soc. Am. Bull. 11, 15-60 (1900).

(97) R. E. Zartman, G. J. Wasserburg, J. H. Reynolds, "Helium, argon, and carbon in some natural gases," J. Geophys. Res. 66, 277-306 (1961).

(98) J. D. Kleeman, D. H. Green, J. F. Lovering, "Uranium distribution in ultramafic inclusions from Victorian basalts," Earth Planet. Sci. Letters 5, 449-458 (1969).

(99) G. J. Wasserburg, E. Mazor, R. E. Zartman, "Isotopic composition of some terrestrial natural gases," In Earth Science and Meteoritics (J. Geiss, E. D. Goldberg, eds.) North-Holland, Amsterdam, 1963, pp. 219-240.

(100) E. R. Oxburg, "Physical evidence for the presence of amphibole in the upper mantle and its petrogenetic and geophysical implications," Geol. Mag. 101, 1-19 (1964).

(101) P. Spindler, R. Lindner, "Diffusion of xenon-133 in UO_2 single crystals," Z. Naturforsch. 21, 1723 (1966).

(102) K. I. Amirkhanoff, S. B. Brandt, E. N. Bartnitsky, "Radiogenic argon in minerals and its migration," Ann. N. Y. Acad. Sci. 91, 235-275 (1961).

(103) J. T. Kimura, "Radiogenic argon diffusion in two Hawaiian Basalts," Undergraduate Honors Thesis, Department of Chemistry, University of Hawaii, 1968.

(104) H. Fechtig, S. Kalbitzer, "The diffusion of argon in potassium-bearing solids," In Potassium Argon Dating (O. A. Schaeffer, J. Zahringer, eds.), Springer-Verlag New York, Inc., New York, N. Y., 1966, pp. 68-107.

(105) G. R. Tilton, G. W. Reed, "Radioactive heat production in eclogite and some ultramafic rocks," In Earth Science and Meteoritics (J. Geiss, E. D. Goldburg, eds.) North-Holland, Amsterdam, 1963, pp. 31-43.

(106) J. Zahringer, "Rare gases in stony meteorites," Geochim. Cosmochim. Acta 32, 209-237 (1968).

(107) G. G. Brown, Unit Operations, John Wiley and Sons, Inc., New York, N. Y., 1950, p. 28.

(108) E. S. Dana, A Textbook of Mineralogy, John Wiley and Sons, Inc., New York, N. Y., 1964, p. 559.

(109) G. A. Macdonald, T. Katsura, "Chemical composition of Hawaiian lavas," J. Petrology 5, 82-133 (1964).

(110) G. A. Macdonald, "Composition and origin of Hawaiian lavas," Geol. Soc. Am. Memoir 116, 477-522 (1968).

(111) C. K. Wentworth, Field Notebook Number 23, Honolulu Board of Water Supply, Honolulu, Hawaii.